Efficacy of *Moringa oleifera* proteins as coagulants in a sustainable sand filter for drinking water treatment

Submitted in partial fulfillment of the requirements for

the degree of

Doctor of Philosophy

in

Chemical Engineering

Brittany A. Nordmark

B.S. Chemical Engineering, University of Maryland, Baltimore County

Carnegie Mellon University

Pittsburgh, PA

April, 2018

© Brittany A. Nordmark, 2018
All Rights Reserved

Acknowledgements

Thank you to my advisors, Bob Tilton and Todd Przybycien (committee chairs), for your guidance, patience, and encouragement during my time at Carnegie Mellon. Thank you to my committee members, Annette Jacobson, James Schneider, and Greg Lowry, for your input and suggestions to strengthen my thesis work. Thank you to my collaborators at the Pennsylvania State University, Stephanie Velegol and Darrell Velegol, for bringing the *Moringa* project to Carnegie Mellon, and thank you to Toni Bechtel for teaching me the *Moringa* basics. Thank you to my funding sources, the Mahmood I. Bhutta Graduate Fellowship in Chemical Engineering at Carnegie Mellon University and Bob Tilton's discretionary account.

Thank you to the coordinators of the Colloids, Polymers, and Surfaces program, Rose Frollini, Annette Jacobson, Susana Steppan, and Ilhem Hakem, for teaching me valuable laboratory skills both inside and outside of class. Thank you to Paul Sides for teaching me how to use the ZetaSpin and for reminding me of why I chose a career in research.

Thank you to the members of the Tilton and Przybycien groups, both past and present, especially Alex Bertuccio, Qin Gu, Yun-Ru Huang, Steve Iasella, Danish Iqbal, and Bhagyashree Lele, and Henry Chu. All of the great conversations, laughs, late nights, and Tilton Group lunches helped me get through this program. Thank you also to department friends, especially Becca Ball, Kathy Fein, Lisa Kasiewicz, Kal Hajj, Nick Lamson, Randy Gamble, Kyle Cochran, Travis Armiger, Bruce Yan, Toni Bechtel, Irem Sen, Anirudh Subramanyam, Ben Sauk, Charles Sharkey, Dana McGuffin, Michael Davidson, Pablo García, and Andrew Fox.

Thank you to Rachael Rindler and Justin Schaeffer for your encouraging words, and thank you to my volleyball teammates, Kevin Martin, Dena Carron, Lindsey Berkebile, Connor Ward, and Zack Tanczos on the Lucky Charms for building me up. Thank you to my Maryland

friends, Camille Vu, Caroline Kemp, Michelle Ma, Celina Szymanski, and Sam Celmer for supporting me while I was away from home. Thank you to my church family at North Way Christian Community, especially Sara Zakutney, Kara VanHoudnos, Amber Okai, Christina Law, Sam Sutherland, Deborah Neuhaus, and Abby Cunningham for your love, prayer, support, and compassion. Thank you to all my friends I made in Pittsburgh, especially Sarah Feicht, Sean Segreti, and Pei Hong Tan.

Thank you to my Mom and Dad and my sister Christina for always being there for me through the good and the bad. Thank you to Grammy and Grandpa and to Baci and Pop for always telling me how proud you are of my accomplishments. Thank you to the members of my extended family for coming to visit me and for your love and support.

Abstract

Cationic proteins from the seeds of the *Moringa oleifera* tree are of interest as sustainable coagulants for drinking water treatment in regions with poor access to potable water in tropical and subtropical regions of the world. They have been shown to reduce turbidity in natural water sources as well as in various model freshwaters. To identify the active components in the seed extract, high performance liquid chromatography was employed. Eight *M. oleifera* cationic protein fractions were isolated and characterized using gel electrophoresis, dynamic light scattering, and circular dichroism. Coagulation performance experiments were conducted using a micro-coagulation assay that was validated by comparison to a standard jar test. Fraction coagulation performances were compared individually and in various combinations against kaolin clay suspensions in model freshwaters of varying hardness. The unfractionated protein extract was found to be effective across a broad range of protein dosages. Coagulation activity for this extract was further investigated against humic acid and mixtures of kaolin clay and humic acid in model freshwaters of varying hardness. The coagulation mechanism of *Moringa oleifera* proteins was demonstrated to be adsorption and charge neutralization. Adsorption isotherms were measured using ellipsometry to investigate the effects of water hardness, fractionation, and fatty acid extraction on protein adsorption to silica surfaces. The zeta potentials of the resulting protein-decorated surfaces were measured by the rotating disk streaming potential method. Sands can be effectively modified with *M. oleifera* proteins using small amounts of seed extract under various local water hardness conditions. Gravity sand filters packed with *Moringa oleifera* modified sand were constructed and shown to be effective against kaolin and humic acid. Protein layer coverage and composition did not affect filter performance. These studies may aid in the design of a simple, effective, and sustainable water purification device for developing nations.

Table of Contents

List of Tables

List of Figures

Chapter 1: Introduction

1.1. Motivation

The motivation for this work stems from the Millennium Development Goals set by the United Nations in 2000. The seventh of these goals is to "Ensure Environmental Sustainability," with one of its targets being to "Halve, by 2015, the proportion of the population without sustainable access to safe drinking water and basic sanitation." Although this goal was met by 2010, it was reported that in 2012, approximately 748 million people were still without access to an improved source of drinking water and that 40% of these people live in sub-Sahara Africa, a region of the world where the *Moringa oleifera* grows[19].

M. oleifera is known as the "miracle tree" because parts of the tree are rich in nutrients, have several medical benefits, and can be used to treat drinking water [1–9]. People in many developing nations treat drinking water by first shelling and grinding the seeds into a powder. Fatty acids are pressed from the grounds, collected, and sold as a commodity. The defatted seeds are then added to a small container of water and shaken to extract cationic proteins that act as coagulants and antimicrobial agents. This protein solution is poured through a cloth into a larger container of water designated for drinking. This water is stirred and particulate matter is allowed to settle, at which time the water is potable[10]. Although *M. oleifera* cationic proteins are highly effective coagulants and antimicrobial agents (reducing water turbidity up to 99.5%[11–23] and achieving 1 to 4 log removal of microorganisms[21,24,25]), this procedure provides only short term benefit. Natural organic matter from the seeds remains in the treated water and supports the growth of residual microorganisms, causing the water to become unsafe to drink after 24 hours[10,26]. In many developing nations, drinking water is scarce or difficult to obtain, so methods of reducing natural organic matter in *M. oleifera* treated water are of great interest.

Our collaborators at the Pennsylvania State University have developed a novel solution to purify drinking water with *M. oleifera* proteins to decrease natural organic matter in treated water[27]. Sand granules are incubated in a solution of *M. oleifera* proteins to allow the proteins to adsorb to the granules and after incubation, excess organic matter is rinsed away. The protein-functionalized sand granules, referred to as "f-sand", are then employed in a gravity sand filter. Particulate matter and microorganisms adhere to the adsorbed proteins as water passes through the filter. Our collaborators showed that a slurry of f-sand is able to reduce the turbidity of kaolin suspensions and that the adsorbed proteins retain their ability to bind and disrupt the membranes of microorganisms[27]. They also found that f-sand filters can achieve 3-4 log removal of 1 µm polystyrene particles and 8 log removal of *E. coli*.[28] Li and Pan[29] found that sand modified by *M. oleifera* proteins can remove between 20-80% of algal bloom cells depending on the algae species. Nisha *et al*.[30] found that a filter packed with *M. oleifera* cationic protein-coated sand (referred to as MOCP c-sand) was able to produce a reduction in water hardness of ~33% and a reduction in chloride ion concentration of ~43%. Williams *et al.* showed that *E. coli* will attach to f-sand packed in a column and that these microbes can be removed with a surfactant rinse[31]. These findings suggest that f-sand formed simply using *M. oleifera* seeds, sand, and locally available water has the potential to produce potable drinking water in the developing world. The work in this dissertation answers several fundamental questions pertinent to the development of *M. oleifera* seed proteins as water purification agents, both as water-soluble coagulants and as the basis for the f-sand filter.

1.2. Background

1.2.1. Characteristics of Moringa oleifera cationic proteins

M. oleifera cationic proteins have been called $MO_{2.1}$[32], Flo (the recombinant protein)[33], and MOCP[27]. They are approximately 1.2 ± 0.2% w/w of the seeds[34]. Various molecular weights determined from SDS-PAGE have been reported in the literature for the active protein species in *M. oleifera* seeds, including reduced molecular weights of approximately 6.5 kDa[19,25,27,32,35], 20 kDa[35], 30 kDa[36], and 66 kDa[37], and native molecular weights of approximately 13 kDa[19,34] and 26 kDa[34]. The two studies reporting native molecular weights identified these species as oligomers of 6.5 kDa cationic proteins.

The 6.5 kDa *M. oleifera* proteins contain eight regions of positive charge and have an isoelectric point around 10.8[38]. The primary structures of several isoforms of the 6.5 kDa species have been determined[32,34,38]. These isoforms consist of 17-18 different amino acids and are 60 residues in length. The secondary and tertiary structures of these proteins are not well-established. A study which employed circular dichroism to determine secondary structure features showed that it consisted of 60% alpha helices, 30% unordered structures, and 10% beta sheets[39]. Another study modeled the secondary and tertiary structures by using the amino acid sequence and the secondary and tertiary structures of 2S seed albumin proteins from various plants because of their high degree of similarity to *M. oleifera* proteins[38]. The model showed that these proteins are mainly composed of alpha helices. This study also isolated the regions of the proteins that are responsible for coagulant and antimicrobial properties.

1.2.2. Moringa oleifera proteins as coagulants

The strong positive charge density of the *Moringa oleifera* proteins is integral to their functionality as coagulants[38]. Suspended contaminants in drinking water, which often include clays, humic acids, and bacteria, are typically negatively charged, and are either stably suspended in solution or require a long period of time to sediment. *M. oleifera* proteins remove these particles through adsorption, which induces coagulation via charge neutralization within a finite range of protein concentrations [13–15,17,24,40–45]. These destabilized particles undergo flocculation via either Brownian motion, fluid shear, or differential sedimentation[46]. Particles less than 200 nm will flocculate via Brownian motion, where particles collide from random thermal motion; particles 200 nm – 500 μm will flocculate via fluid shear, where particles collide because of a velocity gradient; and particles greater than 500 μm will flocculate via differential sedimentation, when particles collide because of varying rates of settling[47].

Several research groups have studied the coagulation activity of *Moringa oleifera* proteins. The aforementioned procedure used to extract proteins by communities in developing nations is typically used for coagulation studies in laboratory settings[11–18,21,41]. Variations in this procedure include removing fatty acids from the crushed seeds using an organic solvent and extracting proteins using a salt solution or various solvents [19,20,24,25,34,36,44,45,48–57]. Ion exchange has been employed to remove excess dissolved organic carbon in the form of non-cationic proteins [24,25,32,34,37,44,48,50,52–57]. It has also been used to isolate individual cationic protein fractions or various combinations of cationic protein fractions [25,32,37,52,57]. These studies used dissimilar chromatographic and micro-coagulation assay conditions, and therefore reported different fractions with varying levels of coagulation activity. The cationic proteins have been found to reduce water turbidity 50-99.5% depending on initial turbidity[11–22].

In Chapters 4 and 5, coagulation activities were determined with a micro-coagulation assay validated in Chapter 3. The standard method for testing coagulation activity for water treatment purposes is the jar test. However, jar tests are not practical when large amounts of the experimental coagulant are unavailable. Micro-coagulation assays that implement volumes on the order of microliters to a few milliliters have been used to conserve and to examine the turbidity reduction capabilities of *M. oleifera* cationic proteins [25,33,38,58,59]. Yet, the correspondence between coagulation micro-assays and jar tests has not been established. The conditions under which the jar test and the coagulation micro-assay yield similar values for useful characteristics such as the critical coagulation concentration and the most effective coagulant dosage are identified here in Chapter 3.

Aqueous extracts from *M. oleifera* seeds consist of various cationic proteins, non-cationic proteins, and other water-soluble compounds [8,19,25,32,48], and it is currently unknown if these component interactions have antagonistic or synergistic impacts on coagulant performance. Therefore, a systematic evaluation of the coagulation activities of extracts with varying levels of purification is needed to determine the protein fraction or combination of fractions that has high coagulation activity at low concentrations. This would establish whether a simple fractionation technology should be developed to eliminate inactive fractions and minimize the dissolved organic carbon added to water. In Chapter 4, a variation of the high pressure liquid chromatography procedure of Gassenschmidt *et al.* (1995) was employed, and eight cationic protein fractions were isolated from an extract from seeds from which fatty acids had been removed. Select fractions were characterized using SDS-PAGE, dynamic light scattering, and circular dichroism. Coagulation activity was examined against kaolin in model freshwaters with four different levels of hardness to determine how electrolyte composition would affect

coagulant performance. The coagulative activities of the four most abundant of these fractions were tested individually as well as three combinations of various cationic fractions. Two unfractionated protein extracts were also tested, one where fatty acids had been removed from the seeds and the other where fatty acids had been left intact.

The coagulation activity of *M. oleifera* proteins has been tested on natural water sources [8,10,11,15,17,20,36,40,50,51,53,56,60–62] and on model freshwaters, including kaolin in deionized or distilled water [13,14,41,42,63], kaolin in tap water [19,24,25,44,45,48,52,57], kaolin in Environmental Protection Agency (EPA) model freshwaters of varying hardness [43], humic acid in deionized water [12], and mixtures of kaolin and humic acid in distilled water [55]. In this last study, Santos and co-workers [55] examined the effects of protein purification, pH, and kaolin concentration on the clarification of kaolin-humic acid mixtures prepared in distilled water, for a fixed humic acid concentration. They also conducted electrophoretic mobility measurements of humic acid, kaolin, their *M. oleifera* protein extract, and a humic acid mixture with the protein extract at various pHs while holding the concentrations of all constituents constant. Since natural waters will vary widely in hardness and natural organic matter content, in the current study we examine the effects of water hardness and humic acid concentration on kaolin removal in EPA model freshwaters in Chapter 5. We complemented these findings with dynamic light scattering and electrophoretic mobility measurements of kaolin, humic acid, and a mixture of the two, all with *M. oleifera* proteins at various concentrations, to probe the effects of humic acid on the coagulation mechanism and effectiveness of the *M. oleifera* proteins.

The purpose of coagulation studies in model waters is to reveal the mechanistic roles of different system components that are likely to be important in complex, highly variable natural water sources. An important aspect of such model studies is to systematically introduce multi-

component interactions that would exist in natural waters. *M. oleifera* proteins adsorb to suspended clay colloids, such as kaolin, and induce coagulation via charge neutralization within a finite range of protein concentrations [13–15,17,24,40–45]. In addition, these proteins are electrostatically driven to bind to natural organic matter, such as humic acids, which are primarily negatively charged. The presence of both suspended clay colloids and natural organic matter sets up a competition between protein adsorption to the clay and protein complexation with the natural organic matter. In addition, humic acids may adsorb to the weakly positively charged faces of the kaolin colloids [64] and contribute to their colloidal stability. Here, the influence of these competitive interactions on the effective concentration range for kaolin coagulation by *M. oleifera* seed proteins is determined by varying humic acid concentration in model freshwaters with varying hardness. By altering the strength of electrostatic interactions, increasing water hardness alters the adsorption of *M. oleifera* seed proteins to oppositely charged surfaces [65] and is expected to significantly influence the effects of humic acid on *M. oleifera* protein-induced coagulation of kaolin.

1.2.3. Moringa oleifera protein adsorption to silica

Adsorption of *M. oleifera* seed proteins to silica surfaces has yet to be extensively studied. Kwaambwa *et al*.[66] used neutron reflectometry with a silicon crystal (111 plane) to construct an adsorption isotherm for cationic *M. oleifera* proteins extracted from seeds from which fatty acids had been removed. This isotherm reached a surface excess concentration plateau of 5.7 mg/m^2 at a 250 µg/mL bulk protein concentration. Their findings suggested multilayer adsorption for the cationic protein fraction studied. The extent to which varying levels of *M. oleifera* extract purification affect adsorption to silica, the main constituent of sand, under various water conditions has yet to be studied. In Chapter 6, we used ellipsometry to construct

adsorption isotherms for the proteins on the native oxide layer on silicon wafers, a model silica surface. The following five protein extract/model source water cases were examined: 1) all-water-soluble proteins, with fatty acids removed, in EPA model hard freshwater; 2) all-water-soluble proteins, with fatty acids removed, in EPA model soft freshwater; 3) all-water-soluble proteins, with fatty acids removed, in deionized water; 4) cationic proteins, with fatty acids, in deionized water and 5) cationic proteins, with fatty acids removed, in deionized water. With these adsorption isotherms, we were able to determine whether non-cationic species play a significant role in the creation of f-sand. We also determined whether fatty acid removal prior to protein extraction affects the adsorption of the proteins. The latter is an important practical issue, as oil removed from the seeds is commonly sold as a commodity before using the seeds to treat drinking water[10]. Finally, by comparing model freshwaters, we determined what effects should be anticipated for variations in local water source hardness.

In addition to ellipsometry, we used the rotating disk streaming potential method[67,68] to measure zeta potential isotherms for the aforementioned cases. These measurements identified the protein concentration at which the silica surface undergoes charge reversal from net anionic to net cationic. Since the cationic character of the f-sand filter material is critical for solids removal and antimicrobial potency, these results will assist in determining the minimum protein concentration required to produce effective f-sand and enable the design of simple water treatment beds that conserve the *M. oleifera* seed resource. Finally, we showed that rinsing with a concentrated sodium chloride solution desorbs the proteins from the silica surfaces, providing a simple method for regenerating f-sand. We address the influences of water hardness and of different modes of protein fractionation that may impact the manner in which these protein extracts are deployed for drinking water treatment systems.

In Chapter 7, we studied the effects of water hardness on *M. oleifera* protein adsorption to sand granules, the composition of the adsorbed protein layer on f-sand granules, and the influence of layer composition on f-sand filter efficiency. Four f-sands with differing amounts of adsorbed protein were created by exposing various quantities of sand to similar aliquots of protein solution containing all-water-soluble proteins extracted from defatted seeds. In Chapter 6, we showed that this protein solution, in both EPA model soft and hard freshwater, adsorbs the most mass to silica surfaces[65]. The supernatants of the protein solutions exposed to these different quantities of sand were collected, concentrated, and fractionated using a cation exchange column and high performance liquid chromatography. Three fractions were collected from the supernatants: the non-cationic flow-through, a fraction containing moderately cationic species, and a fraction containing highly cationic species. These fractions were quantified to determine the composition of the adsorbed protein layer on the f-sands as well as the percent of each fraction adsorbed to the sand granules. It was found that the non-cationic fraction is a negligible component of the adsorbed protein layer for all sand-protein ratios in both soft and hard water. The highly cationic species were the more prevalent fraction in the adsorbed protein layer for the highest protein-sand ratio in both waters. In soft water, the moderately cationic species were the most abundant component in the adsorbed protein layer for the three lowest protein-sand ratios whereas in hard water, the highly cationic species were the most abundant component for these f-sands. In both soft and hard water, the highly cationic fraction has a higher adsorption affinity to sand granules than the moderately cationic fraction.

In Chapter 6, we found that low protein surface coverage on silica surfaces causes charge reversal from negative to positive[65]. *M. oleifera* protein activity as a coagulant and an antimicrobial has been attributed to its positive charge[38]. Therefore f-sand filters were created

using different sand-protein ratios to manipulate adsorbed protein surface coverage and determine if f-sand created with a low protein-sand ratio (low coverage) would be as effective as a filter created using a high protein-sand ratio (high coverage). The four f-sands were packed into disposable chromatography columns to create filters. These filters were tested against humic acid, kaolin, and a mixture of the two in both soft and hard water. It was found that the four f-sand filters performed similarly under all conditions studied, confirming that low protein coverages are sufficient to produce effective f-sand for use in potable water treatment. This finding is very significant, as using dilute solutions to create f-sand would conserve seed protein resource and reduce the amount of natural organic matter in contact with treated drinking water. The latter would reduce residual microbe growth and extend the shelf life of drinking water treated with *M. oleifera* proteins.

1.2.4. Sand filtration

Sand filtration is used to remove particulate matter and natural organic matter from turbid water[69]. The two most prevalent types of gravity sand filtration are slow sand filtration and rapid filtration. In slow sand filtration, the filter granular media is less uniform in size, creating void spaces that are smaller than the particles being filtered. For this reason, straining is the mechanism by which particulates are removed, and particulate destabilization prior to filtration is unnecessary. These particles are retained within the top few centimeters of the bed. The filter bed typically never reaches breakthrough. When water ceases to flow through the filter, the top several centimeters are scraped away. Slow sand filtration works best against waters with turbidity less than 50 NTU with little to no colloidal clay[69].

In rapid filtration, the filter granular media is more uniform in size than is typically found in nature, creating void spaces that are significantly larger than the particles being filtered[69]. For

this reason, straining is not the mechanism by which particulates are removed. Instead, particulates in turbid water are destabilized using a coagulant to eliminate electrostatic repulsions between particulates and filter media to allow them to adhere to filter grains or previously adsorbed particles. Particles are removed from water throughout the entire depth of filter bed. The filter bed is regenerated through a backwash stage, wherein water flows in the opposite direction to remove particulates retained by the filter. Rapid filtration is effective against a wide range of turbid waters given that the water is properly pretreated before filtration[69].

F-sand filters will have characteristics of both slow sand filters and rapid filters. The granular media used to construct f-sand filters will consist of natural sand sources and will therefore be polydisperse in size, similar to slow sand filters. By functionalizing sand with *M. oleifera* proteins, the electrostatic repulsions between particulates and media will be eliminated. This will allow particulates to adhere to the media, which is the mechanism used in rapid filters.

1.3. Dissertation objectives

This dissertation aims to study the fundamentals behind the development of *M. oleifera* proteins as bulk coagulants and their incorporation into the f-sand filter, namely how protein purification and environmental factors affect the ability of *M. oleifera* proteins to act as coagulants and to adsorb to silica surfaces (sand). The first objective was to validate the micro-coagulation assay, which is a scaled-down version of a jar test. Jar tests are the standard method used in drinking water treatment plants to determine effective coagulant dosages. Because our *M. oleifera* protein supply was limited, we needed a method that could predict effective protein coagulant dosages using as little material as possible.

The second objective was to determine the effects of protein purification and environmental factors on the coagulation activity of *M. oleifera* proteins using suspensions of kaolin to model turbid water. Protein purification included the removal of fatty acids from seeds before protein extraction and fractionation via a cation exchange column and high performance liquid chromatography (HPLC). The removal of fatty acids was examined because people in developing nations often remove the oil from seeds prior to water treatment usage and sell it as a commodity. We wanted to confirm that this practice would not interfere with the efficacy of the proteins as coagulants. Fractionation was employed to examine if protein coagulant efficacy would be improved or remain unaffected with the removal of non-cationic species. Removing inactive organic matter would reduce the amount of organic matter in treated water, which allows for the growth of residual microorganisms. Environmental factors that could affect the coagulation activity of *M. oleifera* proteins include water hardness and natural organic matter. Micro-coagulation assays were conducted in model freshwaters created according to recipes supplied by the Environmental Protection Agency. Varying concentrations of humic acid were added to turbid waters containing kaolin clay to model natural organic matter in natural water sources.

The third objective was to determine the effects of protein purification and water hardness on the ability of *M. oleifera* proteins to adsorb to silica surfaces. We wanted to confirm that proteins would be able to adsorb to silica from waters with ionic strengths indicative of natural water sources. Additionally, we wanted to investigate how unfractionated and cationic protein fractions would interact with silica surfaces, namely in terms of mass adsorbed and extent of charge reversal.

The fourth objective was to determine how water hardness and the protein-to-sand ratio in the creation of f-sand affect the composition of the adsorbed protein layer on silica sand granules and then to determine whether the adsorbed layer composition had a significant effect on the performance of f-sand filters.

1.4. Outline of dissertation

Chapter 1 gives an introduction to *Moringa oleifera* and its use in drinking water treatment. Motivation for this thesis is given, as well as background on the research question and dissertation objective.

Chapter 2 is a compilation of materials and methods used in the subsequent five chapters. Materials are listed in alphabetical order by company. Applicable chapters are indicated for each method.

Chapter 3 presents the validation of the micro-coagulation assay employed in Chapters 4 and 5 in place of the commonly used jar test. It was shown that a micro-coagulation assay will yield the same results in terms of critical coagulation concentration and effective concentration range. This work has been published in the *Journal of Environmental Chemical Engineering*: Nordmark, B. A.; Przybycien, T. M.; Tilton, R. D. Comparative coagulation performance study of *Moringa oleifera* cationic protein fractions with varying water hardness. *J. Environ. Chem. Eng.* **2016**, *4* (4A), 4690–4698.

Chapter 4 is focused on the effects of fatty acid removal, protein fractionation, and water hardness on the ability of *M. oleifera* proteins to induce flocculation in kaolin clay. It was shown that the removal of fatty acids does not have an effect on efficacy, that the unfractionated protein extract was most effective at inducing flocculation, and that increasing water hardness broadens

the effective range of coagulating protein concentrations. This work has been published in the *Journal of Environmental Chemical Engineering*: Nordmark, B. A.; Przybycien, T. M.; Tilton, R. D. Comparative coagulation performance study of *Moringa oleifera* cationic protein fractions with varying water hardness. *J. Environ. Chem. Eng.* **2016**, *4* (4A), 4690–4698.

Chapter 5 addresses the effects of humic acid concentration and water hardness on the ability of *M. oleifera* proteins to induce flocculation in kaolin clay. For mixtures of kaolin and humic acid, it was shown that as humic acid concentration increases, the critical coagulation concentration increases, and the range of coagulating protein concentrations broadens. Additionally, as water hardness increases, the critical coagulation concentration decreases, and the range of coagulating protein concentrations broadens. This work has been submitted in the manuscript titled "Effect of humic acids on kaolin coagulation performance of *Moringa oleifera* proteins" to the *Journal of Environmental Chemical Engineering* (2018) by Brittany A. Nordmark, Todd M. Przybycien, and Robert D. Tilton.

Chapter 6 discusses the effects of fatty acid removal, protein fractionation, and water hardness on the ability of *M. oleifera* proteins to adsorb to silica surfaces. It was shown that fatty acids had no effect on the adsorption of proteins to silica, unfractionated protein fractions adsorb more mass to silica than cationic protein fractions, and cationic protein fractions cause a higher charge reversal of silica than unfractionated protein fractions. Additionally, mass of adsorbed proteins increases with water hardness, but charge reversal from negative to positive decreases as water hardness increases. This work was published in *Langmuir:* Nordmark, B. A.; Bechtel, T. M.; Riley, J. K.; Velegol, D.; Velegol, S. B.; Przybycien, T. M.; Tilton, R. D. *Moringa oleifera* seed protein adsorption to silica: Effects of water hardness, fractionation, and fatty acid extraction. *Langmuir* **2018** , *34* (16), 4852–4860.

Chapter 7 examines the effect of water hardness on the composition of the adsorbed layer of unfractionated *M. oleifera* proteins to silica sand granules. This work is part of a manuscript in preparation titled "Selective adsorption of *Moringa oleifera* proteins to quartz sand granules and its role in functionalized sand filter performance" by the authors Brittany A. Nordmark, Todd M. Przybycien, and Robert D. Tilton.

Chapter 8 gives a summary of the conclusions from Chapters 3-7 as well as a discussion of original contributions from this dissertation and future work for the research project.

Chapter 2: Materials and Methods

2.1. Materials

For Chapter 4, *Moringa oleifera* seeds from Nicaragua and Thailand were supplied by Stephanie Velegol at the Pennsylvania State University. For Chapters 5-7, *Moringa oleifera* seeds from Nigeria were purchased through Paisley Farm and Crafts (Paisley, FL). Mini-PROTEAN® TGX™ Precast Protein Gels 4–20% (4561096S), Mini-PROTEAN® Tris-Tricine Gels 10–20% (4563116), 10x Tris/Glycine Buffer for Western Blots and Native Gels (1610734), 2x Laemmli Sample Buffer (1610737), 10x Tris/Tricine/SDS Running Buffer (1610744), Tricine Sample Buffer for Protein Gels (1610739), 2-mercaptoethanol (1610710), Precision Plus Protein™ Kaleidoscope™ Prestained Protein Standards (1610375), and plastic Econo-Pac chromatography columns (7321010) were purchased from Bio-Rad Laboratories, Inc. (Hercules, CA). Sodium bicarbonate (144-55-8) was purchased from EMD Millipore, Inc. (Billerica, MA). Pahokee Peat humic acid standard (1S103H) was purchased from International Humic Substances Society (St. Paul, MN). Silicon wafers were purchased from International Wafer Services, Inc. (Colfax, CA). One thousand Dalton molecular weight cut-off (MWCO) Microcep and Macrocep centrifugal filters (MCP001C46, MAP001C37) were purchased from Pall Corp. (Port Washington, NY). Kaolin clay (K7375), aluminum potassium sulfate dodecahydrate (alum) (237086), 50-70 mesh particle size white quartz sand (274739), sodium phosphate monobasic (S0751), sodium phosphate dibasic (S0876), calcium sulfate dihydrate (C-7411), magnesium sulfate (M2643), potassium chloride (20,800-0), NoChromix (328693), and acetic acid (A6283) were purchased from Sigma-Aldrich, Inc. (St. Louis, MO). A Pierce® 660 nm Protein Assay kit (22662), Coomassie Blue R-250 (BP101), sodium hydroxide (UN1823), RBS 35 detergent concentrate (27952), Nalgene™ Rapid-Flow™ 0.2 µm filters (595-4520), and medium porosity

(9 µm) filter paper (09-801A) were purchased from Thermo Fisher Scientific (Pittsburgh, PA). Clear bottom 96-well plates (89091-010), isopropyl alcohol (67-63-0), hydrochloric acid (BDH7204-1), petroleum ether (470301-956, boiling point 20-75 °C), 0.2 µm cellulose acetate syringe filters (28145-477), and 0.2 µm polyethersulfone syringe filters (28145-501) were purchased from VWR International, LLC (Radnor, PA). A BioSuite™ SP Cation-exchange Column (186002184) was purchased from Waters Corp (Milford, MA). Water was purified to 18 MΩ-cm resistivity by reverse osmosis followed by passage through a Thermo Fisher Barnstead Nanopure Diamond lab water system. All experiments were conducted at room temperature, approximately 22°C.

2.2. Methods

The following section contains all methods for Chapters 3-7.

2.2.1. Model turbid freshwater

Model freshwaters of varying hardness were created using the Environmental Protection Agency (EPA) recipes shown in Table 2.1[70].

Table 2.1. Model freshwaters based on Environmental Protection Agency recipes[70].

Water type	Ionic strength (mM)	pH	$NaHCO_3$ (mg/L)	$CaSO_4 \cdot 2H_2O$ (mg/L)	$MgSO_4$ (mg/L)	KCl (mg/L)
Deionized[a]	0	6.4-6.5	0	0	0	0
Diluted soft[b]	1.15	7.0-7.4	24	15	15	1
Soft	2.29	7.2-7.6	48	30	30	2
Moderately hard	4.58	7.4-7.8	96	60	60	4
Hard	9.17	7.6-8.0	192	120	120	8

[a] Deionized is obtained directly from the Barnstead water purification system with no additives. pH was measured in the laboratory.

[b] Diluted soft water is not an EPA model freshwater. It is simply a two-fold dilution of EPA model soft water. pH range for diluted soft water was interpolated from EPA data.

Model turbid water was created by adding kaolin (Chapter 3: 0.4 g/L Chapters 4-5: 1 g/L; Chapter 7: 0.05 g/L) humic acid (Chapter 5: 5, 10 and 20 ppm; Chapter 7: 5 ppm), or kaolin and humic acid (Chapter 5: 1 g/L kaolin with either 5, 10, 20 ppm humic acid; Chapter 7: 0.05 g/L kaolin with 5 ppm humic acid) to the appropriate model freshwater (Chapter 3: deionized water; Chapter 4: all five model waters; Chapter 5: all five model waters; Chapter 6: deionized, soft, and hard water; Chapter 7: soft and hard water).

2.2.2. Protein extraction

For Chapters 4-7, The protein extraction procedure was adapted from Jerri et al. (2012). Seeds were shelled and then crushed using a mortar and pestle. For certain samples, fatty acids were removed by adding crushed seeds to petroleum ether at a concentration of 10 mg/mL and mixing for 1 h using an Argos RotoFlex™ Plus Tube Rotator. The crushed seeds were separated from the petroleum ether and allowed to dry under vacuum before being added to either 10 mM phosphate buffer pH 7.5 (Chapters 4-6), EPA model soft water (Chapter 7), or EPA model hard water (Chapter 7) at a concentration of 10 mg/mL and mixing for 1 h. For samples with fatty acids, the crushed seeds were immediately mixed with buffer or model water as described above without the petroleum ether extraction step. The supernatant was then either filtered through filter paper and a 0.2 µm polyethersulfone syringe filter or filtered through a Nalgene™ Rapid-Flow™ 0.2 µm filter to remove particulate matter.

2.2.3. Transfer of proteins to appropriate model freshwater

For Chapters 4-6, proteins extracted using 10 mM phosphate buffer were transferred into the appropriate model freshwaters by first concentrating filtered solutions for 1 h using 1,000 MWCO centrifugal filters at 3,220 ×g to less than 1 mL. This concentrate was then diluted to 5

mL with either deionized water, model soft freshwater, or model hard freshwater and concentrated again to less than 1 mL. This cycle was repeated five times to exchange the extracted proteins into each of the model waters. Protein samples in Chapter 7 were extracted directly using soft and hard water and therefore did not need to be transferred.

2.2.4. Preparative high pressure liquid chromatography

Moringa oleifera cationic protein fractions were prepared via preparative chromatography using a Waters Alliance Separations Module HPLC system (model 2690) equipped with a Waters Photodiode Array Detector (model 996) for UV absorbance detection at 280 nm. Various salt gradients were used to elute desired fractions from the BioSuite™ SP cation-exchange column (7.5 × 75 mm) depending on the application. Buffer A was 10 mM phosphate buffer pH 7.5, and buffer B was 2 M sodium chloride in buffer A. The elution flow rate was 1 mL/min.

2.2.4.1. Collection of fractionated cationic proteins

For Chapter 4, eight individual protein fractions were collected. *Moringa oleifera* protein solution was concentrated to less than 1 mL using 1,000 MWCO centrifugal filters and injected onto the cation-exchange column. Proteins were eluted using a piecewise linear gradient: 0% B from 0-10 minutes and then 0-65% B from 10-114 minutes. Cationic protein fractions were collected and subsequently concentrated to less than 1 mL using the centrifugal filters. The concentrated fractions were desalted by diluting with 5 mL of model freshwater and re-concentrating to less than 1 mL five times. This cycle was repeated five times in the centrifugal filters.

2.2.4.2. Collection of all cationic proteins and non-cationic proteins

For Chapter 6, cationic proteins were collected as one fraction. *Moringa oleifera* protein solution was concentrated to less than 1 mL using 1,000 MWCO centrifugal filters and injected onto the cation-exchange column. Proteins were eluted using a piecewise linear gradient: 0% B from 0-10 minutes and then 65% B from 10-45 minutes. The cationic proteins were collected and subsequently concentrated to less than 1 mL using the centrifugal filters. The concentrated proteins were desalted by diluting with 5 mL of model freshwater and re-concentrating to less than 1 mL five times. Non-cationic proteins, operationally defined as proteins not retained by the cation-exchange column, were collected from the flow-through for injected protein samples.

2.2.4.3. Collection of low and high cationic protein fractions

For Chapter 7, three fractions were collected: the non-cationic flow-through (operationally defined as proteins not retained by the cation-exchange column), a fraction of moderately cationic species, and a fraction of highly cationic species. *Moringa oleifera* protein solution was concentrated to less than 1 mL using 1,000 MWCO centrifugal filters and injected onto the cation-exchange column. A piecewise step gradient was used to collect these fractions: 0% B from 0-10 minutes to collect the non-cationic flow through, 40% B from 10-30 minutes to collect the moderately cationic fraction, and 65% B from 30-50 minutes to collect the highly cationic fraction. Protein fractions were collected and subsequently concentrated to 0.5 mL using 1,000 MWCO centrifugal filters. Protein concentration was determined using the Pierce® 660 nm Protein Assay and was used to establish the composition of the adsorbed protein layer.

2.2.5. Determination of protein concentration

The Pierce® 660 nm Protein Assay was used to determine the protein concentration of the resulting *M. oleifera* protein solutions. This assay uses bovine serum albumin (BSA) standard solutions for calibration and has a protein-to-BSA variation in color response ratio of 0.7364, meaning that on average, the assay under-reports protein concentration by approximately 26% [71]. Concentrations determined from the BSA standards were therefore adjusted by this ratio.

2.2.6. Jar tests

For Chapter 3, a Phipps & Bird Gang Stirrer was used to conduct the jar tests. The jar test procedure employed was provided by the PPG Industries Colloids, Polymers and Surfaces Laboratory at Carnegie Mellon University. A 200 mg/L suspension of kaolin (approximately 320 NTU) in a 140 mg/L sodium bicarbonate solution was used to model high turbidity water. The sodium bicarbonate produced an equivalent alkalinity of 84 mg/L calcium carbonate. Six 600 mL beakers were placed under the impellers of the gang stirrer. Varying alum dosages were added to turbid water to produce 300 mL sample volumes with 200 mg/L suspended kaolin and alum concentrations ranging from 0.5 to 1500 ppm. The suspensions were mixed at 85 rpm for 30 seconds, then at 60 rpm for 15 min. After 15 min, the gang stirrer was turned off, and the suspensions were allowed to settle for either 0.25, 1.0, or 3.0 h. After the settling time had been reached, a volumetric pipette was used to collect a 15 mL sample from the center of each jar. Sample turbidities were measured in NTU using a Hach 2100P Portable Turbidimeter. Aliquots of 150 µL of each sample were then pipetted into clean wells of a 96-well plate, and the optical density at 660 nm (OD_{660}) was measured using a SpectraMax M2 plate reader. The NTU readings were plotted against the OD_{660} measurements to create a calibration curve to convert OD_{660} measurements from the micro-coagulation assay with alum to NTU.

2.2.7. Micro-coagulation assays

Assays were conducted in clear-bottom 96-well plates. Aliquots of 150 µL of turbid water were added to wells in the plate followed by aliquots of 150 µL of protein solution at various concentrations. The well plate was shaken on a Corning LSE™ Digital Microplate Shaker (6780-4) at 500 rpm for 15 min, and turbid water samples were allowed to settle. After the settling time had been reached, 150 µL of supernatant was pipetted from just under the liquid surface from each well and dispensed into clean wells. A SpectraMax M2 plate reader was used to measure the OD_{660} of the supernatants.

2.2.7.1. Alum as a coagulant

For Chapter 3, a 0.4 mg/L kaolin suspension with 280 mg/L sodium bicarbonate in deionized water was used to model turbid water. Varying alum dosages in deionized water were added to each well containing kaolin suspension to prepare 300 µL samples with 0.2 g/L kaolin, 140 mg/L sodium bicarbonate and 0.5 to 1500 ppm alum, matching the jar test conditions. The samples were allowed to settle for either 0.25, 1.0, or 3.0 h.

2.2.7.2. Moringa oleifera proteins as a coagulant

For Chapter 4, 1 g/L kaolin suspensions in each of the five EPA freshwaters were used to model turbid water. This high turbidity was used to provide a stringent test for the coagulation activity of the protein fractions. Varying *M. oleifera* protein dosages in each of the five model freshwaters were added to each well containing kaolin suspension to prepare 300 µL samples with 0.5 g/L kaolin and 1-20 µg/mL protein. The samples were allowed to settle for 3.0 h.

For Chapter 5, model turbid water contained either 1 g/L kaolin; 5, 10 or 20 ppm humic acid; or 1 g/L kaolin with 5, 10, or 20 ppm humic acid. These turbid waters were in each of the

five EPA freshwaters. Varying *M. oleifera* protein dosages in each of the five EPA freshwaters were added to each well containing model turbid water to prepare 300 µL samples with either 0.5 g/L kaolin and 2.5-30 µg/mL protein; 2.5, 5, or 10 ppm humic acid and 2.5-250 µg/mL protein; or 0.5 g/L kaolin, 2.5, 5, or 10 ppm humic acid, and 2.5-250 µg/mL protein. The samples were allowed to settle for 3.0 h.

2.2.8. Sodium dodecyl sulfate-polyacrylamide gel electrophoresis (SDS-PAGE)

For Chapter 4, Bio-Rad 4–20% Mini-PROTEAN® TGX™ Precast Protein Gels were used to estimate the molecular weights of the native protein fractions, and Bio-Rad 10–20% Mini-PROTEAN® Tris-Tricine Gels were used to estimate the molecular weights of reduced protein fractions. The TGX™ gels were run in Bio-Rad 10x Tris/Glycine Buffer for Western Blots and Native Gels, and samples were loaded in Bio-Rad 2x Laemmli Sample Buffer. The Tris-Tricine gels were run in Bio-Rad 10x Tris/Tricine/SDS Running Buffer, and samples were loaded in Bio-Rad Tricine Sample Buffer for Protein Gels and 2-mercaptoethanol (5% by volume of loaded sample). Bio-Rad Precision Plus Protein™ Kaleidoscope™ Prestained Protein Standards were used as a molecular weight ladder. Each sample lane was loaded with 0.6 µg of protein fraction. The gels were run at 150 V until the sample front had passed through the gel, approximately 45 minutes. Gels were then fixed in a solution of 25% isopropyl alcohol and 10% acetic acid in water for 1 hour, stained in a solution of 10% acetic acid in water with 60 mg/L Coomassie Brilliant Blue R-250 for 1 h, and allowed to de-stain in a solution of 10% acetic acid in deionized water for 1-3 h.

2.2.9. Circular dichroism

For Chapter 4, a Jasco J-810 Spectropolarimeter was used to examine the secondary structure of select fractions at concentrations of 500 µg/mL. Samples were loaded into a 1 mm quartz cuvette and five spectra were recorded across the wavelength range of 190 to 260 nm at 0.1 nm intervals and averaged. The scanning speed was 200 nm/min with a band width of 1 nm.

2.2.10. Electrophoretic mobility and dynamic light scattering

For Chapters 4-5, electrophoretic mobility and dynamic light scattering measurements were made on kaolin suspensions, humic acid solutions, and kaolin-humic acid mixtures using a Malvern Zeta-sizer Nano Series Nano Z-S. These measurements provided zeta potential and hydrodynamic radius of the aforementioned species (Chapters 4-5) as well as for kaolin suspension with *Moringa oleifera* proteins (Chapter 4) and kaolin-humic acid mixtures with *Moringa oleifera* proteins (Chapter 5). Zeta potential was calculated from the electrophoretic mobility using the Smoluchowski approximation for Henry's function[72].

2.2.11. Adsorption substrate preparation

For Chapter 6, silicon wafers with a 2 nm thick native oxide layer were used for adsorption experiments with ellipsometry. The wafers were cut into 1 cm^2 squares using a carbide-tipped pen. The wafers were cleaned as follows: soaking in RBS 35 detergent for five minutes, in sulfuric acid with NoChromix for 20 minutes, in 6 N hydrochloric acid for 20 minutes, and in 10 mM sodium hydroxide for 30 minutes. The wafers were rinsed with copious amounts of deionized water between steps. Substrates were stored in deionized water and used within 24 hours of cleaning.

2.2.12. Ellipsometry

For Chapter 6, the surface excess concentration of protein adsorbed to the native silicon dioxide (silica) layer on silicon wafers was measured in-situ using phase-modulated ellipsometry (Picometer Ellipsometer, Beaglehole Instruments). The ellipsometer was equipped with a 632.8 nm HeNe laser. The angle of incidence was scanned between 71° and 72° near the water/silicon Brewster angle, which is where ellipsometry is most sensitive to interfacial films.

2.2.12.1. Protein adsorption to silicon wafers

Silicon wafer squares were placed in a Petri dish filled with 30 mL of deionized water. Previously described light guides[73] similar to those of Benjamins *et al*.[74] were used to bypass the air/water interface to probe the silica/water interface. A multi-angle scan of each wafer in deionized water was conducted to confirm the silicon oxide layer thickness. The wafers were then moved while wet to individual Petri dishes, and 30 mL of the desired protein solution were added to each Petri dish. Multi-angle scans were recorded at 1 h, 3 h, and 5 h adsorption time points to ensure that protein adsorption had equilibrated by 5 h.

The protein surface excess concentration was determined from the effective optical thickness of the adsorbed layer, $d_{avg}(n_{avg}-n_0)$, where d_{avg} and n_{avg} are the optical average thickness and refractive index of the adsorbed protein layer, and n_0 is the refractive index of the bulk solution. TFCompanion software (Version 3.0, Semicon Software Inc.) was used to fit the thickness of the protein layer numerically using a homogeneous, four-layer optical model: semi-infinite silicon, silicon dioxide, adsorbed protein, and semi-infinite water layers with refractive indices of 3.882 + 0.019i, 1.457, 1.450 (by assumption)[75], and 1.331, respectively. Error in the assumed protein layer refractive index is compensated by a corresponding error in the fitted

optical average layer thickness, such that the effective optical thickness and protein surface excess concentration are correct to within ~5%[75]. Because the oxide layer thickness was measured prior to protein adsorption, the optical average thickness of the adsorbed protein layer was the only quantity regressed.

The de Feijter Equation[76] was used to determine the surface excess concentration of the adsorbed protein from the effective optical thickness of the layer:

$$\Gamma = \frac{d_{avg}(n_{avg} - n_0)}{dn/dc} \tag{2.1}$$

The refractive index increment *dn/dc* was measured for each of the five protein extract/source water cases studied (Reichert AR7 Series Automatic Refractometer, Reichert Technologies, Depew, NY). The average and standard deviation of the five refractive index increments was 0.19 ± 0.01 cm^3/g, which is within the typical range for protein solutions of 0.18 ± 0.03 cm^3/g [77]. There was no relationship between *dn/dc* and water hardness or the particular type of protein isolate.

2.2.12.2. Protein desorption and re-adsorption to silicon wafers

To measure desorption and re-adsorption of the adsorbed protein layer, an experiment was conducted with a 1 cm^2 wafer square placed at the bottom of a custom-built flow cell (15 mL volume), described previously[73], that allows one solution to be displaced by another. The cell was initially filled with deionized water. After a multi-angle scan to confirm the oxide layer thickness and a time-resolved measurement to ensure a stable baseline, 50 mL of a 50 µg/mL solution of cationic *M. oleifera* proteins with fatty acids in deionized water were pumped through the flow cell at a rate of 0.64 mL/min using a peristaltic pump. This was followed by a deionized

water rinse, then 50 mL of a 0.5 M sodium chloride solution, and finally 50 mL of a 1 M sodium chloride solution. A multi-angle scan was recorded to confirm whether complete protein desorption had been achieved. A time-resolved measurement was initiated before the flow cell was rinsed again with deionized water and another 50 mL of a 50 µg/mL solution of cationic *M. oleifera* proteins with fatty acids in deionized water was pumped through the flow cell to determine if protein would re-adsorb to the silica surface.

2.2.13. Streaming Potential Measurements

Silica surface streaming potential measurements were conducted using a ZetaSpin instrument (Zetamatrix Inc.). The rotating disk apparatus and method of data analysis have been described in detail by Sides and co-workers[67,68]. Circular, 2.54 cm diameter silicon wafers with the native oxide layer were attached to a cylindrical polycarbonate mount and bathed in a 400 mL reservoir of either 0.5 mM sodium chloride, EPA model soft freshwater, or EPA model hard freshwater. The 0.5 mM NaCl solution was used instead of deionized water since a known ionic strength is necessary for reliable interpretation of electrokinetic measurements. The conductivity and pH of each electrolyte solution were monitored. The wafer was then rotated at a rate of Ω = 4000 rpm at five second intervals during which the streaming potential was measured.

The rotating wafer generates a streaming potential ϕ_s along the silica surface that is measured between a silver/silver chloride reference electrode at a distance z = 1 mm from the center of the wafer surface and a silver/silver chloride electrode far from the disk in the electrolyte reservoir. After obtaining a stable bare substrate baseline, protein solution was injected into the cell while streaming potential measurements were being recorded, and the adsorption kinetics were monitored. The rotating wafer allowed for well-mixed conditions in the reservoir. The measured streaming potential ϕ_s yields the surface zeta potential ζ, according to[68]:

$$\zeta(z) = \frac{1.96\phi_s\kappa_i\sqrt{\frac{\nu}{\Omega^3}}}{\varepsilon a\left(\frac{1-2\bar{z}\sqrt{1+\bar{z}^2}+2\bar{z}^2}{\sqrt{1+\bar{z}^2}}\right)} \quad (2.2)$$

The parameters κ_i, ν, ε, and $\bar{z}$ are the bulk solution ionic conductivity, kinematic viscosity, dielectric constant, and electrode-surface distance normalized by the disk radius, respectively.

2.2.14. Protein adsorption to quartz sand for composition studies

Quartz sand was measured out in 4, 8, 16, and 32 g quantities and added to 30 mL aliquots of 100 µg/mL protein solution containing all water soluble proteins in either soft water or hard water to create mixtures with 12, 21, 35, and 52% w/w of sand. The protein-sand mixtures were allowed to mix for 3 h using the Argos RotoFlex™ Plus Tube Rotator. For adsorbed layer composition studies, the centrifugal tubes were stood upright to allow the quartz sand to settle and the supernatant was filtered through medium porosity (9 µm) filter paper. The supernatant was then concentrated to less than 1 mL using a 1,000 MWCO centrifugal filter. High pressure liquid chromatography (see Section 2.2.4.3) was used to collect three fractions from the supernatant: the non-cationic flow-through, a fraction containing moderately cationic proteins, and a fraction containing highly cationic proteins. These fractions were quantified to determine the coverage and composition of the adsorbed protein layer on the sand granules.

2.2.15. Bare sand and f-sand filter construction

For both bare sand and f-sand filters, 16 g of quartz sand were added to 30 mL of either soft or hard water. This wetted sand was then transferred to a plastic chromatography column to create a 10 mL bed and rinsed with 15 bed volumes (150 mL) of soft or hard water. For bare sand filters, a 30 µm polyethylene bed support was placed on top of the packed sand to prevent

disturbance. After this step, the bare sand filters were ready for experimentation. For f-sand filters, the 16 g of rinsed sand was distributed between 4, 2, 1, or 0.5 aliquots of 30 mL of 100 µg/mL protein solution in soft water or hard water to create 12, 21, 35, and 52% w/w sand mixtures, respectively. The protein-sand mixtures were allowed to mix for 3 h using the Argos RotoFlex™ Plus Tube Rotator. The f-sand was then returned to the plastic chromatography column and rinsed with 15 bed volumes (150 mL) of soft or hard to remove residual, un-adsorbed proteins and other natural organic matter. A 30 µm polyethylene bed support was then placed on top of the packed sand to prevent disturbance. After this step, f-sand filters were ready for experimentation.

2.2.16. Filtration experiments

Six turbid waters were created to test the performance of the f-sand filters: 5 ppm humic acid, 0.05 g/L kaolin, and a mixture of 5 ppm humic acid and 0.05 g/L kaolin, each in EPA soft and hard water. A metal stand was used to position a separatory funnel above the plastic chromatography column. The capped column was filled with 10 mL of turbid water, and the separatory funnel was filled with 20 bed volumes (200 mL) of turbid water. The separatory funnel was used to maintain 10 mL of turbid water above the column to produce a constant pressure head and volumetric flow rate. Once the column was uncapped to allow flow through the column, successive 1 mL samples were collected and saved for optical density readings. For the bare sand filters, every 1 mL sample was collected for the first 10 mL, and then every tenth 1 mL sample was collected for the next 190 mL. For the f-sand filters, every tenth 1 mL sample was collected for the entire 200 mL. Aliquots of 150 µL of each collected sample were pipetted into a 96-well plate and optical density measurements were taken at 300 nm (instead of 660 nm) to increase sensitivity to turbidity.

Chapter 3: Validation of the micro-coagulation assay

3.1. Introduction

This work has been published in the *Journal of Environmental Chemical Engineering*: Nordmark, B. A.; Przybycien, T. M.; Tilton, R. D. Comparative coagulation performance study of *Moringa oleifera* cationic protein fractions with varying water hardness. *J. Environ. Chem. Eng.* **2016**, *4* (4A), 4690–4698. We utilized an efficient 96 well plate optical density-based micro-coagulation assay to conserve *M. oleifera* proteins. Turbidity reduction results from a conventional jar test using aluminum potassium sulfate dodecahydrate (alum), a standard coagulant, were used to validate the micro-coagulation assay as an accurate scale-down of the jar test. Micro-coagulation assays that implement volumes on the order of microliters to a few milliliters have been used in several studies to examine the turbidity reduction capabilities of *M. oleifera* cationic proteins.[25,33,38,58,59] Yet, the correspondence between micro-coagulation assays that use micro- to low macro-volumes and the larger volume jar tests conventionally used in water treatment plants to evaluate coagulant performance has not been established. To be most useful, micro-coagulation assays should indicate degrees of turbidity reduction and values for both the CCC and the most effective coagulant dosage that are similar to the jar test. This chapter identifies the conditions under which the jar test and the micro-coagulation assay yield similar results, using a kaolin suspension to model turbid water and aluminum potassium sulfate dodecahydrate (alum) as a coagulant.

3.2. Results and Discussion

3.2.1. Jar test and micro-coagulation assay comparison with the kaolin/alum system

It was impractical to use jar tests to determine the coagulation performance of *M. oleifera* protein fractions due to our limited supply of seeds. Micro-coagulation assays, which

use on the order of 10^3 times less material, were better suited for the task. The jar tests and micro-coagulation assays that used alum to clarify a kaolin suspension were performed to determine whether a micro-coagulation assay was a suitable scaled-down substitute for the jar test. Alum is a commonly used coagulant in drinking water treatment plants, inducing flocculation by either sweep flocculation or charge neutralization, depending on pH, coagulant concentration, and particle concentration [46]. When lower alum concentrations are added to water with a high turbidity, aluminum cations destabilize particles through charge neutralization, allowing particles to flocculate when contacting other particles. As alum concentration is increased, particles are re-stabilized, and when alum concentration is increased further, aluminum hydroxide precipitates form and reduce turbidity through sweep flocculation, wherein the precipitates remove particles as they sediment under gravity [46]. As will be shown, there was a range of alum dosages that was able to reduce water turbidity in the jar tests and micro-coagulation assays, but when the alum dosage was increased, the particles were re-stabilized. This behavior suggests that kaolin turbidity was reduced via adsorption and charge neutralization [46], the expected coagulation mechanism of kaolin using *M. oleifera* proteins.

Turbidimeter nephelometric turbidity units (NTU) readings from the kaolin/alum jar test samples were plotted against their corresponding OD_{660} measurements from the SpectraMax M2 plate reader in Figure 3.1. Note that the gap in the data at intermediate NTU/OD_{660} values represents systems that were not colloidally-stable under our experimental conditions. Higher NTUs correspond to stable kaolin suspensions wherein the alum dosage was below the critical coagulation concentration. Lower NTUs correspond to destabilized kaolin suspensions wherein the alum dosage was at or above the critical coagulation concentration. The strong linear correlation between NTU and OD_{660} ($R^2 = 0.9943$) was used to convert OD_{660} measurements

from the kaolin/*M. oleifera* micro-coagulation assays to conventional turbidity units to facilitate direct comparison between jar test and micro-coagulation assay results.

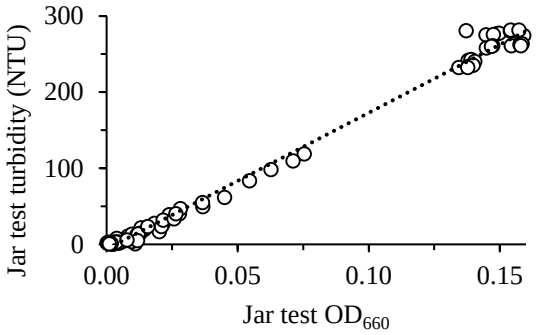

Figure 3.1. Calibration of kaolin suspension turbidity and optical density. The linear least squares regressed calibration line shown (R2 = 0.9943) was used to convert OD660 values to NTU to compare jar tests and micro-coagulation assays. Higher NTUs correspond to stable kaolin suspensions wherein the alum dosage was below the critical coagulation concentration. Lower NTUs correspond to destabilized kaolin suspensions wherein the alum dosage was at or above the critical coagulation concentration

Results for the jar tests and micro-coagulation assays with varying settling times over a range of alum dosages are shown in Figure 3.2. The critical coagulation concentration (CCC) for the jar tests at each settling time were between 5 and 10 ppm alum. The most effective alum dosages for the jar tests for each settling time were between 100 and 200 ppm alum. The CCC values and most effective alum dosages for the jar tests were independent of settling time. The CCC values for the micro-coagulation assays were 50, 20, and 10 ppm alum for 0.25, 1.0, 3.0 h settling times, respectively. The most effective alum dosage for the micro-coagulation assays was 200 ppm alum for 0.25 and 1.0 h, and 100 ppm alum for 3.0 h.

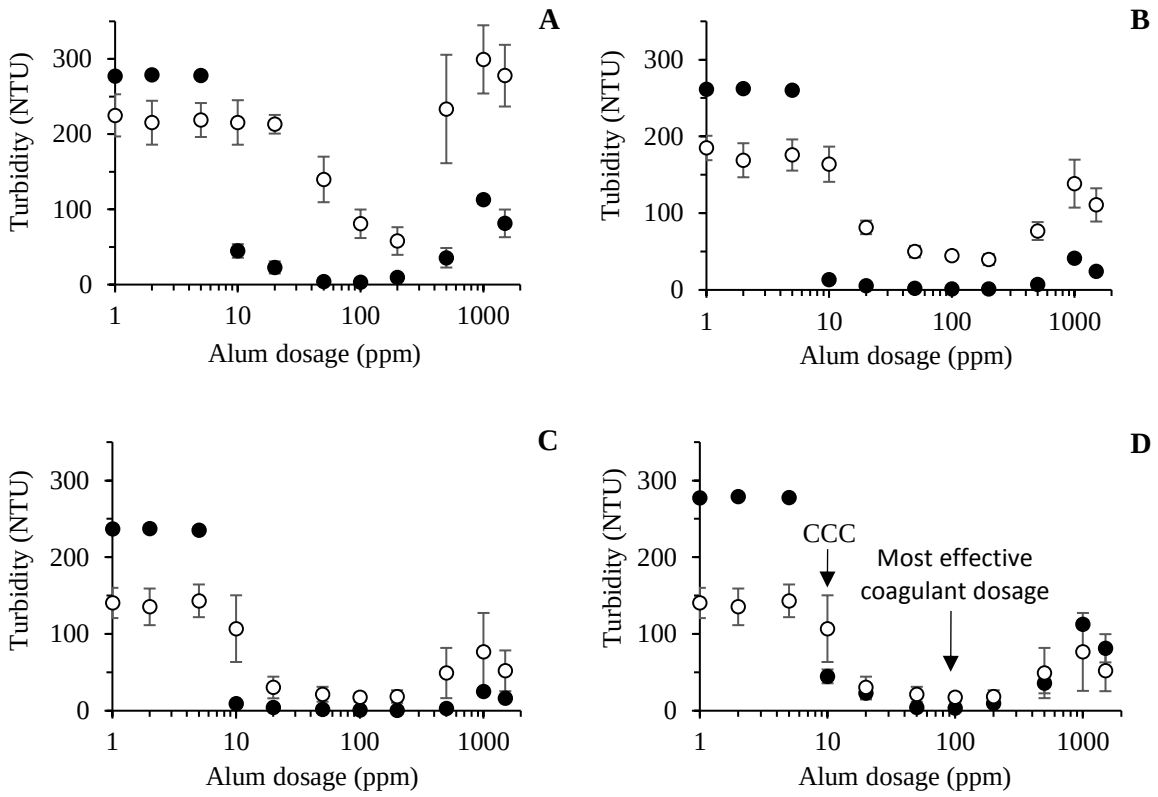

Figure 3.2. Comparison of jar test turbidities (black circles) and micro-coagulation assay calibrated turbidities (white circles) with varying alum dosages for 0.25 h (A), 1.0 h (B), and 3.0 h (C) settling times. The jar test with a 0.25 h settling time indicates the same CCC and most effective dosage as the micro-coagulation assay with a 3 h settling time (D). Error bars represent the standard deviation of three measurements for the jar tests and nine measurements for the micro-coagulation assays. Spearman's rank correlation coefficients for the jar test and micro-coagulation assay turbidities for A, B, C, and D are $\rho = 0.580$ ($P < 0.05$), $\rho = 0.906$ ($P < 0.001$), $\rho = 0.902$ ($P < 0.001$), and $\rho = 0.923$ ($P < 0.001$), respectively.

The jar test and micro-coagulation assay results are strongly correlated: Spearman's rank correlation coefficients for settling times of 0.25 h (Figure 3.2A), 1 h (Figure 3.2B), and 3 h (Figure 3.2C) are $\rho = 0.580$ ($P < 0.05$), $\rho = 0.906$ ($P < 0.001$), and $\rho = 0.902$ ($P < 0.001$), respectively. Using the 0.25 h settling time results for the jar test as a convenient reference, the largest correlation coefficient was found with the micro-coagulation assay with a 3 h settling time (Figure 3.2D), $\rho = 0.923$ ($P < 0.001$). Thus, a 3 h settling time was used for all subsequent

micro-coagulation assays with *M. oleifera* proteins. It should be noted that for all settling times, calibrated micro-coagulation assays turbidities were generally less than jar test turbidities below the alum CCC and generally greater above the CCC. Therefore, it is not recommended that micro-coagulation assays be used to determine what coagulant dosage will reduce water turbidity to meet regulatory standards [78]. However, since the appropriate micro-coagulation assay indicates the same CCC value and most effective coagulant dosage as the jar test, it provides a suitable comparative screen for coagulant performance when experimental coagulants are limited.

3.3. Conclusions

Micro-coagulation assays can be used in place of standard jar tests to evaluate performance of scarce coagulants. These well plate assays should be shaken for 15 minutes and allowed to settle for 3 h to produce critical coagulation concentrations and most effective coagulant dosages similar to those that would result from a jar test.

Chapter 4: Comparative coagulation performance study of *Moringa oleifera* cationic protein fractions with varying water hardness

4.1. Introduction

This work has been published in the *Journal of Environmental Chemical Engineering*: Nordmark, B. A.; Przybycien, T. M.; Tilton, R. D. Comparative coagulation performance study of *Moringa oleifera* cationic protein fractions with varying water hardness. *J. Environ. Chem. Eng.* **2016**, *4* (4A), 4690–4698. Extracts containing cationic proteins from *Moringa oleifera* seeds are used to reduce drinking water turbidity in developing regions where the plant grows. To identify the active components in the seed extract, high performance liquid chromatography was employed, and eight *M. oleifera* cationic protein fractions were isolated. The protein fractions were characterized using gel electrophoresis (native molecular weights range from 12-48 kDa, reduced molecular weights range from 7-30 kDa), dynamic light scattering (radii of strongly cationic fractions are 1.2-1.5 nm), and circular dichroism (strongly cationic fractions are mainly comprised of alpha helices). Coagulation performance experiments were conducted using the micro-coagulation assay validated in Chapter 3. Fraction coagulation performances were compared individually and in various combinations against kaolin clay suspensions in model freshwaters of varying hardness. Ionic strengths of the model freshwaters ranged from 2.29-18.33 mM, and protein fraction concentrations ranged from 0-20 μg/mL. A combination of the weakly cationic fractions did not show coagulation activity. In diluted soft through moderately hard water, the individual strongly cationic fractions were effective at low dosages across a narrow range. Combinations of the strongly cationic fractions, of all cationic fractions, and of all cationic and non-cationic fractions were effective across broad ranges that encompassed low and medium dosages. The range of effective coagulant concentrations broadened for all individual

fractions and combinations as water hardness increased. In model hard water, kaolin is inherently unstable, so protein additives are unnecessary to induce flocculation.

4.2. Results and Discussion

4.2.1. Fractionation and analysis of Moringa oleifera cationic proteins

We adapted the procedure of Gassenschmidt *et al*. (1995) using a single strong cation exchange column and a linear sodium chloride gradient to fractionate the extracts from Nicaraguan and Thai *M. oleifera* seeds. The chromatograms revealed numerous peaks, when only a few were expected based on previous fractionation reports.

4.2.1.1. Fractionation

The chromatograms in Figure 4.1 revealed that Nicaraguan and Thai cationic protein extracts are comprised of the same fractions with slightly different mass percentages. Fractions are indicated by the numbered boxes and were collected and subjected to micro-coagulation assays individually and in various combinations.

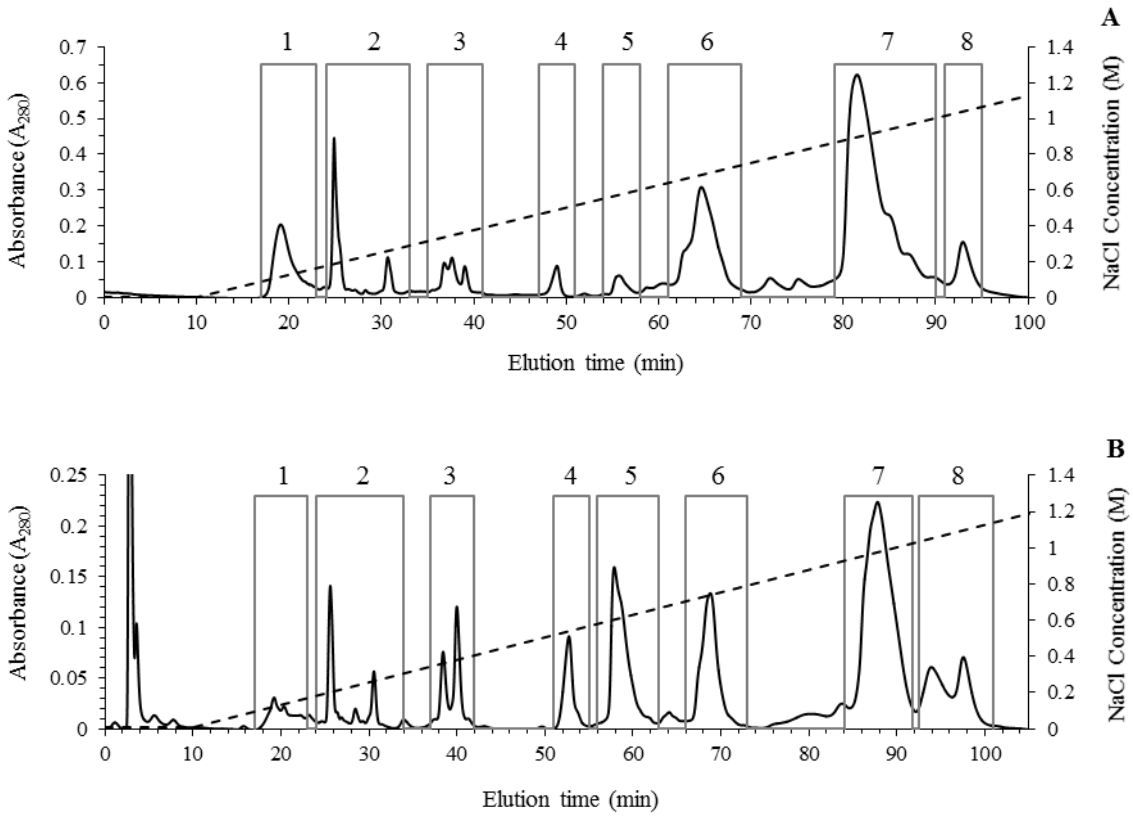

Figure 4.1. Chromatograms of Nicaraguan (A) and Thai (B) *M. oleifera* proteins eluted from the strong cation exchange column and detected by absorbance at 280 nm. Buffer A was 10 mM phosphate buffer pH 7.5, and Buffer B was 2 M sodium chloride in A. Gradient was 0% B from 0-10 minutes, 0-65% B from 10-114 minutes at a flow rate of 1 mL/min. Fractions are boxed and labeled numerically.

Increased elution time correlates with increased affinity of protein fractions for the cation exchange media. Therefore, higher fraction numbers are expected to have higher adsorption affinities for suspended solids with a net negative surface charge, such as kaolin at moderate and high pH. These fractions are referred to pragmatically as "strongly cationic." Since electrostatically driven protein adsorption can be dictated as much by details of charge distribution as by the overall net charge of a protein[79,80], the elution time may not strictly indicate the net charge.

4.2.1.2. Relative mass of fractions

The mass percent of each cationic fraction for Thai seeds is shown in tabular form in Table 4.1. This table also reports the area under the peaks for each fraction as well as the area per mass for each fraction. The area per mass indicates the degree of aromaticity of that fraction. Fractions 1-4 combined and fraction 5 have the highest absorbance per mass, suggesting that these fractions have greater aromatic content.

Table 4.1. Comparison of masses of fractions 5, 6, 7, 8, and 1-4 from Thai seeds rounded to the nearest 50 µg. Fractions 5, 6, 7, and 8 combined account for over 90% of the *Moringa oleifera* cationic proteins. Area under each fraction and area per mass were determined and reported for each fraction.

Fraction	Fraction mass (µg)	Mass percent	Area under curve (A_{280}·min)	Area/Mass (A_{280}·min/µg)·10^5
5	2,150	27.9%	0.435	87
6	2,100	27.3%	0.116	5.4
7	2,300	29.9%	0.335	15.9
8	650	8.4%	0.303	13.2
1-4	500	6.5%	0.315	48.4

As shown by Table 4.1, *M. oleifera* cationic proteins from Thai seeds are approximately 6.5 wt% fractions 1- 4, which are weakly cationic fractions, and approximately 93.5 wt% fractions 5-8, which are strongly cationic fractions. *C*ationic proteins from Nicaraguan seeds are approximately 5.1 wt% fractions 1-4 and approximately 94.9 wt% fractions 5-8. These percentages were estimated using the area per mass values determined for Thai proteins.

4.2.1.3. Sodium dodecyl sulfate-polyacrylamide gel electrophoresis (SDS-PAGE)

Proteins from Nicaraguan seeds were used to determine the molar masses for fractions 5, 6, 7, 8 and the combination of fractions 1-4 in their native and 2-mercaptoethanol-reduced forms were estimated by SDS-PAGE and reported in Table 4.2. SDS-PAGE images are shown below in Figure 4.2. The left image shows the molecular weights of the protein fractions in their native form, and the right image shows the molecular weights of the protein fractions in their 2-mercaptoethanol reduced form.

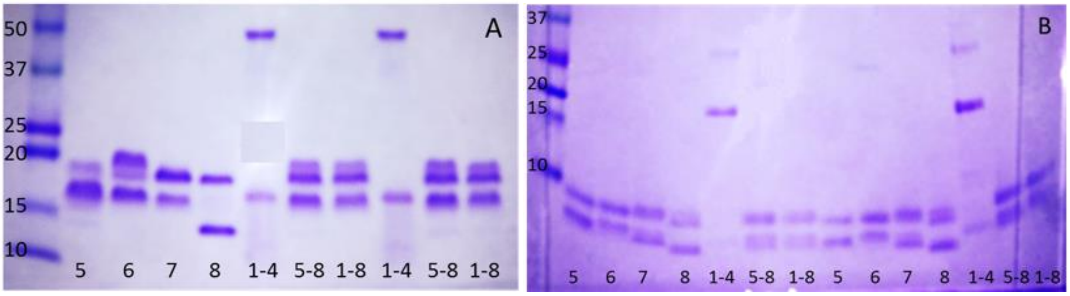

Figure 4.2. SDS-PAGE for fractions 5, 6, 7, 8, and 1-4 in their native (A) and 2-mercaptoethanol reduced (B) forms. The first lane of each gel contains a standard protein molecular weight calibration ladder. The molecular weights of the ladder bands are given in kDa.

The curvature in the gel bands seen in Figure 4.2B was accounted for as follows: A curve was fit to the migration front after it had passed through the gel (not shown). This curve was applied to each standard molecular weight marker in the gel, with the slope of the edges of the curve being adjusted to match each marker (higher molecular weights have a lower angle from the horizontal than lower molecular weights). A molecular weight calibration curve was then created using the method established by Lin et al. [81].

Each fraction yielded two or three bands in the native and reduced forms, with each band corresponding to distinct proteins. For fractions 5, 6, 7, and 8, the native molecular weights were 12-19 kDa, and the reduced molecular weights were 7-9 kDa. For the combination of fractions 1-4, the native molecular weights were 11-48 kDa, and the reduced molecular weights were 8-30 kDa. Various molecular weights determined from SDS-PAGE have been reported in literature for the active species in *M. oleifera* seeds, including reduced protein molecular weights of approximately 6.5 kDa [19,25,27,32,35], 20 kDa [35], 30 kDa [36], and 66 kDa [37]. Ndabigengesere et al. (1995) reported a native protein molecular weight of 13 kDa, and Shebek et al. (2015) reported native protein molecular weights of 13 kDa and 26 kDa. Both studies identified these species as oligomers of 6.5 kDa cationic proteins. Okuda et al. (2001) [48] reported a non-proteinaceous species with a molecular weight of 3 kDa.

Table 4.2. Native and reduced form molar masses for protein fractions 5, 6, 7, 8, and 1-4 as estimated by SDS-PAGE. Upper and lower bounds were calculated from band widths.

	Native		**Reduced**	
Fraction	**Number of bands**	**Molar mass (kDa)**	**Number of bands**	**Molar mass (kDa)**
5	2	19 ± 0.1	2	9 ± 1.1
		16 ± 0.2		8 ± 1.0
6	2	19 ± 0.2	2	9 ± 1.1
		15 ± 0.1		8 ± 1.0
7	2	18 ± 0.1	2	9 ± 1.1
		15 ± 0.1		8 ± 1.0
8	2	17 ± 0.1	2	9 ± 1.1
		12 ± 0.1		7 ± 1.0
1-4	3	48 ± 0.1	3	30 ± 1.4
		15 ± 0.1		19 ± 1.4
		11 ± 0.1		8 ± 1.0

Though not precisely matched by any of the SDS-PAGE bands in Table 4.2, the most commonly reported reduced molecular weight of 6.5 kDa comes close to the several reduced protein bands we observed in the 7 to 8 kDa range. Since fractions 5, 6, 7 and 8 are distinguished by their cation exchange retentions but have similar molecular weights, these proteins may differ by a small number of basic or acidic amino acids. Detailed sequence analysis on the highly resolved HPLC fractions collected here remains a subject for future research. Comparing the molar masses of the native bands to those of the reduced bands, it appears that most of the distinct proteins are likely composed of either homogenous or heterogeneous disulfide-linked dimers. The 12 ± 0.1 kDa band in fraction 8 and the 11 ± 0.1 kDa band from fractions 1-4 cannot be reconstructed from the molar masses of the reduced bands within experimental error, but it is possible that some reduced protein bands may fall below the lower detectability limit of the SDS-PAGE gels.

4.2.1.4. Circular Dichroism

Circular dichroism was used to examine the secondary structure contents of fractions 5, 6, 7, 8, and 1-4 from Nicaraguan and Thai seeds as shown in Figure 4.3. Average molar masses determined from SDS-PAGE were used to calculate the molar ellipticity per residue for each fraction.

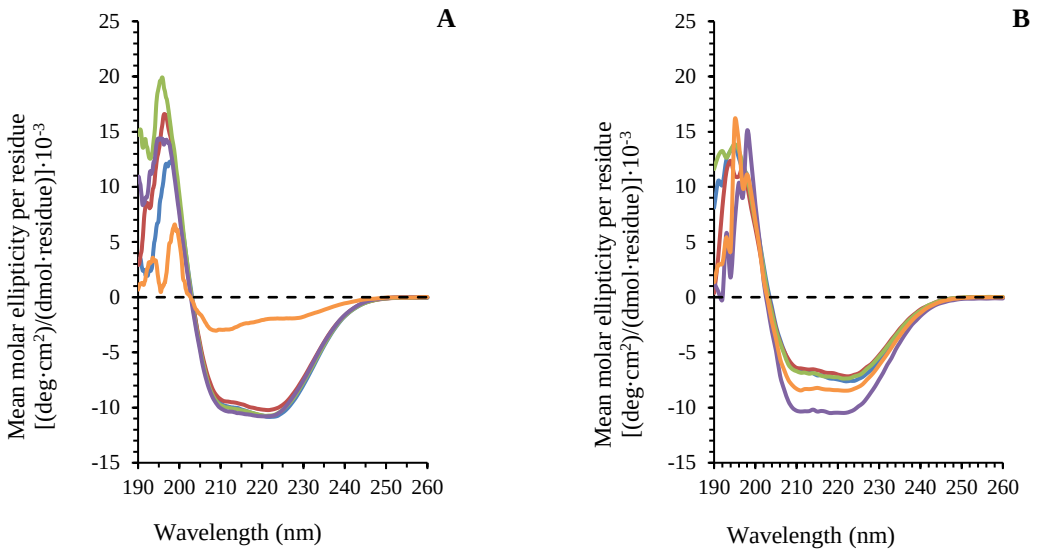

Figure 4.3. Far UV circular dichroism spectra of fractions 5 (blue), 6 (red), 7 (green), 8 (purple), and 1-4 (orange) for Nicaraguan seeds (A) and Thai seeds (B). Fractions were at a concentration of 500 µg/mL. Features at 208 nm and 222 nm are characteristic of alpha helix content.

The spectra showed that for Nicaraguan seeds, fractions 5, 6, 7, and 8 have similar secondary structures, mainly in the form of alpha helices as indicated by the characteristic spectral signatures at 208 nm and 222 nm[82]. The combination of weakly cationic fractions 1-4 has significantly less alpha helical content compared to the other fractions analyzed, which might play a role in explaining the combination's lack of activity in the subsequent micro-coagulation assays. For Thai seeds, all five fractions have similar secondary structures in the form of alpha helices. The combination of weakly cationic fractions 1-4 has alpha helical content comparable to the other fractions analyzed, which could explain why this combination displayed coagulation activity in the subsequent coagulations assays.

Suarez *et al*. (2005) isolated the segment of a *M. oleifera* cationic protein monomer responsible for coagulation activity. This segment was mainly comprised of one of the protein's alpha helices. Given the presence of proteins with distinct molar masses in each fraction, we

refrain from quantitative spectral analysis to estimate the relative proportions of distinct secondary structural elements. Kwaambwa and Maikokera (2008) reported that the secondary structure of a combination of all cationic proteins extracted from seeds from *M. oleifera* from Botswana consisted of 58 ± 4% alpha helices, 10 ± 3% beta sheets, and 33% unordered structure. Suarez *et al*. (2005) used computational modeling to predict the secondary structure of the *M. oleifera* monomer sequenced by Gassenschmidt *et al*. (1995) called MO2.1. Their model predicted that 29 of the 60 residues of MO2.1 were within three alpha-helical regions with the remaining residues comprising loops or unordered structures[38].

4.2.1.5. Dynamic light scattering

The hydrodynamic radii of the more cationic protein fractions were measured in triplicate in deionized water using DLS. The hydrodynamic radii for fractions 5, 6, 7 and 8, respectively, were 1.2 ± 0.1, 1.3 ± 0.1, 1.5 ± 0.4 and 1.2 ± 0.2 nm, where the error is the standard deviation of the three measurements. A one-way ANOVA indicated that these fractions did not significantly differ in size (P = 0.45). Fractions 1-4 could not be gathered in sufficient concentrations for DLS analysis. No *M. oleifera* cationic protein size data could be found for comparison in the literature.

4.2.2. Kaolin coagulation by Moringa oleifera protein fractions

The micro-coagulation assay was used to compare the kaolin coagulation performance of individual and combined *M. oleifera* fractions. Fractions 5, 6, 7, and 8 were studied individually because they are strongly cationic and were expected to be more effective coagulants for the negatively charged suspended clays. Additionally, these fractions are the most abundant by mass of the *M. oleifera* cationic proteins. Fraction combinations were studied to determine if

competitive adsorption of multiple distinct proteins might alter coagulation performance. In a practical sense, the performance of fraction combinations would also systematically indicate the level of protein purification necessary, if any, to obtain a more effective coagulant. The combinations that were studied include fractions 1-4, fractions 5-8, fractions 1-8, "all proteins" (all water soluble cationic and non-cationic proteins), and "all proteins with fatty acids" (all water soluble cationic and non-cationic proteins extracted from seeds where fatty acids had not been removed with petroleum ether).

The micro-coagulation assays were performed in waters of varying hardness to determine how coagulation performance depends on electrolyte composition and whether different fractions or combinations are better suited for specific water hardness conditions. Each model water, with no kaolin or humic acid present, had a normalized optical density of zero. Protein-free samples acted as a negative control for the assays. EPA policy states that 95% of drinking water samples per month must be equal to or less than 0.3 NTU with the maximum turbidity not exceeding 1 NTU if conventional or direct filtration is used or 5 NTU if other methods of filtration are used [78]. We have shown previously that a kaolin clay suspension with a turbidity of 5 NTU corresponds to an OD_{660} of 0.006 [43]. If the optical density of a sample supernatant was less than 0.006, then that concentration was considered effective as a coagulant.

4.2.2.1. Micro-coagulation assays for Nicaraguan seed proteins

Results from the micro-coagulation assays for Nicaraguan seed proteins are shown in Figure 4.4. The following discussion provides performance comparisons of the various fractions and combinations for each water hardness condition.

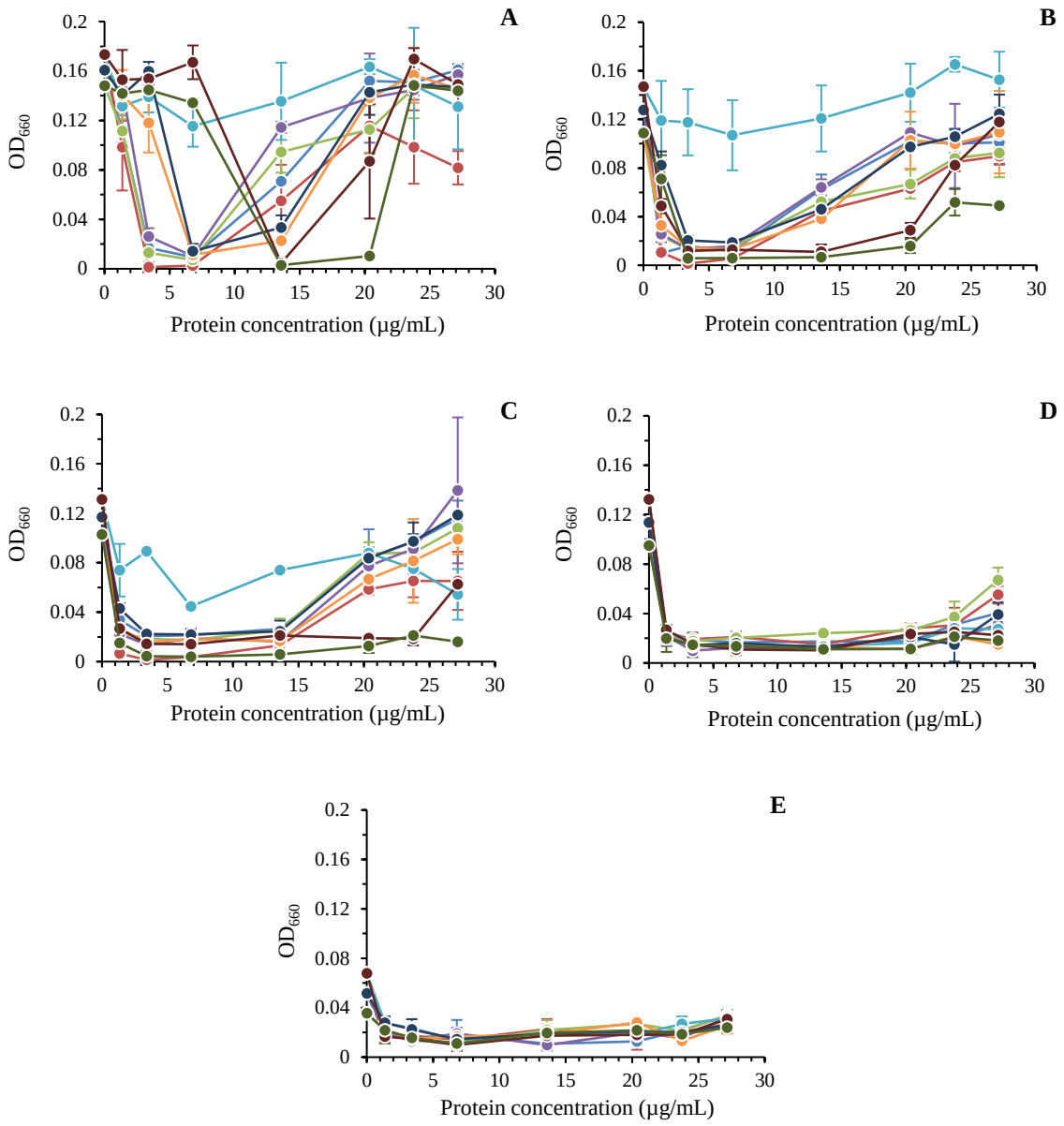

Figure 4.4. Micro-coagulation assays for Nicaraguan *M. oleifera* protein fractions in deionized water (A), diluted soft water (B), soft water (C), moderately hard water (D), and hard water (E). Fractions studied are fraction 5 (blue), fraction 6 (red), fraction 7 (green), fraction 8 (purple), fractions 1-4 (teal), fractions 5-8 (orange), fractions 1-8 (navy), all proteins (maroon), and all proteins with fatty acids (olive). Data points are the average of two trials. Lines connect the averages to guide the eye. Error bars are standard deviations of two trials.

4.2.2.1.1. Deionized water

Although deionized water is not a realistic model freshwater, it is the most stringent test of a neutralization-based coagulation mechanism, since electrostatic double layer repulsions are strongest at low ionic strength conditions. In deionized water, none of the protein fractions differed significantly in supernatant OD_{660} from the negative controls for concentrations less than 3 µg/mL. The individual fractions 5, 6, 7, and 8 each had a critical coagulation concentration (CCC) of 3 µg/mL. The combined fractions 5-8 and combined fractions 1-8 both had a CCC of 7 µg/mL, and the "all proteins" and "all proteins with fatty acids" both had a CCC of 14 µg/mL. The combined fractions 1-4, the least cationic of the cationic proteins, did not induce coagulation at any concentration considered.

All fractions that demonstrated coagulation enhancement at some lower concentration also demonstrated re-stabilization at a higher concentration. The individual fractions 5, 6, 7, and 8 exhibited less coagulation enhancement at 14 µg/mL and higher concentrations, with fraction 6 being the only sample to show slight coagulation enhancement at the highest concentration, 27 µg/mL. Combined fractions 5-8, and combined fractions 1-8 were effective at both 7 and 14 µg/mL and demonstrated decreasing coagulation enhancement at 20 and 27 µg/mL. "All proteins" and "all proteins with fatty acids" exhibited less coagulation enhancement at 20 and 24 µg/mL, respectively. The diminished coagulation performance at higher concentrations is attributed to net charge reversal on the kaolin particles associated with charge overcompensation by cationic protein adsorption, as discussed further below.

4.2.2.1.2. Diluted soft water

As in deionized water, combined fractions 1-4 did not show turbidity reduction capabilities at the considered concentrations in diluted soft water. Individual fractions 5, 6, 7, and

8, combined fractions 5-8, and combined fractions 1-8 behaved similarly to each other, exhibiting significant turbidity reduction between 3 and 7 µg/mL and modest but finite turbidity reduction just outside this range. The range of effective protein concentrations for the "all proteins" and "all proteins with fatty acids" combinations broadened to 3 to 14 µg/mL. In deionized water, the individual fractions 5, 6, 7, and 8 had the lowest effective protein concentration at 3 µg/mL. In diluted soft water, however, all individual fractions and combination of fractions except for combined fractions 1-4 were effective coagulants at this concentration.

4.2.2.1.3. Soft water

In soft water, fractions 1-4 again failed to enhance coagulation. The "all proteins with fatty acids" combination exhibited the widest range of effective protein concentrations, yielding supernatant optical densities similar to kaolin-free water from 1 to 27 µg/mL. The "all proteins" combination exhibited the second widest range of effective proteins concentrations from 1 to 24 µg/mL. All the other combinations and individual fractions exhibited significant turbidity reduction for concentrations between 1 and 14 µg/mL.

4.2.2.1.4. Moderately hard water

In moderately hard water, coagulation performance was indistinguishable for all individual fractions and combinations at concentrations between 1 and 20 µg/mL. Between 3 and 20 µg/mL, all protein combinations tested reduced OD_{660} to levels similar to kaolin-free controls, and nearly did so at 1 µg/mL. The "all proteins" and "all proteins with fatty acids" combinations decreased OD_{660} to the kaolin-free water level at 24 and 27 µg/mL as well, again being distinguished as the two protein combinations with the widest ranges of effective concentrations.

4.2.2.1.5. Hard water

In hard water, the negative controls produced the same supernatant optical densities as the kaolin-free water, indicating that the kaolin suspension was inherently unstable in hard water. Supernatant optical densities for all protein fractions and combinations were also indistinguishable from the negative controls. This shows that not only was protein not needed for kaolin coagulation in hard water, but also that cationic protein adsorption, if it occurred at all, was not able to re-stabilize the kaolin suspension. As ionic strength increases, the electrostatic double layer repulsion weakens, allowing attractive van der Waals forces to drive kaolin aggregation [46].

4.2.2.2. Micro-coagulation assays for Thai seed proteins

Results from the micro-coagulation assays using Thai seeds are shown in Figure 4.5. The following discussion provides performance comparisons of the various fractions and combinations across the five water hardness.

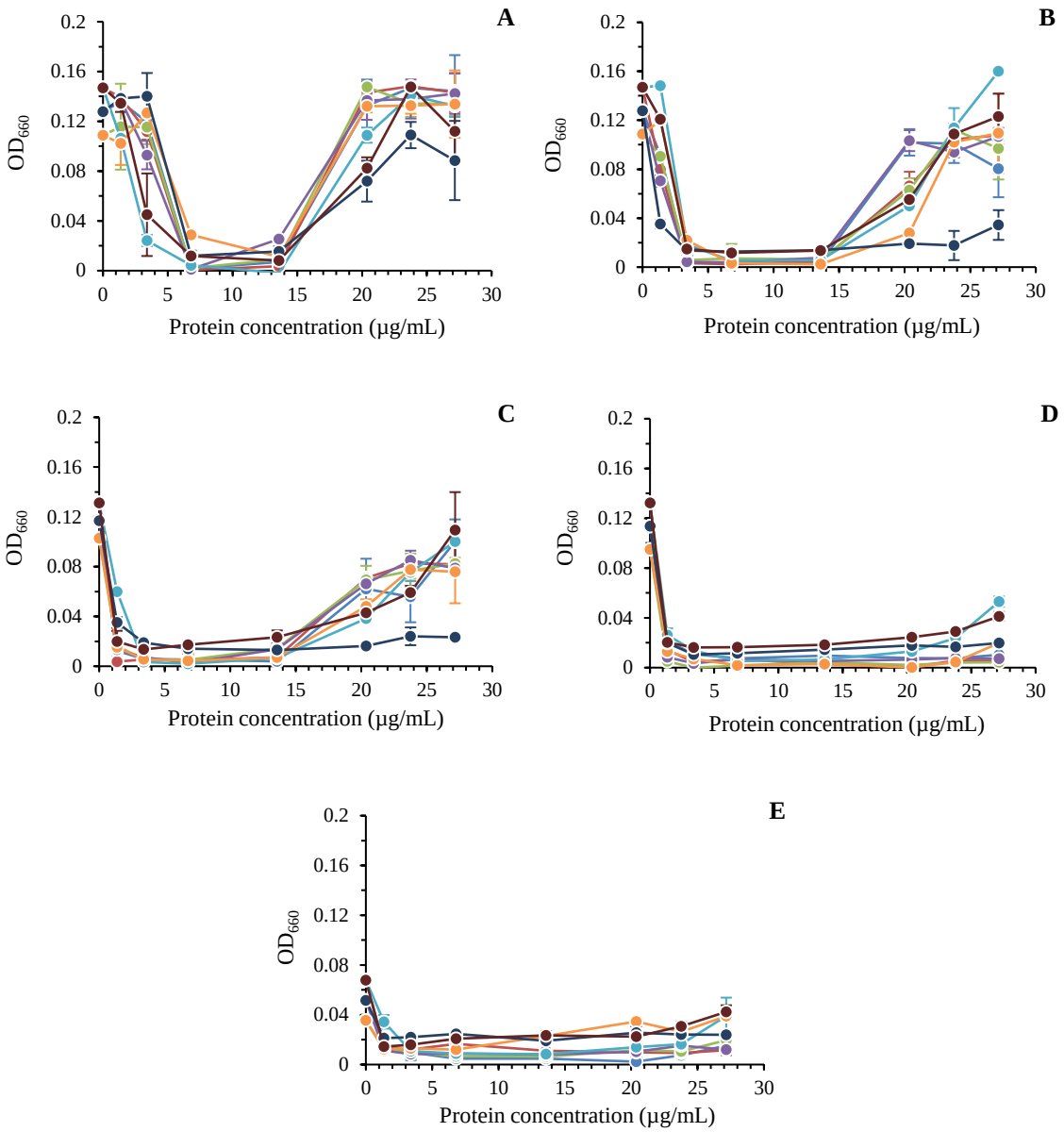

Figure 4.5. Micro-coagulation assays for Thai *M. oleifera* protein fractions in deionized water (A), diluted soft water (B), soft water (C), moderately hard water (D), and hard water (E). Fractions studied are fraction 5 (blue), fraction 6 (red), fraction 7 (green), fraction 8 (purple), fractions 1-4 (teal), fractions 5-8 (orange), fractions 1-8 (navy), and all proteins (maroon). Data points are the average of two trials. Lines connect the averages to guide the eye. Error bars are standard deviations of two trials.

As with the Nicaraguan seeds, *M. oleifera* proteins from Thai seeds reduced optical densities to kaolin-free water levels for all water hardness conditions, and most fractions exhibited re-stabilization at higher concentrations for softer waters. As water hardness increased, the range of effective protein concentrations widened and the critical coagulation concentrations decreased. The effective range of the protein fractions broadened from 7-14 µg/mL in deionized water to 1-24 µg/mL in moderately hard water, and the critical coagulation concentrations decreased from between 3-7 µg/mL in deionized water to 1 µg/mL in moderately hard water. In hard water, proteins were not needed for kaolin coagulation and did not produce re-stabilization.

The micro-coagulation assay results for the Thai seeds were similar to those of Nicaraguan seeds, with some notable differences. The Thai seed results had diminished diversity in coagulation performance in deionized water. The effective ranges of fraction concentrations were more similar to each other with the Thai seeds than with the Nicaraguan seeds. Another notable difference was that the Thai combined fractions 1-8 exhibited the broadest concentration range for effective coagulation in softer waters rather than the "all proteins with fatty acids" combination exhibited by the Nicaraguan seeds.

Most notably, whereas the combination of fractions 1-4 was ineffective at any concentration for Nicaraguan seeds, it did exhibit effective coagulation at intermediate concentrations in deionized, diluted soft, soft, and moderately hard water. When subjected to circular dichroism (Figure 4.3), the combined fractions 1-4 from Thai seeds had similar alpha helix content to those of fractions 5, 6, 7, and 8. This higher alpha helix content compared to the combined fractions 1-4 from the Nicaraguan seeds could explain why the Thai combined fractions 1-4 reduced turbidity in the micro-coagulation assays whereas the Nicaraguan combined fractions 1-4 did not.

4.2.3. Coagulation mechanism via Moringa oleifera proteins

The proposed mechanism of coagulation via addition of *M. oleifera* proteins is flocculation due to charge neutralization caused by protein adsorption [9,10,19,32,44,49,59,66]. Because the *M. oleifera* proteins are much smaller than the kaolin particles (DLS indicated an average kaolin hydrodynamic radius of 240 ± 11 nm in deionized water), it is unlikely that the proteins are causing bridging flocculation. Bridging is more commonly observed for high molecular weight polymeric flocculants [46,83]. It is more likely that the cationic proteins adsorb to the kaolin particles, neutralizing their negative charge and weakening the electrostatic double layer repulsion such that van der Waals forces drive flocculation [19]. The re-stabilization, or lack of kaolin coagulation observed at higher protein concentration, is attributed to charge overcompensation due to additional protein adsorption at the higher concentrations [46]. Net surface charge reversal is not uncommon when proteins adsorb to oppositely charged surfaces [80,84,85]. To test this hypothesis, kaolin particle zeta potentials were measured with different concentrations of the combination of "all proteins with fatty acids" in diluted soft water (pH ~ 7) and plotted in Figure 4.6 together with the corresponding OD_{660} values from the micro-coagulation assay.

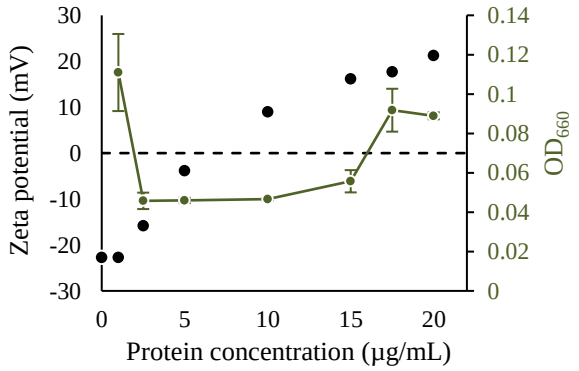

Figure 4.6. Zeta potential of kaolin with varying concentrations of the "all proteins with fatty acids" combination in diluted soft water (pH ~ 7). Black circles represent the average of three zeta potential measurements. Error bars represent standard deviation for these measurements and are smaller than the markers. The green line and markers are the OD_{660} measurements for "all proteins with fatty acids" in diluted soft water from Figure 4.3. Error bars represent the standard deviation of duplicate measurements.

Figure 4.6 confirms that negatively charged kaolin becomes less negatively charged with increasing protein concentration, passing through neutrality and experiencing charge reversal at higher protein concentrations. This charge reversal occurs at an intermediate protein concentration of approximately 8 µg/mL, which is very near to the median of protein concentrations that induce coagulation in the micro-coagulation assay. The optical density minima observed in the softer waters can thus be explained as follows: at lower protein concentrations, there is insufficient adsorption of positively charged proteins to neutralize the negative charge of the kaolin particles and significantly diminish the electrostatic double layer repulsion. At intermediate protein concentrations, kaolin particles become weakly charged so that van der Waals attractions are stronger than the electrostatic double layer repulsions and flocs can form. At higher concentrations, charge overcompensation by protein adsorption restores a net repulsion between the particles [46].

4.2.4. Water treatment implications

M. oleifera proteins were effective coagulants against kaolin in deionized water as well as in model freshwaters ranging from diluted soft water to moderately hard water. In these waters, 3-20 µg/mL protein was an effective dosage range for "all proteins" and "all proteins with fatty acids" to clarify a 920 NTU kaolin suspension. Shebek et al. (2015) reported that *M. oleifera* cationic proteins are 1.2 ± 0.2% w/w of the seeds. Using this information, our effective fraction dosage range can be converted to approximately 250-1,700 µg crushed seeds/mL. It has been reported that for water with high turbidities ranging from 250-430 NTU, the effective dosage ranges from 15-400 µg crushed seeds/mL [10,24,25,41]. This is near the effective range observed, considering the high turbidity model water used in this study, that suspended matter morphology affects required dosage, and that genetic differences or environmental factors affect the protein content of the seeds. Additionally, the mass fraction of cationic proteins in *M. oleifera* seeds reported by Shebek et al (2015) may be an underestimate, as this value was determined from water extracts, and it has been shown by Madrona et al. (2010) that salt solution extracts yield a higher percent of proteins from the seeds.

The combination of weakly cationic fractions 1-4 was unable to induce flocculation of kaolin particles in any of the model freshwaters tested. The coagulation activity of a combination of fractions 1-8 did not differ significantly from that of a combination of fractions 5-8, showing that fractions 1-4 neither augment nor diminish coagulation performance. The coagulation performance of fractions 5, 6, 7, and 8 individually did not differ from a combination of these strongly cationic fractions, showing that combining these fractions does not have a synergetic effect. In model freshwaters with lower hardness, fractions 5, 6, 7, and 8 were effective at low dosages across a narrow range, approximately 3-7 µg/mL of protein. Using these fractions

individually or in combination would add the least amount of dissolved organic carbon when treating water with *Moringa oleifera* seeds. However, because the strongly cationic fractions are effective across a narrow concentration range, coagulant overdosing could more easily occur, resulting in re-stabilization of suspended matter.

The combination of "all proteins" was effective at high dosages across a broad range, approximately 3-20 µg/mL of protein, which suggests a desirable robustness for water treatment applications. Using this fraction combination, the water treatment process would be less vulnerable to re-stabilization caused by a protein overload, which would otherwise be difficult to anticipate given the likely plant-to-plant variability in total protein content and varying extraction yields under field operating conditions. However, because this combination is effective at high dosages and likely contains other water soluble material in addition to the cationic proteins, using it would add more dissolved organic carbon content, which would more readily lead to bacterial growth in treated water.

The coagulant performance of the "all proteins with fatty acids" combination did not differ significantly from the "all proteins" combination, showing that removing fatty acids prior to protein extraction does not have a detrimental effect on coagulant performance, which agrees with the findings of Ghebremichael *et al*[25]. This is important because oil from *M. oleifera* seeds is a valuable commodity that can be collected and sold prior to using the seeds for water treatment [1,4–10].

The micro-coagulation assay was also performed using protein fractions extracted from Thai seeds The key trends were similar for protein fractions from Nicaraguan and Thai seeds, but a few subtle differences were noted. These differences can likely be attributed to differences in seed composition developed due to genetic differences or environmental factors where the *M.*

oleifera trees grew. Since the kaolin coagulation process is the result of the complex, multi-component, competitive adsorption of a diverse population of proteins, small differences in relative protein abundance, amino acid content, and charge distributions could produce the observed differences. Without detailed compositional, structural and competitive adsorption studies, the exact cause of the differences cannot be identified, yet the results obtained with both seed sources indicate that additional protein purification beyond aqueous extraction is not warranted for field applications in water treatment.

4.3. Conclusions

More than eight distinct cationic protein subpopulations exist in aqueous extracts of *M. oleifera* seeds. Collected fractions had molecular weights ranging from 11-48 kDa non-reduced and 7-30 kDa reduced. The strongly cationic protein fractions are 1.2-1.5 nm in radius and are mainly comprised of alpha helices. The mechanism of kaolin flocculation by *M. oleifera* cationic proteins is adsorption and charge neutralization. As such, coagulation occurs within a finite coagulant concentration range, depending on water hardness, as the range of effective coagulant dosages broadens for all fractions as water hardness increases. Kaolin suspensions are inherently unstable in hard water due to electrostatic screening and do not need the addition of coagulant proteins to induce flocculation. Fatty acids do not significantly affect coagulation activity.

The differences in coagulation results between the Thai and Nicaraguan seeds can likely be attributed to seed compositional differences developed due to genetic differences or environmental factors where the *M. oleifera* trees grew. Since the kaolin coagulation process is the result of the complex, multi-component, competitive adsorption of a diverse population of proteins, small differences in relative protein abundance, amino acid content, and charge distributions could produce the observed differences. Without detailed compositional, structural

and competitive adsorption studies, the exact cause of the differences cannot be identified, yet the results obtained with both seed sources indicate that additional protein purification beyond aqueous extraction is not warranted for field applications in water treatment.

These results indicate that many of the individual or combined protein fractions studied could be used to achieve turbidity reduction using low protein dosages so as to minimize dissolved organic carbon. However, to produce a water treatment process that is robust against uncertainty in the concentration of seed extracts, protein combinations should be used because they are effective coagulants over broader concentration ranges. These conclusions are based on model waters where clays are the only suspended materials. It remains to be determined how *Moringa oleifera* cationic protein fractions would compare in their coagulation performance in complex waters with significant suspended or dissolved organic matter.

Chapter 5: Effect of humic acids on kaolin coagulation performance of *Moringa oleifera* proteins

5.1. Introduction

This work has been submitted in the manuscript titled "Effect of humic acids on kaolin coagulation performance of *Moringa oleifera* proteins" to the *Journal of Environmental Chemical Engineering* (2018) by Brittany A. Nordmark, Todd M. Przybycien, and Robert D. Tilton. Cationic proteins from *Moringa oleifera* seeds are of interest as sustainable coagulants for drinking water treatment in regions with poor access to potable water. They have been shown to reduce turbidity in natural water sources as well as in various model freshwaters. Prior research on kaolin suspension coagulation by fractionated *M. oleifera* protein extracts demonstrated that coagulation occurred by adsorption and charge neutralization. Negatively charged natural organic matter may interfere with this coagulation mechanism by complexing with *M. oleifera* proteins or adsorbing to suspended kaolin particles. In this study, kaolin suspensions in model waters with varying concentrations of humic acid were used to model surface water. Electrophoretic mobility and dynamic light scattering measurements showed evidence of humic acid adsorption to kaolin particles. Coagulation micro-assays, which are validated, scaled-down versions of jar tests, were used to determine the coagulation activity of the *M. oleifera* proteins in EPA model freshwaters (ionic strengths ranging from 1.15-9.17 mM) as a function of humic acid concentration. Electrophoretic mobility measurements confirmed that the coagulation mechanism of the proteins against a mixture of kaolin and humic acid is neutralization induced by adsorption, but increasing humic acid concentrations necessitated higher protein concentrations to achieve similar degrees of turbidity reduction. The range of effective coagulating protein doses broadened as humic acid concentration increased and as water hardness increased. These coagulation studies reveal the mechanistic roles of particulate and

natural organic matter that will likely contribute to the development of methods to treat natural water using *M. oleifera* seed proteins.

5.2. Results and Discussion

5.2.1. Coagulation by M. oleifera proteins

The coagulation micro-assay was used to compare the coagulation performance of a combination of all-water-soluble *M. oleifera* proteins with fatty acids removed against suspended kaolin particles, humic acid, and mixtures of kaolin and humic acid in various model freshwaters. For each measurement, the optical density recorded in wells containing only the model waters, with no kaolin or humic acid present, was used as a baseline for all supernatant analyses. Protein-free samples act as a negative control for the assays.

EPA policy states that 95% of drinking water samples per month must have turbidity equal to or less than 0.3 NTU, with the maximum turbidity not exceeding 1 NTU if conventional or direct filtration is used or 5 NTU if other methods of filtration are used [78]. We have shown previously that a kaolin suspension with a turbidity of 5 NTU corresponds to an OD_{660} of 0.006 in the coagulation micro-assay [43]. If the optical density of a sample supernatant was less than 0.006, then the protein concentration used in that sample was considered effective as a coagulant. Therefore, an effective protein coagulation concentration range (EPCC) is the range of concentrations that reduce the sample turbidity below an OD_{660} of 0.006.

The critical coagulation concentration (CCC) is also examined for each micro-micro-coagulation assay. The CCC is the lowest protein concentration at which coagulation is first observed, but not necessarily the lowest protein concentration at which water turbidity is reduced to an established metric. We report the CCC as the midpoint concentration between the data

point where coagulation is first evident and its predecessor. The error reported with this quantity corresponds to ± one-half of the spacing between these two points.

5.2.1.1. Model waters containing kaolin clay

Figure 5.1 shows the coagulation performance of *M. oleifera* proteins against kaolin clay in each of the four model freshwaters and deionized water, with no humic acid present. The concentration of kaolin was held constant at 0.5 g/mL.

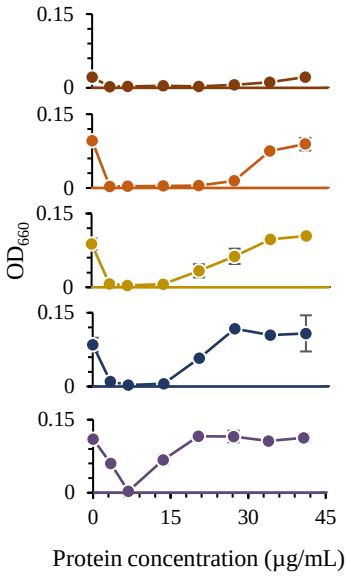

Figure 5.1. Kaolin micro-coagulation assays performed in (from bottom to top) deionized water (purple), diluted soft freshwater (dark blue), soft freshwater (mustard), moderately hard freshwater (orange), and hard freshwater (maroon). Kaolin concentration was held constant at 0.5 g/L. Error bars represent the standard deviation of two replicates and are frequently smaller than the symbol size.

Consistent with our prior work [43], the EPCC range broadens as water hardness increases from a narrow range around 5-10 µg/mL in deionized water to 2-30 µg/mL in hard water. Diluted soft water and soft water results are not significantly different from each other, but the

EPPC ranges in moderately hard and hard water are significantly broader. Even in the absence of the proteins, kaolin flocculates in hard water, as indicated by the low optical density of the supernatant at 0 μg/mL protein concentration. Nevertheless, there is still a range of protein concentrations at which the supernatant optical density is less than that obtained in the absence of proteins. The CCC is between 2 and 5 μg/mL across the five model waters for kaolin. Thus, the primary effect of increasing water hardness is to increase the upper limit on the EPCC range. Both of these phenomena are likely due to increased electrostatic screening with increasing ionic strength in the model freshwaters and its effects on protein adsorption to kaolin and on long-range inter-particle electrostatic double layer repulsions [46].

The key effect of cationic protein adsorption is to modify the net surface charge of the kaolin particles. The optical density minima observed in the above and following micro-coagulation assays can be explained as follows: at low protein concentrations, the surface concentration of adsorbed cationic proteins is insufficient to diminish the electrostatic double layer repulsions of the negatively charged kaolin particles to the point that the suspension is destabilized. At intermediate protein concentrations, the extent of cationic protein adsorption is sufficient to neutralize the kaolin charge, at which point van der Waals attractions become dominant and the suspension is destabilized. At high concentrations, more extensive adsorption of cationic proteins causes a surface charge reversal from negative to positive, re-stabilizing the kaolin suspension. Similar qualitative trends will be reported below for kaolin suspensions in the presence of humic acid, and this proposed charge neutralization mechanism will be checked by electrophoretic mobility measurements.

5.2.1.2. Model waters containing humic acid

Figure 5.2 shows the coagulation micro-assay performance of *M. oleifera* proteins against humic acid in each of the model waters, starting with the lowest ionic strength deionized water and progressing to hard water. The concentration of humic acid was varied from 2.5 to 10 ppm, and no kaolin was present.

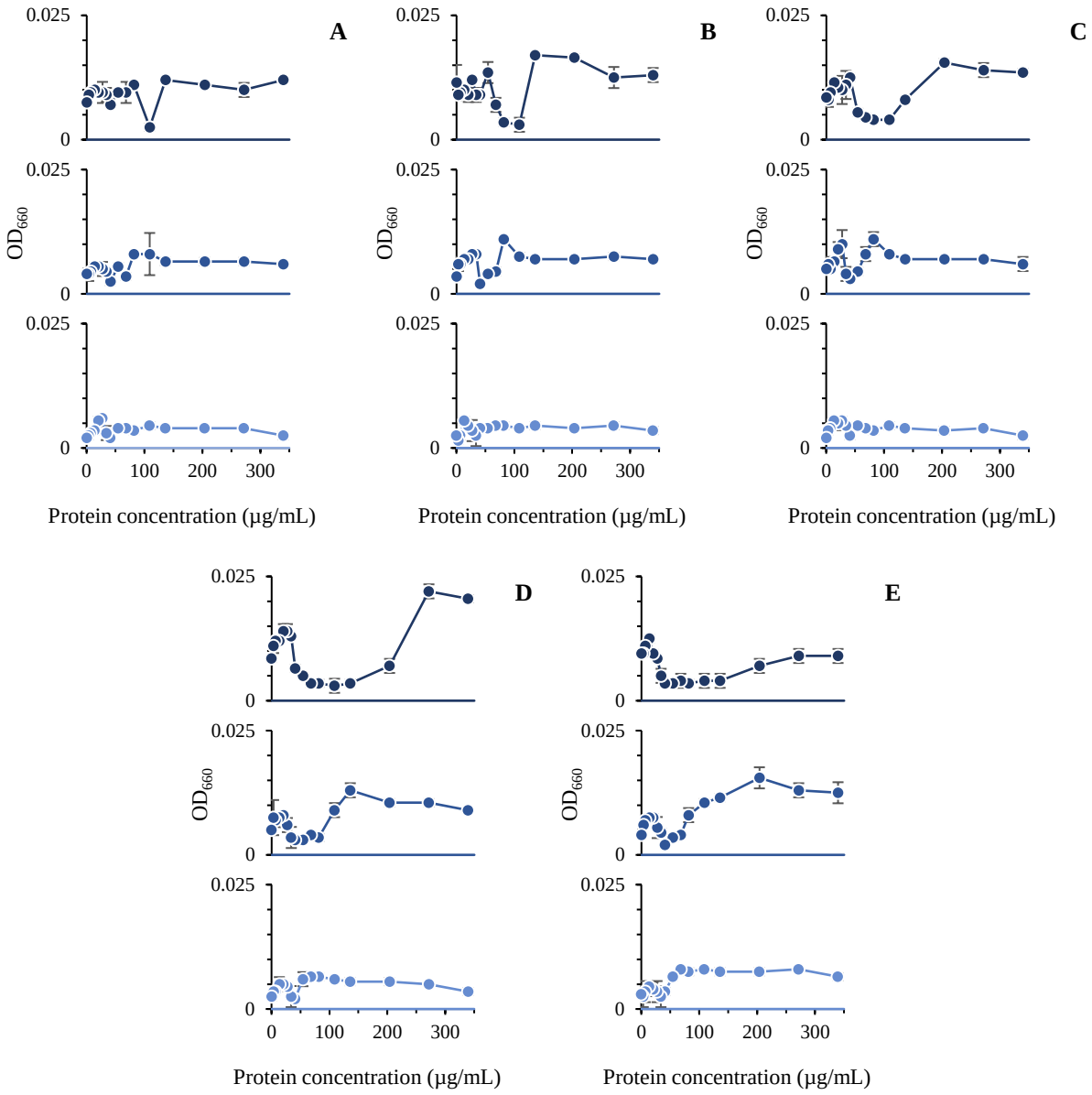

Figure 5.2. Humic acid coagulation micro-assays performed in (A) deionized water, (B) diluted model soft freshwater (1.15 mM), (C) model soft freshwater (2.29 mM), (D) model moderately hard freshwater (4.58 mM), and (E) model hard freshwater (9.17 mM). Humic acid concentrations studied were (from bottom to top in each panel) 2.5 ppm (light blue), 5 ppm (medium blue), and 10 ppm (dark blue). Error bars represent the standard deviation of two replicates.

The coagulation micro-assays for humic acid follow similar qualitative trends as those for kaolin. Note that the OD_{660} for these humic acid solutions are an order of magnitude less than those for 0.5 g/L kaolin suspensions presented above. As water hardness increases, the EPCC range broadens. This is most noticeable for the 10 ppm humic acid case, where the EPCC range broadens from 95-122 µg/mL in deionized water to 38-170 µg/mL in hard water. Additionally, the CCC decreases with increasing water hardness, but increases with decreasing humic acid concentration. For 10 ppm humic acid, the CCC decreases from 95 ± 14 µg/mL in deionized water to 30 ± 4 µg/mL in hard water. In diluted soft water, the CCCs for 2.5, 5 and 10 ppm humic acid are 23 ± 4, 37 ± 4, and 61 ± 7 µg/mL, respectively.

For the micro-coagulation assays with humic acid, in all but the 10 ppm humic acid in hard water case, the supernatant optical densities initially increase at lower protein concentrations before decreasing at the critical coagulation concentration, only to increase again at high protein concentrations to values that exceed the optical density of the corresponding protein-free humic acid solution. Note that OD_{660} is negligible for a simple solution of the proteins. This optical density trend is attributed to increasing extents of complexation and flocculation as protein concentration increases. With the onset of protein-humic acid binding at low protein concentrations, complexes form that are larger and scatter more light, but their size is not yet sufficient for the flocs to sediment from solution. With further complexation at higher protein concentrations, flocs approach electrical neutrality, macroscopic phase separation occurs, and sedimentation clarifies the supernatant. At higher protein concentrations, protein-humic acid complexes become charge-reversed and colloidally stable. As these complexes grow, their light scattering cross-section increases. This complexation is addressed by electrophoretic mobility and dynamic light scattering measurements described below.

5.2.1.3. Model waters containing kaolin and humic acids

Figure 5.3 shows the effect of humic acid on the coagulation performance of *M. oleifera* proteins against kaolin in each of the model waters, starting with deionized water and progressing to hard water. The kaolin concentration was held constant at 0.5 g/L, and the humic acid concentration was varied from 2.5 to 10 ppm.

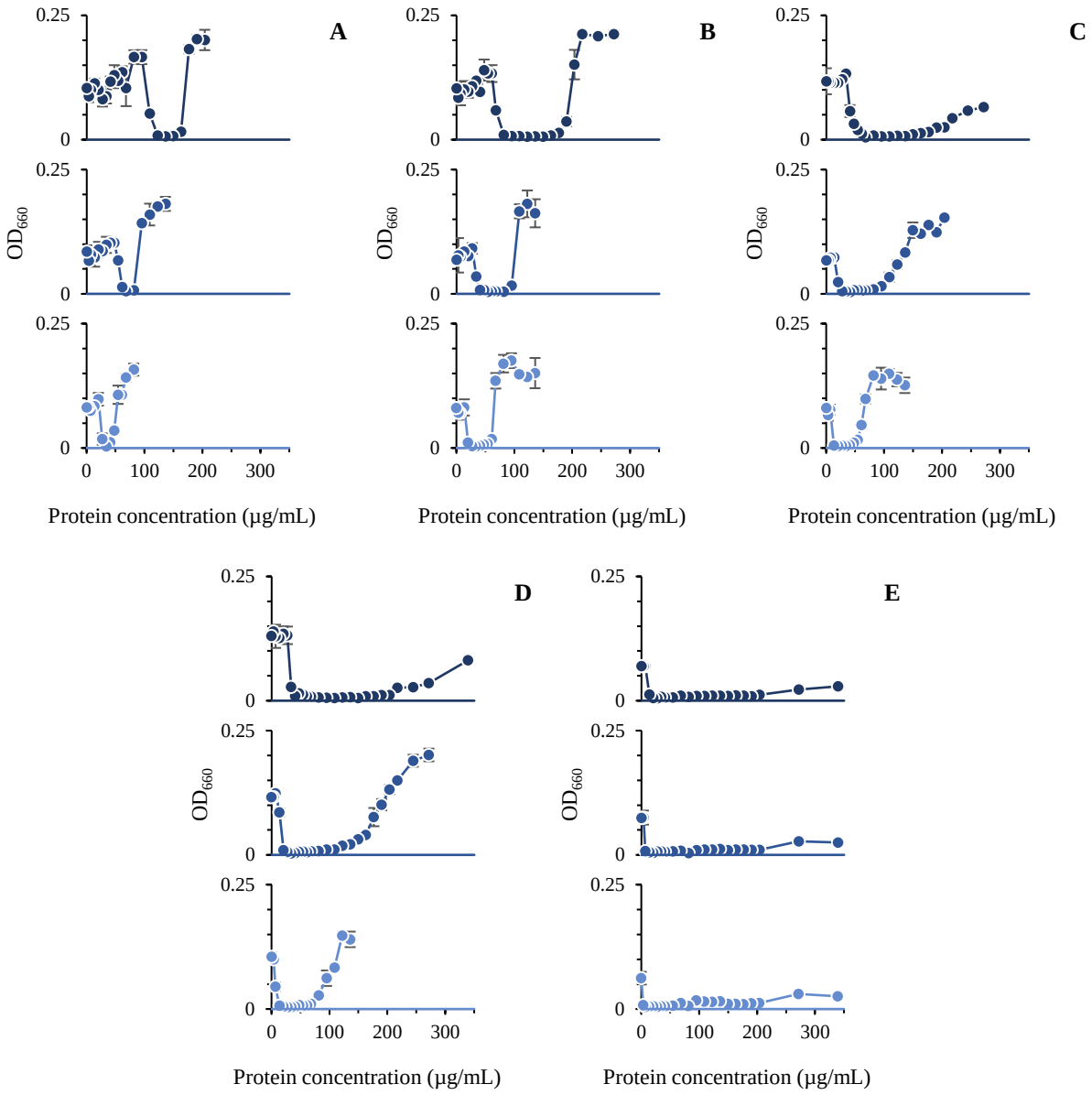

Figure 5.3. Kaolin-humic acid mixture coagulation micro-assays performed in (A) deionized water, (B) diluted model soft freshwater (1.15 mM), (C) model soft freshwater (2.29 mM), (D) model moderately hard freshwater (4.58 mM), and (E) model hard freshwater (9.17 mM). Kaolin concentration was held constant at 0.5 g/L while humic acid concentration was varied. Humic acid concentrations studied were (from bottom to top in each panel) 2.5 ppm (light blue), 5 ppm (medium blue), and 10 ppm (dark blue). Error bars represent the standard deviation of two replicates.

The coagulation micro-assays for the mixtures of kaolin and humic acid share similar attributes to those for kaolin and humic acid individually. As water hardness increases, the EPCC range broadens. For the mixture of kaolin with 10 ppm humic acid, the range broadened from 116-170 µg/mL in deionized water to 17-238 µg/mL in hard water. The EPCC ranges for the mixtures are broader than those for either material alone in the same type of water. This has practical significance since mixtures of suspended clays and natural organic matter are common in natural surface waters, and a broad EPCC range lends itself to robust water treatment performance.

The effective protein coagulation dosages reported here differ from those reported by Santos *et. al.* [55], who found that 1-180 µg/mL is the effective range to reduce the turbidity of a mixture of 0.45 g/L kaolin and 9 ppm humic acid prepared in distilled water. One may have expected results in distilled water to resemble those obtained here in de-ionized water. A possible reason for this difference could be that subsequent to their extraction of *M. oleifera* proteins using a 0.15 M solution of sodium chloride, they did not desalt their extracts. A rough calculation reveals that if indeed no desalting occurred, the overall ionic strength of the turbid water with protein in their micro-coagulation assays would be approximately 17 mM (exceeding the ionic strength of EPA model hard water) which would explain the broad range of effective protein coagulation dosages that they reported.

Similar to the humic acid coagulation micro-assays, the CCCs for the mixtures decrease with increasing water hardness and increase with increasing humic acid concentration. For mixtures with 10 ppm humic acid, the approximate CCC decreases from 95 ± 14 µg/mL in deionized water to 10 ± 4 µg/mL in hard water. In diluted soft water, the approximate CCCs for mixtures with 2.5, 5 and 10 ppm humic acid are 17 ± 3, 30 ± 4, and 61 ± 7 µg/mL, respectively.

The EPCC ranges and CCCs for the micro-coagulation assays shown in Figures 5.1-5.3 are summarized in Table 5.1.

Table 5.1. Summary of effective protein coagulation concentration ranges (EPCC range) and the critical coagulation concentrations (CCC) for the micro-coagulation assays in Figures 5.1-5.3. EPCC range is the range of concentrations that reduce the sample turbidity below an OD_{660} of 0.006. CCC is reported as the midpoint concentration between the data point where coagulation is first evident and its predecessor. The error reported with this quantity corresponds to ± one-half of the spacing between these two points.

Turbid water	Quantity (µg/mL)	Deionized	Diluted soft	Soft	Moderately hard	Hard
0.5 g/L kaolin	EPCC range	5-10	2-17	2-17	2-23	2-30
	CCC	2 ± 2	2 ± 2	2 ± 2	2 ± 2	2 ± 2
2.5 ppm humic acid	EPCC range	38-47	31-37	38-47	31-47	24-47
	CCC	30 ± 4	23 ± 4	30 ± 4	23 ± 4	17 ± 3
5 ppm humic acid	EPCC range	38-47	38-74	31-61	31-95	31-74
	CCC	37 ± 4	37 ± 4	30 ± 4	23 ± 4	23 ± 4
10 ppm humic acid	EPCC range	95-122	75-122	47-122	62-170	38-170
	CCC	95 ± 14	61 ± 7	47 ± 7	37 ± 4	30 ± 4
2.5 ppm humic acid and 0.5 g/L kaolin	EPCC range	31-37	24-57	11-51	11-74	2-238
	CCC	23 ± 4	17 ± 3	10 ± 4	5 ± 2	2 ± 2
5 ppm humic acid and 0.5 g/L kaolin	EPCC range	58-88	38-88	24-88	17-116	5-238
	CCC	47 ± 7	30 ± 4	17 ± 3	10 ± 4	5 ± 2
10 ppm humic acid and 0.5 g/L kaolin	EPCC range	116-170	75-170	65-156	38-183	17-238
	CCC	95 ± 14	61 ± 7	37 ± 4	30 ± 4	10 ± 4

Note that the EPCC ranges and the CCCs for the mixtures of kaolin and humic acid more closely resemble those of humic acid than those of kaolin, even though kaolin is the dominant source of turbidity (OD_{660}). For example, the EPCC ranges for kaolin, 10 ppm humic acid, and the mixture of kaolin and 10 ppm humic acid in soft water are 2-17 µg/mL, 47-122 µg/mL, and 65-156 µg/mL, respectively, and the CCCs for these samples are 2 ± 2, 47 ± 7, and 37 ± 4 µg/mL, respectively. The EPCC ranges are broader for the mixtures of kaolin and humic acid than for their individual components at all humic acid concentrations in each model freshwater.

The CCCs for the mixtures are either equal to or less than those for humic acid and always greater than those for kaolin.

These differences could be attributed to competition between protein adsorption to kaolin and protein complexation with humic acid. A key effect of humic acid addition to the kaolin suspension is to shift the CCC to higher values compared to the kaolin-only suspensions. For each water hardness, the optical density of most of the humic acid solutions increases somewhat by the addition of proteins at the lowest measured concentration (3 μg/mL). This is strong evidence for protein complexation with humic acid at these low concentrations, even if the extent of complexation is not sufficient to cause humic acid sedimentation from solution. As a result of this complexation, the concentration of unbound cationic proteins in the kaolin-humic acid mixtures is decreased. Higher total concentrations of protein must be added to the mixture to achieve the same degree of kaolin net charge neutralization as would be required in the absence of humic acid. Also note that the OD_{660} contribution of humic acids, and especially the change in OD_{660} caused by protein-driven coagulation of humic acid (Figure 5.2), is very small compared to the kaolin contribution. Thus small changes in OD_{660} that might occur due to protein-humic acid complexation in the mixtures are not distinguishable.

In a similar line of reasoning, protein-humic acid complexes could adsorb to kaolin. These complexes would be less positively charged, in fact negatively charged at the lowest protein concentrations, and would therefore be far less effective in neutralizing the kaolin net charge. A further possibility is that humic acid, and/or protein-humic acid complexes that are negatively charged at low protein concentrations, may adsorb to the kaolin particles and thereby increase the net negative charge of said particles. With an increased negative charge, these humic acid-modified kaolin particles would require higher protein concentrations to be neutralized and

coagulated compared to kaolin in the absence of humic acid. These hypotheses are explored further in the next section.

As with the humic acid micro-coagulation assays, many of the micro-coagulation assays with kaolin and humic acid show supernatant optical densities initially increasing at low protein concentrations below the CCC. This could suggest a limited degree of kaolin flocculation induced by adsorption of protein-humic acid complexes. Many of these assays also show larger optical densities as particles are re-stabilized at higher protein concentrations compared to the optical densities measured below the CCC. *M. oleifera* proteins do not contribute significantly to OD_{660} at the protein concentrations studied, and this effect was not significant in kaolin suspensions that had no humic acid. It is possible that at protein concentrations above the EPCC range in the mixture samples, kaolin, humic acid, and proteins are forming flocs that are larger than those formed at lower protein concentrations but still small enough to avoid sedimentation. Larger flocs would scatter more light and result in a larger optical density. It is also possible that the composition or morphology of the flocs at higher protein concentrations differs from that of the flocs at lower protein concentrations, resulting in differing optical densities.

5.2.2. Evidence of humic acid adsorption to kaolin

Electrophoretic mobility and dynamic light scattering measurements were used to explore the possibility of humic acid adsorption to kaolin and the possibility of protein-humic acid complexation in the freshwaters used for the micro-coagulation assays. The zeta potential was determined for kaolin clay (0.5 g/L), humic acid (10 ppm), as well as a mixture of the two species (0.5 g/L kaolin, 10 ppm humic acid) in diluted soft water (1.15 mM ionic strength) as a function of protein concentration. These results are shown in Figure 5.4.

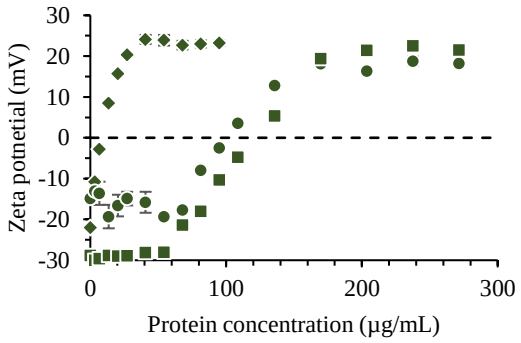

Figure 5.4. Zeta potential of 0.5 g/L kaolin (diamonds), 10 ppm humic acid (circles), and 0.5 g/L kaolin with 10 ppm humic acid (squares) with varying protein concentrations in diluted soft water (pH ~ 7). Data points represent the average of three zeta potential measurements. Error bars are standard deviation of five measurements and are frequently smaller than the markers.

Figure 5.4 shows that in the absence of proteins, humic acid is the least negatively charged species, with a zeta potential of approximately -15 mV, followed by kaolin at -22 mV, then the mixture of the two species at -29 mV. This is clear evidence of humic acid adsorption to kaolin. When adding proteins at increasing concentrations, kaolin is the first sample to pass through neutrality at a protein concentration of approximately 10 µg/mL, followed by humic acid at approximately 100 µg/mL, then the mixture at approximately 120 µg/mL. The shift in neutralization to higher protein concentrations in the kaolin-humic acid mixture is consistent with the observed shift in EPCC range and with the hypothesis proposed above.

Number-averaged hydrodynamic radii for the same samples were determined from dynamic light scattering (DLS) measurements in deionized water, soft water (2.29 mM ionic strength), and hard water (9.17 mM ionic strength). These results are shown in Table 3 along with the Polydispersity Index (PdI) as defined by ISO standard document ISO 22412:2017. In

reference to DLS, highly monodisperse standards will have a PdI around 0.05, and samples with a PdI greater than 0.7 are considered highly polydisperse [86].

Table 5.2. Number average hydrodynamic radii of humic acid (10 ppm), kaolin (0.5 g/L) and a mixture of humic acid and kaolin (10 ppm and 0.5 g/L, respectively) in deionized, soft, and hard water. Reported values are the average of five measurements. Error is reported as the average half width at half maximum of five measurements.

Water type	Sample	Hydrodynamic radius (nm)	Polydispersity Index
Deionized	Humic acid	4 ± 2	0.39 ± 0.05
	Kaolin	190 ± 130	0.42 ± 0.03
	Mixture	160 ± 120	0.37 ± 0.06
Soft	Humic acid	3 ± 1	0.42 ± 0.04
	Kaolin	430 ± 300	0.43 ± 0.05
	Mixture	380 ± 250	0.48 ± 0.03
Hard	Humic acid	11 ± 5	0.56 ± 0.09
	Kaolin	550 ± 300	0.57 ± 0.06
	Mixture	440 ± 250	0.53 ± 0.08

DLS revealed that humic acids are approximately 1-10 nm in radius and that kaolin particles are approximately 200 nm in radius. Humic acids are complex mixtures that may contain discrete molecules or small aggregates [87]. Kaolin particles are hexagonal plate-like structures with strongly negatively charged edges and either weakly positively or negatively charged faces (depending on pH) that form aggregates by adsorbing face to face, edge to edge, or face to edge [64]. This is important to consider when interpreting DLS, which reports radii of spheres with diffusion coefficients equivalent to those of the scattering species.

PdI for the three samples increased slightly as water hardness increased, but all nine indices were between 0.37 and 0.57. The slight increase in PdI could be indicative of flocculation. The hydrodynamic radii of kaolin and the mixture increase significantly in soft and hard waters relative to deionized water, also suggesting flocculation. This is consistent with the

coagulation micro-assay results for hard water in Figures 5.1 and 5.3. Increased screening weakens the electrostatic double layer repulsions as ionic strength increases, which allows van der Waals forces to drive flocculation [46].

The mixture's scattering objects are smaller than the kaolin particles in all three waters. Adsorption of humic acid could be preventing kaolin particles from aggregating in the model freshwaters. This adsorption is likely occurring at the faces of the kaolin particles, which have a near-zero charge density [64]. If humic acid were adsorbing to kaolin, the negative charge density of the kaolin particles would become even more negative, as was observed in Figure 5.4. Greater negative charge would require higher concentrations of positively charged species in the form of *M. oleifera* proteins to induce flocculation, as hypothesized above, which is indeed observed when comparing Figures 5.1 and 5.2 to Figure 5.3.

5.2.3. Kaolin coagulation mechanism via M. oleifera proteins in the presence of humic acid

Charge neutralization of suspended particles is achieved through *M. oleifera* protein adsorption [9,10,19,32,43,44,49,59,66]. Both *M. oleifera* proteins and humic acid are significantly smaller than kaolin particles, so bridging flocculation, which is more commonly observed for high molecular weight flocculants [46,83], is an unlikely kaolin coagulation mechanism. A shown previously [43], kaolin coagulation is induced by protein adsorption and charge neutralization, and continued protein adsorption causes re-stabilization at high concentrations. To test if this holds true for kaolin in the presence of humic acids, zeta potentials and hydrodynamic radii data for mixtures of 0.5 g/L kaolin and 10 ppm humic acid with *M. oleifera* proteins in diluted soft water (pH ~ 7) are directly compared with coagulation micro-assay results in Figure 5.5 (C). Zeta potentials and hydrodynamic radii data for 0.5 g/L kaolin (Figure 5.5 A) and 10 ppm humic acid (Figure 5.5 B) separately are also provided.

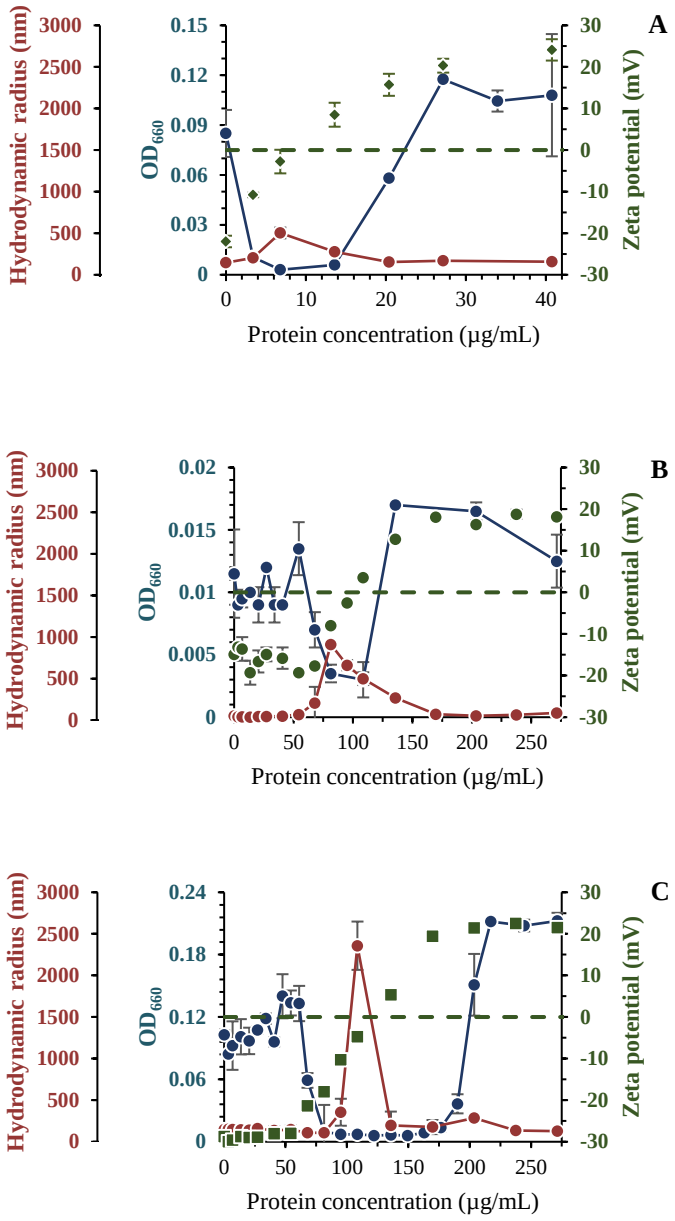

Figure 5.5. Superposition of coagulation micro-assay data from Figure 5.1 for 0.5 g/L kaolin (A), from Figure 5.2 for 10 ppm humic acid (B), and from Figure 5.3 for a mixture of 0.5 g/mL kaolin and 10 ppm humic acid (C) in diluted soft water with zeta potentials from Figure 5.4 and hydrodynamic radii from dynamic light scattering. Error bars represent the standard deviation of two replicates for coagulation micro-assays and three replicates for zeta potentials and hydrodynamic radii.

As previously stated, charge reversal occurs at a protein concentration of approximately 10, 100, and 120 µg/mL for kaolin, humic acid, and the mixture, respectively. Dynamic light scattering revealed a spike in particle size at 7, 81, and 109 µg/mL for kaolin, humic acid, and the mixture, respectively. The charge reversal concentrations and the particle size spike concentrations are both near the midpoint of the EPCC range for their corresponding turbid water sample. It is clear that as coagulants, *M. oleifera* proteins adsorb to and neutralize particles, which leads to flocculation, sedimentation, and ultimately, clarified water. Comparing the hydrodynamic radii at the particle size spike concentration, protein-kaolin aggregates have the smallest size at approximately 500 nm, followed by protein-humic acid aggregates at approximately 880 nm, and then protein-kaolin-humic acid aggregates at approximately 2,400 nm. Although an indirect comparison because of differences in ionic strength, these protein-particle aggregates are larger than the particle aggregates reported for soft water in Table 5.2. Finally, a small increase in hydrodynamic radius is observed at high protein concentrations for the three turbid water samples, which may be the cause of the increased optical density observed in the coagulation micro-assay.

5.3. Conclusions

M. oleifera proteins are effective coagulants against kaolin, humic acid, and mixtures of kaolin and humic acid in EPA model freshwaters. As water hardness increases, the range of effective coagulating protein concentrations broadens. Increasing water hardness also decreases the critical coagulation concentration for humic acid and the mixtures, but has no effect for kaolin. The critical coagulation concentration is an order of magnitude higher for humic acid and the mixtures than it is for kaolin. As humic acid concentration increases, the range of effective coagulating protein concentrations broadens, and the critical coagulation concentration increases.

Electrophoretic mobility and dynamic light scattering measurements suggest that humic acid adsorbs to kaolin in the model freshwaters. In diluted EPA model soft freshwater, a mixture of 0.5 g/L kaolin and 10 ppm humic acid has a more negative zeta potential than its individual components. The concentration at which charge reversal occurs was an order of magnitude lower for kaolin than for humic acid or the mixture, though the mixture required a higher protein concentration to cause charge reversal than humic acid alone. Size measurements show that particle size increases significantly for kaolin and the mixture as water hardness increases. The particle size of the mixture is on the same order of magnitude as the particle size of kaolin, but is consistently smaller, suggesting that kaolin was somewhat less aggregated in the presence of humic acid. These methods also confirm that the coagulation mechanism for kaolin using *M. oleifera* proteins in the presence of humic acid is adsorption and charge neutralization. The protein concentrations at which charge reversal and a spike in particle size occur closely resemble the median concentrations of the ranges of effective protein concentrations for kaolin, humic acid, and the mixture.

By systematically increasing the complexity of model freshwaters to include humic acid as a model for natural organic matter along with kaolin clay as a model for particulate matter, we have shown that *M. oleifera* proteins remain effective as coagulants when used to reduce turbidity in a multi-component system. Competitive adsorption between kaolin, humic acid, and the proteins creates a need for higher coagulant dosages in order to successfully clarify water, but it also broadens the protein concentration range for effective coagulation. It is likely that this trend will persist as other predominantly negatively charged components, such as microbes, are added to the water to be treated.

Chapter 6: *Moringa* oleifera seed protein adsorption to silica: Effects of water hardness, fractionation, and fatty acid extraction

6.1. Introduction

This work has been published in *Langmuir:* Nordmark, B. A.; Bechtel, T. M.; Riley, J. K.; Velegol, D.; Velegol, S. B.; Przybycien, T. M.; Tilton, R. D. *Moringa oleifera* seed protein adsorption to silica: Effects of water hardness, fractionation, and fatty acid extraction. *Langmuir* **2018** , *34* (16), 4852–4860. Motivated by the proposed use of cationic protein-modified sand for water filtration in developing nations, this study concerns the adsorption of *Moringa oleifera* seed proteins to silica surfaces. These proteins were prepared in model waters of varying hardness and underwent different levels of fractionation, including fatty acid extraction and cation exchange chromatography. Adsorption isotherms were measured by ellipsometry, and the zeta potentials of the resulting protein-decorated surfaces were measured by the rotating disk streaming potential method. The results indicate that the presence of fatty acids has little effect on the *M. oleifera* cationic protein adsorption isotherm. Adsorption from the unfractionated extract was indistinguishable from that of the cationic protein isolates at low concentrations but yielded significantly greater extents of adsorption at high concentrations. Adsorption isotherms for samples prepared in model hard and soft freshwaters were indistinguishable from each other over the measured bulk solution concentration range, but adsorption from hard or soft water was more extensive than adsorption from deionized water at moderate protein concentrations. Streaming potential measurements showed that adsorption reversed the net sign of the zeta potential of silica from negative to positive for all protein fractions and water hardness conditions at protein bulk concentrations as low as 0.03 μg/mL. This suggests that sands can be effectively modified with *M. oleifera* proteins using small amounts of seed extract under various local water hardness conditions. Finally, ellipsometry indicated that *M. oleifera* proteins adsorb

irreversibly with respect to rinsing with these model freshwaters, suggesting that the modified sand would be stable on repeated use for water filtration. These studies may aid in the design of a simple, effective, and sustainable water purification device for developing nations.

6.2. Results and Discussion

6.2.1. Adsorption isotherms

The following adsorption isotherms are compared: all-water-soluble proteins and isolated cationic proteins, both in deionized water and both with fatty acids removed (Figure 6.1); cationic proteins in deionized water with and without fatty acids (Figure 6.2); and all-water-soluble proteins with fatty acids removed in deionized water, EPA model soft freshwater, and EPA model hard freshwater (Figure 6.3).

6.2.1.1 All-water-soluble proteins versus cationic proteins

Figure 6.1 compares the adsorption isotherm for all-water-soluble proteins in deionized water to the isotherm for cationic proteins in deionized water, each with fatty acids removed. Comparing these adsorption isotherms isolates the effects of fractionating *M. oleifera* protein extracts, with no interference from residual bound fatty acids. Although deionized water is not a model for any natural water source, its extremely low ionic strength provides a stringent test of electrostatic interaction effects that may differentiate between protein samples that differ in their charge characteristics.

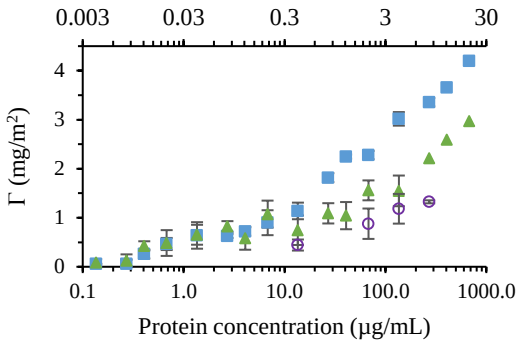

Figure 6.1. Adsorption isotherms for solutions of all-water-soluble proteins (blue squares), cationic proteins (green triangles), and non-cationic proteins (open purple circles), all with fatty acids removed and in deionized water. The primary horizontal axis indicates concentration for the solutions of all-water-soluble and cationic proteins. The secondary (upper) horizontal axis indicates concentration for the solutions of non-cationic proteins. Error bars are standard deviations of two to four replicate measurements.

The isotherms display three distinct regimes. A shoulder at intermediate concentrations separates two regimes at low and high concentrations where the surface excess concentration increases with bulk concentration. The all-water-soluble proteins isotherm and the cationic proteins isotherm are indistinguishable at protein concentrations up to 7 µg/mL. It should be noted that at these low concentrations, protein depletion from the bulk caused by adsorption could range from 17-85%, which could influence the shape of the isotherm. At concentrations of 14 µg/mL and above, adsorption from the all-water-soluble proteins sample produces significantly higher surface excess concentrations than the cationic protein fraction. The difference in surface excess concentrations far exceeds any difference that could be attributed to the two samples having slightly different refractive index increments.

An additional set of experiments was conducted to probe the source of the difference in the extent of adsorption at the higher bulk concentrations. The all-water-soluble proteins sample

consists of all of the cationic proteins plus all of the non-cationic proteins (operationally defined as proteins not retained on the cation-exchange column). The goal of the additional experiments was to determine whether the extent of adsorption from the all-water-soluble proteins samples at higher bulk concentrations was simply a linear combination of the extent of adsorption of cationic proteins and non-cationic proteins acting independently, or whether strong interactions among the different components yielded a more complex adsorption process.

Analysis of the seed protein extracts using the Pierce 660 nm Protein Assay showed that the protein extracts were 97 ± 0.3 wt% cationic proteins and 3 ± 0.3 wt% non-cationic. Thus, solutions of non-cationic proteins (with fatty acids removed) were collected from the cation-exchange column effluent and prepared in deionized water at four concentrations ranging from 0.4 to 8 μg/mL. This concentration range matches the concentrations of non-cationic proteins that are present in the all-water-soluble protein samples at total concentrations ranging from 14 to 272 μg/mL.

Ellipsometry results for non-cationic protein adsorption are also plotted in Figure 6.1 on the secondary (upper) horizontal axis, which is scaled so that the non-cationic protein data can be aligned with the corresponding total protein concentration for the all-water-soluble proteins. In all cases, the sum of the surface excess concentrations produced by the cationic and non-cationic proteins is similar to the surface excess concentrations produced by the all-water-soluble proteins samples. It appears that non-cationic and cationic proteins adsorb in a simple additive manner, with no significant contribution from interactions between those components.

Kwaambwa *et al.*[66] used neutron reflectometry with a silicon crystal (111 plane) to construct an adsorption isotherm for cationic *M. oleifera* proteins from which fatty acids had

been removed. Their isotherm reached a surface excess concentration plateau of 5.7 mg/m^2 at a 250 µg/mL bulk protein concentration. At the same bulk concentration, our cationic protein isotherm shows a surface excess concentration of ~2.2 mg/m^2, and the adsorption isotherm had not yet reached a plateau at 680 µg/mL, the highest concentration considered here. The discrepancy may derive from variation in protein content depending on the seed origin[43]. *M. oleifera* seeds have more than eight distinct cationic protein fractions with different cation exchange resin affinities and molecular weights, and these vary in their relative amounts according to the geographical seed source[43]. This discrepancy could also be attributed to the methods by which protein concentration was determined. Kwaambwa *et al*. measured lyophilized protein powder, whereas this study used a protein assay. There were also differences in protein fractionation methods, which could be significant since fractionation was shown here to have quite significant effects on the adsorption isotherms. For these reasons, we emphasize the relative effects of different degrees of seed extract purification and different water compositions in this study more than absolute quantitative values for surace excess concentrations.

6.2.1.2. Fatty acids versus fatty acids removed

M. oleifera seeds are approximately 35 wt% fatty acids[19], with the main fatty acids being oleic acid (69 wt%), palmitic acid (10 wt%) and stearic acid (8 wt%)[88]. Protein-bound fatty acids may be expected to affect the adsorption affinity of cationic *M. oleifera* proteins on negatively charged silica by altering the protein net charge and by introducing hydrophobic alkyl chains to the protein surface. The protein-surface interactions could be expected to change, as could inter-protein interactions within an adsorbed layer. In order to analyze the amount of fatty acids that are associated with the aqueous protein extracts, an aqueous seed extract was lyophilized (Vertis Unitrap II, Gardiner, NY) and the resulting powder was de-fatted with petroleum ether using the

same procedure described above for de-fatting crushed seeds. Comparing the mass before and after de-fatting showed that the aqueous seed extract was approximately 90 wt% protein and 10 wt% fatty acids; not all fatty acids from the seeds are extracted with the proteins. Figure 6.2 compares adsorption isotherms for cationic *M. oleifera* proteins in deionized water, with or without fatty acid removal. This comparison shows that protein-bound fatty acids have no significant effect on the adsorption behavior of the cationic proteins. The three distinct isotherm regimes noted in Figure 6.1 are present and are indistinguishable in the isotherms for proteins with or without fatty acids.

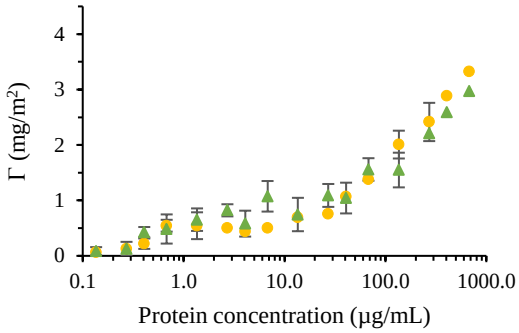

Figure 6.2. Adsorption isotherms for solutions of cationic proteins with fatty acids (yellow circles) and cationic proteins with fatty acids removed (green triangles, data replotted from Figure 6.1), both in deionized water. Error bars are standard deviations of two to four replicate measurements.

6.2.1.3. Effect of water hardness

Figure 6.3 shows a comparison of the adsorption isotherms for all-water-soluble proteins with fatty acids removed in deionized water, model soft freshwater, and model hard freshwater. The adsorption isotherms for soft and hard water are quite similar to each other, but they do differ from the deionized water isotherm. The primary effect of water hardness appears in the transitional region of the isotherm, observed at intermediate protein concentrations between 1

and 27 µg/mL. There, the isotherm for deionized water exhibits significantly lower surface excess concentrations than its soft water and hard water counterparts. At protein concentrations lower than 1 µg/mL and higher than 27 µg/mL, the three isotherms display similar surface excess concentrations.

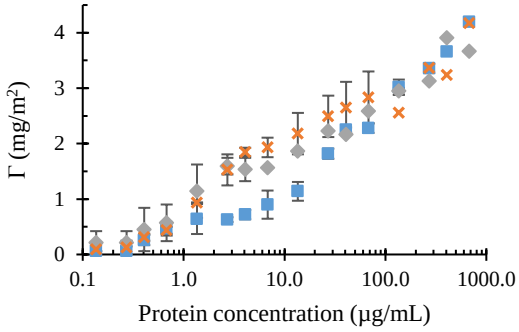

Figure 6.3. Adsorption isotherms for solutions of all-water-soluble proteins in deionized water (blue squares, data replotted from Figure 6.1), in model soft freshwater (gray diamonds), and in model hard freshwater (orange crosses), all with fatty acids removed. Error bars are the standard deviation of two to four replicate measurements.

The model soft and hard waters differ in ionic strength and slightly in pH. The Debye lengths are 6.4 nm and 3.2 nm in soft and hard water, respectively. Since the dilute ionic compositions of the protein solutions in deionized water are not known, we cannot reliably estimate a Debye length, but it is certain that it is larger than the Debye length in the soft and hard model waters. It is notable that the only distinction between isotherms occurs in the intermediate transitional region of the isotherm where the effects of intermolecular interactions on the adsorbed layer organization may be expected to be important. Evidently, it is here where the long range electrostatic interactions associated with the very large Debye lengths expected in the deionized water samples are most influential. Although they do differ from each other, the

Debye lengths in model soft and hard water are both roughly on the order of *M. oleifera* protein dimensions (1.3 nm hydrodynamic radius[43]). As a result, lateral electrostatic interactions among adsorbed proteins would be mostly limited to nearest neighbor interactions in the soft and hard waters, while they may exert more long ranged effects on layer organization in deionized water.

The similar surface excess concentrations between the deionized, soft and hard water isotherms outside of the intermediate concentration regime indicate that the levels of electrostatic screening in these waters are insufficient to significantly affect the protein affinity for the bare, negatively charged silica surface at the lowest concentrations or the energetics of filling in a dense adsorbed layer at the higher concentrations.

6.2.1.4. Area fraction coverage

All five isotherms exhibit a shoulder in surface excess concentration at intermediate bulk concentrations, although the effect is weakest for the hard water isotherm in Figure 6.3. Shoulders in isotherms have been attributed in some cases to a transition from monolayer to multilayer adsorption or to absorbed layer rearrangements[80,89,90]. In order to explore the origins of the isotherm shoulders, the surface excess concentration at which a complete monolayer forms, Γ_{mon}, was estimated for both the hexagonal close packing (HCP) limit and for the random sequential adsorption (RSA) jamming limit. HCP ordering requires post-adsorption mobility of proteins and is the extreme case for monolayer packing. The RSA jamming limit presumes no post-adsorption protein mobility and represents a lower bound for monolayer saturation. Protein layers may contain both mobile and immobile proteins[91–94], so actual monolayer limits will likely fall in between these two cases. These estimates of Γ_{mon} were compared to the surface excess concentrations achieved in the five adsorption isotherms to judge whether multilayer adsorption

might be occurring. Since the protein samples are heterogeneous, the purpose of this analysis is to make a reasonable determination of the likelihood of multilayer adsorption.

The surface excess concentration at which a complete monolayer forms was predicted according to these two-dimensional packing considerations as:

$$\Gamma_{mon} = \frac{M_w \Theta_m}{\pi R_h^2 N_A} \tag{6.1}$$

Here, M_w is the molecular weight of the adsorbed species, Θ_m is the area fraction that specifies saturated monolayer coverage, R_h is the hydrodynamic radius of the adsorbing species, and N_A is Avogadro's number. Θ_m = 0.91 for HCP and 0.545 for RSA[95], assuming spherical proteins. This expression predicts surface excess concentration at which a complete monolayer forms based on area fraction.

Given the likely heterogeneity of the adsorbed layer composition, an alternative approach was considered as well, where the effective three-dimensional protein mass density of the adsorbed layer was compared to the protein mass per unit volume in the crystalline state, assuming that the crystalline state would represent a reasonable upper bound on protein packing. *M. oleifera* protein crystals contain approximately 50% water[96]. By this reasoning, an upper bound is placed on the surface excess concentration that can be contained in a monolayer if its protein mass per unit volume of the adsorbed layer exceeds that of the crystalline state. Thus a saturated monolayer surface excess concentration can be estimated as:

$$\Gamma_{mon} = \frac{d \rho_w \rho_p}{\rho_w + \left(\frac{\phi_w}{1 - \phi_w}\right) \rho_p} \tag{6.2}$$

Here, d is the monolayer thickness, ρ_w is the density of water, ρ_p is the density of protein, and ϕ_w is the mass fraction of water in the adsorbed layer (taken as 0.5 to be similar to the crystal water content)[96]. For either approach, the hydrodynamic radius was approximated using the empirical correlation:[97]

$$R_h = 0.066 M_W^{\frac{1}{3}} \tag{6.3}$$

This equation yields hydrodynamic radius in nanometers when molecular weight is expressed in Daltons. The hydrodynamic radius was used to calculate protein density in Equation 6.4:

$$\rho_p = \frac{MW}{N_A \frac{4}{3} \pi R_h^3} \tag{6.4}$$

The molecular weights used for these two analyses included the high, low, and weighted average molecular weights of *M. oleifera* proteins as determined by SDS-PAGE from Nordmark *et al*.[43] (48.2, 10.9, and 17.3 kDa) as well as the molecular weights most commonly reported in the literature for *M. oleifera* protein monomers, dimers, and tetramers (6.5, 13.0, and 26.0 kDa)[19,25,27,32,34,35].

The smallest and largest possible values of Γ_{mon} predicted using Equation 6.1 for the RSA jamming limit were 1.2 and 2.4 mg/m^2, calculated for molecular weights of 6.5 and 48.2 kDa, respectively. All adsorption isotherms produced surface excess concentrations that exceeded the RSA upper value for monolayer adsorption. The HCP limit provides a more stringent test for multilayer adsorption. The smallest and largest possible values of Γ_{mon} for the HCP limit using Equation 6.1 were 2.1 and 4.0 mg/m^2, calculated for molecular weights of 6.5 and 48.2 kDa, respectively. Only the isotherms for all-water-soluble proteins in deionized and hard water exceeded the upper value for HCP monolayer adsorption. The isotherms for all-water soluble

proteins in soft water and cationic proteins with fatty acids exceeded the Γ_{mon} for a 26 kDa protein of 3.3 mg/m^2, and the isotherm for cationic proteins without fatty acids exceeded the Γ_{mon} for a 17.3 kDa protein of 2.9 mg/m^2.

Assuming that *M. oleifera* protein layer thickness is equal to twice the protein hydrodynamic radius, Equation 6.2 predicted that the smallest and largest possible values of Γ_{mon} were 1.4 and 2.8 mg/m^2, calculated for molecular weights of 6.5 and 48.2 kDa, respectively. All adsorption isotherms produced surface excess concentrations that exceeded the upper value for monolayer adsorption. Between these two analyses, it is very likely that *M. oleifera* seed proteins adsorb beyond monolayer coverage on silica surfaces. The neutron reflectivity measurements reported by Kwaambwa *et al*.[66] also suggested multilayer adsorption for a cationic *M. oleifera* seed protein fraction.

6.2.2. Streaming potential measurements

It has been established that adsorption of cationic proteins to negatively charged silica surfaces can result in a net surface charge reversal[80,98]. Here we used streaming potential measurements to monitor the change in zeta potential of silica surfaces caused by protein adsorption. The goal of these experiments was to determine the minimum protein concentration required to produce surface charge reversal. Understanding the net charge reversal behavior will be useful for further understanding of how f-sand will interact with negatively charged water contaminants such as natural organic matter, suspended clay particles, or bacteria. While ellipsometry showed that *M. oleifera* seed proteins can produce very large surface excess concentrations that likely exceed monolayer coverage at higher bulk protein concentrations, it may not be necessary to produce such dense adsorbed layers when the goal is simply to electrostatically harvest negatively charged contaminants from drinking water sources. Using the

minimum bulk concentration needed to produce surface charge reversal would conserve materials for f-sand production.

Streaming potential measurements were made at bulk protein concentrations of 0.02, 0.2 and 2 µg/mL for the five protein/water cases studied. Deionized water was replaced by 0.5 mM sodium chloride solutions in order to have an unambiguous ionic strength for zeta potential determination. Zeta potentials produced by protein adsorption from each of the five protein/water combinations are shown in Figure 6.4.

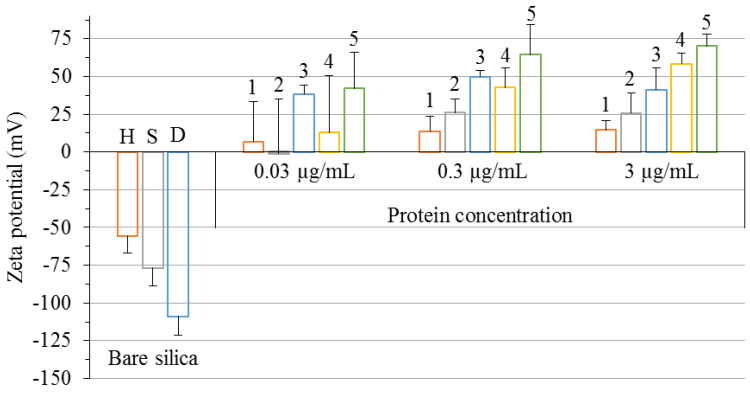

Figure 6.4. Zeta potentials for *M. oleifera* proteins adsorbed to silica. For bare silica H, S, and D denote hard water, soft water and 0.5 mM sodium chloride soluton in otherwise deionized water, respectively. Protein adsorption conditions are denoted by numeric code: 1) all water soluble proteins, hard water, no fatty acids; 2) all water soluble proteins, soft water, no fatty acids; 3) all water soluble proteins, 0.5 mM sodium chloride, no fatty acids; 4) cationic proteins, 0.5 mM sodium chloride, with fatty acids; 5) cationic proteins, 0.5 mM sodium chloride, no fatty acids. Bars represent the averages of three individual trials, and error bars represent the standard deviations. The lower portion of each error bar is omitted to avoid crowding the figure.

The first comparison to be made is between the bare silica surfaces in model hard freshwater, model soft freshwater, and 0.5 mM sodium chloride solution. The Graham Equation was used to estimate the surface charge density for wafers in each of these waters: one negative

charge per 860 $Å^2$ for hard water, one negative charge per 890 $Å^2$ for soft water, and one negative charge per 1,500 $Å^2$ for 0.5 mM sodium chloride. The smaller surface charge density in 0.5 mM NaCl is likely due to the lower pH, 6.0, of this water composition.

Case 3 (all-water-soluble proteins) and case 5 (cationic proteins) were dissolved in 0.5 mM sodium chloride with fatty acids removed. Both cases produced surface charge reversal even at the lowest solution concentration examined, 0.03 μg/mL. Ellipsometry for these cases (in deionized water) showed similar surface excess concentrations for the two cases at bulk protein concentrations of 7 μg/mL and below (Figure 6.1). Nevertheless, the cationic proteins produced a more positive zeta potential than did the all-water-soluble proteins across the three orders of magnitude of bulk protein concentration examined. Although the difference in zeta potential between these two cases was only significant ($p < 0.05$) at a bulk protein concentration of 3 μg/mL, a trend of increasing significance (decreasing p values) was observed with increasing bulk protein concentration. While the same mass was adsorbed per unit area of silica surface at 0.3 μg/mL and 3 μg/mL bulk concentrations (ellipsometry), the charge distributions in the adsorbed layers are different, with the layer formed by cationic proteins presenting more positive charge at the plane of shear.

Comparing cationic proteins with fatty acids to those without fatty acids (case 4 vs. case 5), the cationic proteins without fatty acids (case 5) produced a more positive zeta potential for each of the protein concentrations studied, but the statistical significance of this conclusion is modest ($p = 0.31$, 0.19, and 0.13 for 0.03, 0.3, and 3 μg/mL, respectively). The cationic proteins produced similar surface excess concentrations with and without fatty acids as reported by ellipsometry (Figure 6.2). Although the fatty acids do not significantly alter the adsorption of mass to silica, they do somewhat decrease the positive charge exposed at the shear plane.

Comparing all-water-soluble proteins without fatty acids in model hard and model soft freshwaters to those in 0.5 mM sodium chloride solution (cases 1, 2, and 3, respectively), the proteins in 0.5 mM sodium chloride produced the highest positive zeta potential for the two highest bulk concentrations, followed by the proteins in soft water, and then by the proteins in hard water, as would be expected based on the Debye lengths in these model waters for similar extents of adsorption. In Figure 6.3, all-water-soluble proteins produced similar surface excess concentrations in the three different model waters at 0.3 μg/mL, but higher surface excess concentrations were produced at 3 μg/mL for the proteins in soft and hard water. Most importantly, the proteins produced a significant surface charge reversal in each model water at bulk concentrations of just 0.3 μg/mL.

The zeta potential is the electrical potential at the plane of shear. As such, in the presence of an adsorbed protein layer of finite thickness, it can be sensitive not only to the total charge at an interface but also to the spatial distribution of charge within the adsorbed layer. During protein adsorption, charge is redistributed throughout the layer, and counterions are recruited into the layer to avoid charge buildup[98]. Furthermore, changes in protein orientation as the adsorbed layer builds up may result in differently-charged regions of the protein surface being exposed at the effective shear plane over the complex surface, with a resulting effect on the correlation between surface concentration and zeta potential[80]. Given the heterogeneous protein population in the seed extracts, it is likely that the relative amounts of different protein sub-fractions (with varying degrees of cationic character[43]) in the adsorbed layers are not constant as the surface excess concentration changes. These complexities complicate the relationship between zeta potential and surface excess concentration for proteins relative to the more well-behaved relationship between zeta potential and surface coverage for layers of uniformly charged

spherical colloids[99]. Nevertheless, it is informative to relate the measured zeta potentials to surface excess concentrations.

At the lowest protein concentration considered in ellipsometry experiments, 0.1 µg/mL, the surface excess concentrations were low, falling in the range of 0.05 – 0.25 mg/m^2 for each protein and water sample. This is near the limit of detection for ellipsometry. Streaming potential measurements indicated that protein adsorption from even more dilute solutions of 0.03 µg/mL was sufficient to reverse the surface zeta potential from negative for bare silica to positive for all protein and water cases studied except case 2 (all water soluble proteins, soft water, no fatty acids) which produced a near-zero zet potential. A quick calculation to estimate the surface excess concentration of protein required to cause surface charge reversal (protein surface concentration that just neutralizes the bare surface charge density reported for each water hardness above), assuming the monomeric protein molecular weight and eight positive charges per protein[38] revealed the following: For silica surfaces in 0.5 mM sodium chloride solution, model soft water, and model hard water, the required surface excess concentration to cause charge reversal was estimated to be 0.09, 0.15, and 0.16 mg/m^2, respectively. These surface excess concentrations are comparable to those measured by ellipsometry at the low ends of the adsorption isotherms.

6.2.3. Protein desorption

F-sand performance requires that protein adsorption should be irreversible wth respect to rinsing or else the protein would be washed off the sand during water filtration. A desorption experiment was conducted using ellipsometry in order to establish the robustness of adsorbed *M. oleifera* cationic protein layers (with fatty acids) on silica, the results of which are shown in Figure 6.5.

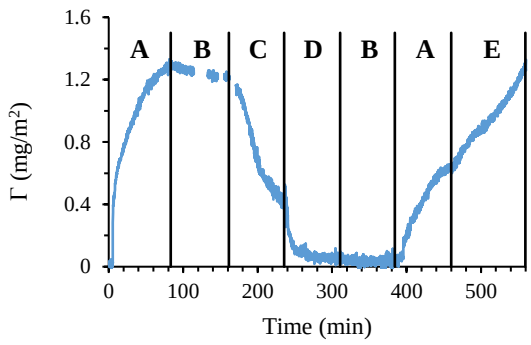

Figure 6.5. Time resolved ellipsometry measurement of a 68 µg/mL solution of all-water-soluble *M. oleifera* proteins with fatty acids in deionized water adsorbing to and then desorbing from a silica suface. A: Protein adsorbing under flow. B: Deionized water rinse. C: 0.5 M sodium chloride rinse. D: 1 M sodium chloride rinse. E: Continued protein adsorption with no flow.

After pumping 50 mL of a 68 µg/mL solution of all-water-soluble proteins with fatty acids in deionized water through the flow cell for 80 minutes, the surface excess concentration reached approximately 1.3 mg/m^2. Subsequent rinsing with deionized water for 80 minutes caused only a slight desorption of 8% of the adsorbed material to a surface excess concentration of 1.2 mg/m^2, indicating that *M. oleifera* proteins adsorb nearly irreversibly to silica at low ionic strength. Next, in order to test the ability to regenerate a *M. oleifera* protein-coated surface, as would be desired for field applicaton of an f-sand filtration system, the adsorbed layer was rinsed with a 0.5 M sodium chloride solution. The surface excess concentration decreased to approximately 0.45 mg/m^2 after 80 minutes, a removal of 58% of the initial adsorbed material. Finally, a 1 M sodium chloride solution rinse was conducted for 80 minutes, during which the surface excess concentration rapidly decreased to approximately 0.05 mg/m^2. This rinse removed an additional 31%, leaving behind only 3% of the initial adsorbed material. Before attempting to

re-adsorb protein, the system was flushed with deionized water for 80 minutes, after which adsorption from a fresh 68 μg/mL protein solution was initiated and produced a similar surface excess concentration as was produced on the fresh silica surfaces. In practical terms, this provides a simple scheme for removing these proteins from negatively-charged sand granules when cleaning and regenerating active f-sand surfaces is required.

6.3. Conclusions

Ellipsometry revealed that adsorption from a solution of all water-soluble *Moringa oleifera* seed proteins produces greater surface excess concentrations on negatively charged silica surfaces than a solution of cationic proteins. Fatty acids do not interfere with the adsorption of *M. oleifera* seed proteins to silica. Water hardness does affect adsorption to silica. Proteins in model soft or hard freshwater adsorb to a greater extent on silica than proteins in deionized water at intermediate bulk protein concentrations, but the extent of adsorption from deionized, soft and hard model waters was indistinguishable at the low and high concentration regimes of the adsorption isotherms. Thus, the primary practical effect of water hardness on *M. oleifera* seed protein adsorption is fairly modest, as it is limited to a shift in a transitional regime of the adsorption isotherm, and soft and hard waters yielded adsorption isotherms that were quite similar to each other. Estimates of the surface excess concentrations that correspond to monolayer saturation suggest that adsorption most likely exceeds saturated monolayer coverage for each combination of protein fractionation and water hardness at higher bulk concentrations.

Streaming potential measurements showed that dilute solutions of *M. oleifera* proteins cause a net charge reversal of silica surfaces from negative to positive and that a solution of cationic proteins will produce a more positive zeta potential than a solution of all-water-soluble proteins. Although fatty acids have no significant effect on the extent of adsorption, they do tend

to somewhat decrease the extent of surface charge reversal caused by cationic protein adsorption to silica. *M. oleifera* seed proteins are capable of producing dense layers that exceed monolayer saturation, but such high coverages are not necessary to produce net charge reversal of silica from negative to positive. This is a particularly significant finding in the practical sense since it suggests that dilute solutions would be sufficient to produce f-sand with a net positive charge for use in potable water treatment in resource-limited regions of the developing world.

It is also significant in the practical sense that adsorbed *M. oleifera* seed protein layers are resistant to desorption during rinsing. The retention of a robust adsorbed layer would allow f-sand to be used to filter large volumes of drinking water. When necessary to clean and regenerate f-sand, the current research indicates that rinsing in concentrated sodium chloride solutions (0.5 to 1 M) would remove nearly all of the adsorbed proteins in a short time and leave the surface in a state that can readily accommodate re-adsorption from a fresh *M. oleifera* seed protein solution.

Chapter 7: Selective adsorption of *Moringa oleifera* proteins to quartz sand granules and its role in functionalized sand filter performance

7.1. Introduction

This work is part of a manuscript in preparation titled "Selective adsorption of *Moringa oleifera* proteins to quartz sand granules and its role in functionalized sand filter performance" by the authors Brittany A. Nordmark, Todd M. Przybycien, and Robert D. Tilton. Filters containing sand functionalized with adsorbed *Moringa oleifera* proteins (f-sand) have the potential to treat drinking water while reducing concentrations of natural organic matter in the treated water. Here we study the effects of water hardness on *M. oleifera* protein adsorption to sand granules, the composition and coverage of the adsorbed protein layer on f-sand granules, and the influence of layer composition on f-sand filter performance. Four f-sands with varying compositions and coverages of adsorbed proteins were created in EPA model soft and hard freshwaters by varying the weight percent of sand in protein-sand slurries. The adsorbed layers were characterized by their non-cationic, moderately cationic, and highly cationic species content as determined by retention on a cation exchange chromatography column using step gradients. *M. oleifera* protein fractions are expected to compete for adsorption to silica sand granules, generally in response to cationic charge. When sand adsorption sites are limited, the highly cationic fraction dominates the adsorbed protein layer composition in both soft and hard water. F-sand filter performance was tested against kaolin, humic acid, and a mixture of the two model contaminants. Adsorbed protein layer composition did not affect f-sand filter performance against the turbid waters, showing that minimal protein surface coverage can produce effective f-sand. For the f-sand filters, 50% breakthrough was observed after 4.9-6.4 column volumes for humic acid and the mixture in soft water, but after 8.0-9.5 column volumes for these model contaminants in hard water. 50% breakthrough was not observed in the f-sand filters against

kaolin. For the negative control non-functionalized sand filter, 50% breakthrough was observed after less than 1 column volume.

7.2. Results and Discussion

7.2.1. Total protein adsorption to sand granules

Previously constructed isotherms for the adsorption of *M. oleifera* proteins onto oxidized silicon wafers[65] were used to estimate the appropriate range of protein-sand ratios for experimentation. It was assumed that sand granules are smooth, spherical, and have radii equal to the mean sand granule radius (127 µm). From our isotherms, it was predicted that it would take approximately 1.5 mg of protein, from the 3 mg of protein contained in a 30 mL solution of 100 µg/mL of all water soluble proteins (in either soft or hard water), to saturate the available surface area of 32 g of sand (52% w/w), leaving 1.5 mg of protein in solution. However, it was found that nearly all 3 mg of protein adsorbed to the 32 g of sand, demonstrating that the surface area of the sand was under-estimated. For this reason, 4, 8, and 16 g of sand (corresponding to 12, 21, and 35% w/w sand) were also exposed to the same identical protein solution aliquots. Figure 7.1 shows the percent of total protein adsorbed from soft and hard water versus the weight percent of sand in each slurry (A) as well as the corresponding adsorption isotherms for proteins adsorbed from soft and hard water (B). Slurries are referred to in the format SX, where X is the weight percent of sand in the slurry.

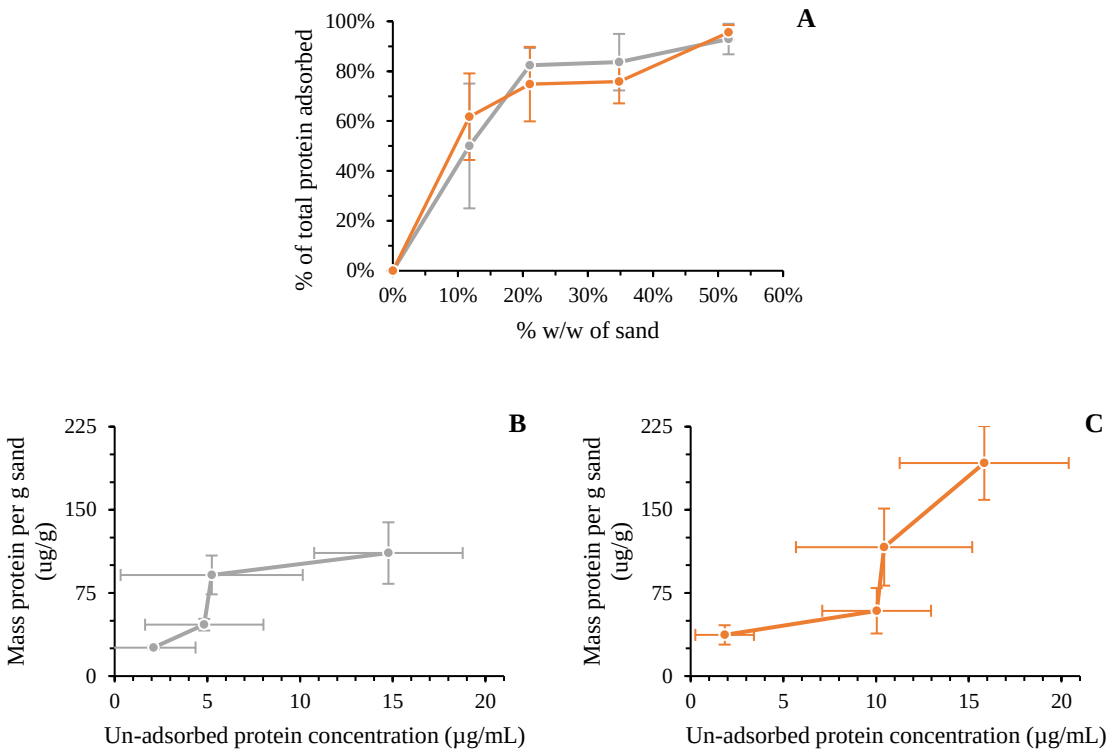

Figure 7.1. Percent of total protein adsorbed to sand versus the weight percent of sand in each slurry (A) for soft (gray) and hard (orange) water as well as the adsorption isotherms for proteins adsorbed to sand in soft (B) and hard (C) water. Proteins were adsorbed from 30 mL aliquots of 136 µg/mL of all-water-soluble protein solution. Error bars are the standard deviation of two to three replicate measurements.

From Figure 7.1A, it is evident that water hardness has minimal effect on the total amount of protein adsorbed from the extract to silica sand granules. From both waters, approximately 50-62% of total protein adsorbs in a slurry containing 12% w/w sand, 74-84% of total protein adsorbs in a slurry containing 21-35% w/w sand, and 93-96% of total protein adsorbs in a slurry containing 52% w/w sand. Figures 7.1B and 7.1C show that the isotherms for soft and hard water have similar shapes with an abrupt increase in slope at some intermediate concentration. The isotherm transition for proteins adsorbed from hard water is shifted to lower

bulk un-adsorbed protein concentrations, likely caused by increased screening of lateral electrostatic repulsions in the adsorbed layers formed in the model hard water.

7.2.2. Composition of the adsorbed protein layer

The supernatants of the protein solutions exposed to sand were collected, concentrated, and injected onto the cation exchange column for analysis. Using HPLC and a stepwise gradient, three fractions were collected: the non-cationic flow-through, the moderately cationic species (proteins that eluted when exposed to 0.8 M sodium chloride) and the highly cationic species (proteins that eluted when exposed to 1.3 M sodium chloride). These fractions were collected, concentrated, and assayed with the Pierce® 660 nm Protein Assay to determine the protein mass through concentration and the known volumes. Figure 7.2 shows the relative compositions of the adsorbed protein layers versus the weight percent of sand in the slurry in soft (A) and hard (B) water.

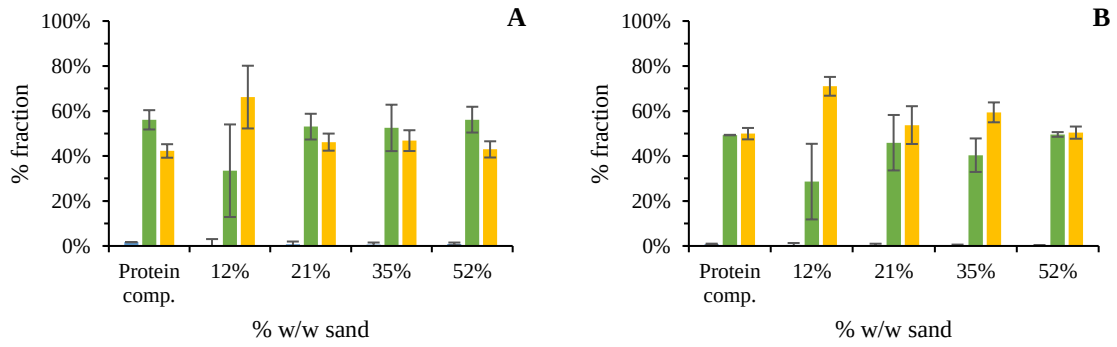

Figure 7.2. Relative compositions of adsorbed protein layers versus weight fraction of sand in soft (A) and hard (B) water. "Protein comp." is the bulk composition of the protein solutions used to create the slurries. The adsorbed layer is composed of three fractions: the non-cationic flow-through (blue), the moderately cationic species (green), and the highly cationic species (yellow). The flow-through is a negligible component of the adsorbed layer and barely visible as the first bars in the figures. Error bars are the standard deviation of two to three replicate measurements.

For both soft and hard waters, the non-cationic flow-through is less than or equal to 1% of the adsorbed layer, making it a negligible component. When sand granule adsorption sites are limited, as with the case for 12% w/w sand slurries, the highly cationic fraction dominates the adsorbed layer in both soft and hard water, comprising approximately 70% of the total adsorbed protein. This implies that there is electrostatic competition between the moderately and highly cationic fractions, with the highly cationic fraction having a higher adsorption affinity to the sand granules. In soft water, the moderately cationic fraction is a consistently higher percentage of the adsorbed layer than the highly cationic fraction from 21-52% w/w sand slurries. In hard water, the opposite is true, with the highly cationic species consistently comprising a higher percentage of the adsorbed layer than the moderately cationic species in 21-52% w/w sand slurries. This can likely be attributed to lateral electrostatic repulsions in soft water favoring adsorption of moderately cationic proteins, while in hard water, these repulsions are screened and adsorption of highly cationic proteins is favored. As the weight percent of sand in the slurry increases and adsorption sites become more plentiful, the composition of the adsorbed layer approaches the composition of the protein solution used to create the slurries.

With the composition of the adsorbed layer established, the adsorption affinities of each fraction as well as the selectivity between fractions were calculated using Equations 7.1 and 7.2, respectively.

$$A_i = \frac{q_i}{c_i} \tag{7.1}$$

$$S_{ij} = \frac{q_i}{q_j} \cdot \frac{c_j}{c_i} \tag{7.2}$$

Here, q is the concentration of proteins adsorbed to sand in µg protein/g sand, and c is the bulk concentration of protein after adsorption in µg protein/mL solution. Affinity has units of mL solution/g sand, and selectivity has no units. Tables 7.1 and 7.2 give the adsorption affinities of the three fractions and the selectivities between the fractions in the soft and hard water slurries, respectively.

Table 7.1. Adsorption affinities for the three fractions in the soft and hard water slurries. Adsorption affinity is given in mL/g sand.

Water type	Fraction	S12	S21	S35	S52
Soft	Non-cationic flow-through	0.4	0.7	0.3	0.2
	Moderately cationic	37	48	24	14
	Highly cationic	73	42	22	11
Hard	Non-cationic flow-through	0.8	0.4	0.1	0.01
	Moderately cationic	55	53	24	18
	Highly cationic	136	63	35	19

The non-cationic flow-through has the lowest adsorption affinity of the three fractions in all soft and hard water slurries. These affinities are consistently less than 1. For the S12 slurry, the case where sand granule adsorption sites are most limited, the highly cationic fraction has the highest adsorption affinity in both soft and hard water. As the weight percent of sand in the slurries increases, the highly cationic fraction continues to have the highest adsorption affinity in hard water, but the moderately cationic fraction has the highest adsorption affinity for these slurries in soft water. The ratio of affinities for the highly cationic fraction to the moderately cationic fraction approaches unity as weight percent of sand in the slurries increases.

Table 7.2. Selectivity between the non-cationic flow-through (F), the moderately cationic fraction (M), and the highly cationic fraction (H), in the soft and hard water slurries.

Water type	Selectivity	S12	S21	S35	S52
Soft	S_{HM}	9	3	4	1
	S_{HF}	30	15	25	17
	S_{MF}	4	6	7	13
Hard	S_{HM}	13	2	6	1
	S_{HF}	15	8	28	536
	S_{MF}	1	4	5	484

The selectivities between the three fractions show that in both waters, the highly cationic fraction adsorbs preferentially to the moderately cationic fraction, and that the moderately cationic fraction adsorbs preferentially to the non-cationic flow-through. There is no adsorption preference between the highly cationic and the moderately cationic fractions for the S52 slurry in soft and hard water, nor between the moderately cationic and non-cationic flow-through fractions for the S12 slurry in hard water. The exceptionally high selectivities in hard water between the highly cationic fraction and the non-cationic flow-through and between the moderately cationic fraction and the non-cationic flow-through seen for the S52 slurry in hard water stems from the very small adsorption affinity of the non-cationic flow-through in this slurry.

7.2.3. F-sand filters

F-sand filters were constructed using the f-sands created with 12, 21, 35, and 52% w/w sand slurries in both soft and hard water to investigate the effect of adsorbed protein layer composition on filter performance. In each case, f-sand was prepared in the same model water as was used to test its filtration performance. Filters are referred to in the format FX, where X is the weight percent of sand in the original slurry. The f-sand filters were tested in their respective EPA freshwaters against three turbid water models: 5 ppm humic acid, 0.05 g/L kaolin, and a

mixture of 5 ppm humic acid and 0.05 g/L kaolin. Non-functionalized sand filters were also constructed and tested against these turbid waters to act as negative controls. All filters were constructed with 16 g of sand, resulting in a column bed volume of 10 mL.

Two metrics were used to access filter performance: the number of column volumes at which 50% breakthrough occurs and the filter capacity per bed volume. 50% breakthrough is defined as the ratio of the optical density of the filter effluent to the optical density of the turbid water entering the filter equaling 0.5. Capacity is a measure of the amount of mass per unit bed volume retained by the filter. This quantity was found by integrating the area between the breakthrough curves up until 50% breakthrough and the $OD_{300}/OD_{300,0} = 1$ line, which gives capacity in units of $OD_{300}/OD_{300,0}$ • mL filtered water per mL filter bed. If multiplied by initial turbid water concentration, capacity can be obtained in terms of particulate mass per mL filter bed. This is valid for turbid waters containing only kaolin or only humic acid. The number of column volumes at which 50% breakthrough occurs and the filter capacity per bed volume are summarized for each breakthrough curve in Tables 4 and 5, respectively.

7.2.3.1. Filters tested against kaolin

Figure 7.3 shows the breakthrough curves for the f-sand filters and the bare sand filters tested against turbid water containing 0.05 g/L kaolin in soft (A) and hard (B) water.

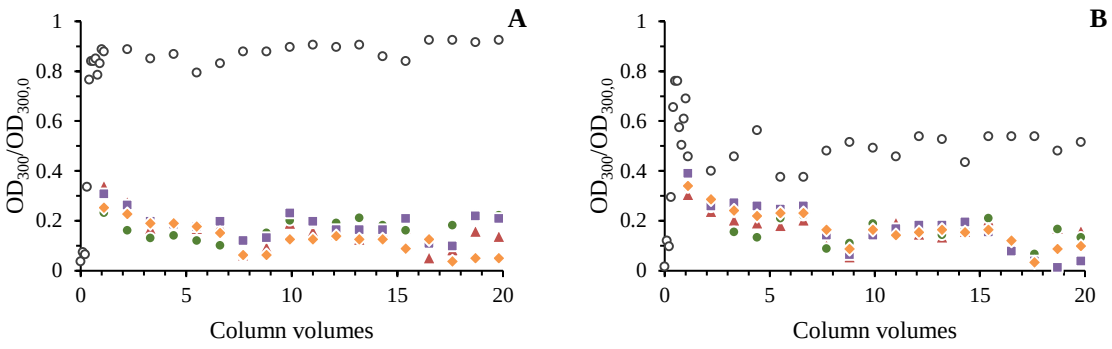

Figure 7.3. Breakthrough curves for f-sand filters tested for removal of 0.05 g/L kaolin in soft (A) and hard (B) water. Filters tested were non-functionalized sand (open black circles), F12 (maroon triangles), F21 (dark green circles), F35 (purple squares) and F52 (peach diamonds).

The four f-sand filters behaved similarly to one another against kaolin in soft and hard water, respectively. In both waters for all f-sand filters, 50% breakthrough of kaolin was never observed. Approximately 35-40% breakthrough was initially observed followed by a decrease in optical density, likely corresponding to aggregated kaolin being retained by the filters. For the bare sand filters, 50% breakthrough was observed after less than one column volume in both soft and hard water. The capacity of the bare filter in both waters was 0.03 $OD_{300}/OD_{300,0}$ • mL filtered water per mL filter bed. The bare sand filter produced hard water with 40% breakthrough between 1 and 20 column volumes. In a previous study[43], we showed that EPA model hard water induces flocculation of kaolin in the absence of proteins. The better performance of the bare sand filter against kaolin in hard water than in soft water could be attributed to kaolin aggregating and either being retained by the filter.

7.2.3.2. Filters tested against humic acid

Figure 7.4 shows the breakthrough curves for the f-sand filters and the bare sand filters tested against turbid water containing 5 ppm humic acid in soft (A) and hard (B) water.

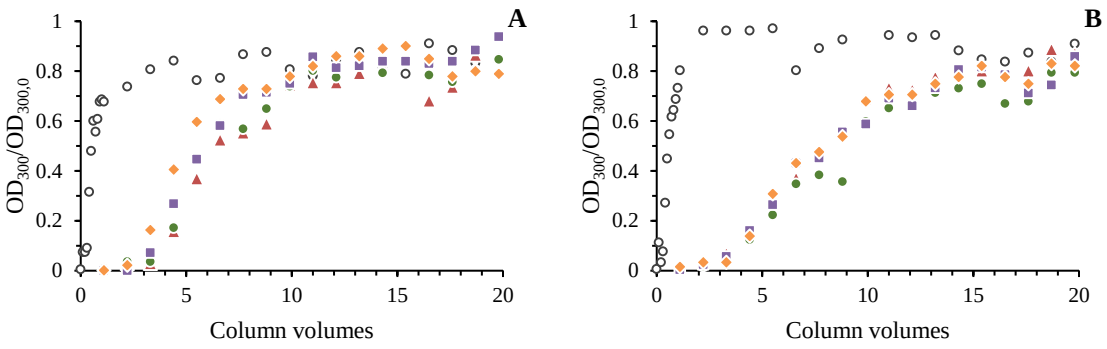

Figure 7.4. Breakthrough curves for f-sand filters tested for removal of 5 ppm humic acid in soft (A) and hard (B) water. Filters tested were bare sand (open black circles), F12 (maroon triangles), F21 (dark green circles), F35 (purple squares) and F52 (peach diamonds).

The four f-sand filters behaved similarly to one another against humic acid in soft and hard water, respectively. The capacities of the filters to remove humic acid was 0.42-0.61 $OD_{300}/OD_{300,0}$ • mL filtered volume per mL bed volume in soft water and 0.64-0.86 $OD_{300}/OD_{300,0}$ • mL filtered water per mL filter bed in hard water. This slight increase in capacity for removing humic acid in hard water could be attributed to humic acid flocculation (see Table 5.2), resulting in aggregates being retained by the filter. For the f-sand filters, 50% breakthrough of humic acid was reached after 4.9-6.5 column volumes for humic acid in soft water and after 8.0-9.5 column volumes for humic acid in hard water. Water hardness had no effect on the capacity of the bare sand filters, which was 0.05 $OD_{300}/OD_{300,0}$ • mL filtered water per mL filter bed for both soft and hard water. For the bare sand filter, 50% breakthrough of humic acid was observed after less than one column volume in both waters.

7.2.3.3. Filters tested against a mixture of humic acid and kaolin

Figure 7.5 shows the breakthrough curves for the f-sand filters and the non-functionalized sand filters tested against turbid water containing 0.05 g/L kaolin and 5 ppm humic acid in soft (A) and hard (B) water.

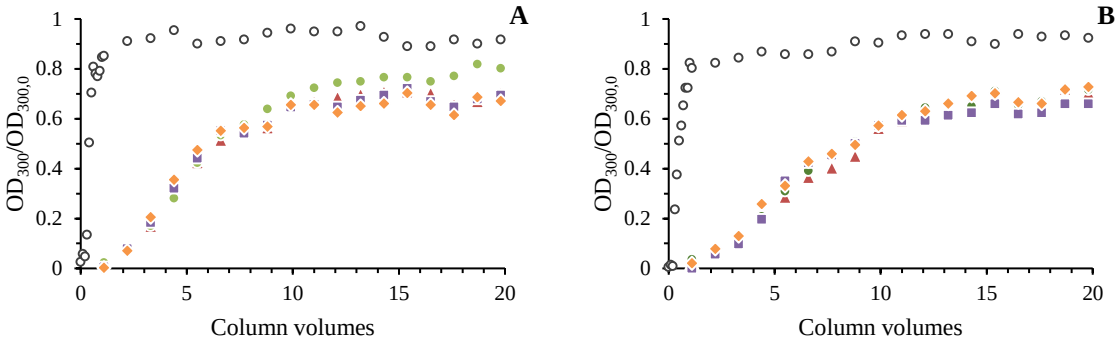

Figure 7.5. Breakthrough curves for f-sand filters tested for removal of a mixture of 5 ppm humic acid and 0.05 g/L kaolin in soft (A) and hard (B) water. Filters tested were bare sand (open black circles), F12 (maroon triangles), F21 (dark green circles), F35 (purple squares) and F52 (peach diamonds).

The four f-sand filters behaved similarly to one another against the mixture in both soft and hard water, respectively. The capacities of the f-sand filters to remove mixture turbidity was 0.91-0.97 $OD_{300}/OD_{300,0}$ • mL filtered water per mL filter bed in soft water and 1.30-1.36 $OD_{300}/OD_{300,0}$ • mL filtered water per mL filter bed in hard water. For the f-sand filters, 50% breakthrough of mixture was reached after 4.9-6.4 column volumes for the mixture in soft water and after 8.6-9.3 column volumes for the mixture in hard water. Water hardness had a very slight effect on the capacity of the bare sand filters, which was 0.06 $OD_{300}/OD_{300,0}$ • mL filtered water per mL filter bed in soft water and 0.08 $OD_{300}/OD_{300,0}$ • mL filtered water per mL filter bed in

hard water. For the bare sand filter, 50% breakthrough of mixture was observed after less than one column volume in both waters.

The breakthrough curves for the mixture more closely resemble the breakthrough curves for humic acid than the breakthrough curves for kaolin. In Chapter 5, we showed that humic acid adsorbs to and colloidally stabilizes kaolin. It is likely that humic acid in the mixture is preventing kaolin particles from aggregating and being retained by the filter, as was seen with the kaolin breakthrough curves, making it more challenging to treat multi-component turbid waters.

7.2.3.4. Summary of filter performances

The number of column volumes at which 50% breakthrough is observed for the filters against the soft and hard turbid waters is provided in Table 7.3. Filter capacities per bed volume for each breakthrough curves are given in Table 5 in unites of $OD_{300}/OD_{300,0}$ • mL filtered water per mL filter bed.

Table 7.3. Column volume at which 50% breakthrough is observed.

Water	Particulate	Bare sand	F12	F21	F35	F52
Soft	Kaolin	0.3	-	-	-	-
	Humic acid	0.5	6.4	5.9	5.9	4.9
	Mixture	0.4	6.4	6.3	6.1	5.9
Hard	Kaolin	0.4	-	-	-	-
	Humic acid	0.6	8.0	9.5	8.2	8.1
	Mixture	0.5	9.3	8.6	8.8	8.9

Table 7.4. Filter capacities for 50% breakthrough in $OD_{300}/OD_{300,0}$ • mL filtered water per mL filter bed.

Water	Particulate	Bare sand	F12	F21	F35	F52
Soft	Kaolin	0.03	-	-	-	-
	Humic acid	0.05	0.61	0.58	0.57	0.42
	Mixture	0.06	0.93	0.97	0.93	0.91
Hard	Kaolin	0.03	-	-	-	-
	Humic acid	0.05	0.76	0.86	0.64	0.75
	Mixture	0.08	1.36	1.32	1.32	1.30

The f-sand filters had similar capacities against each respective soft and hard turbid water, showing that adsorbed protein layer composition does not affect f-sand filter performance. This finding is very significant, as creating f-sand with low protein coverage reduces the amount of natural organic matter in contact with treated drinking water. Limited natural organic matter in treated drinking water would hinder residual microbe growth, extending the shelf life of drinking water treated with *M. oleifera* proteins.

7.3. Conclusions

M. oleifera proteins selectively adsorb to silica sand granules. When sand adsorption sites are limited, the highly cationic species dominate the adsorbed protein layer composition in both soft and hard water. As sand adsorption sites become abundant, the selectivity of the highly cationic fraction to the moderately cationic fraction approaches unity. Non-cationic species are a negligible component of the adsorbed protein layer. With copious adsorption sites, low cationic species are the most abundant component in the adsorbed protein layer when proteins are adsorbed from soft water, whereas high cationic species are the most abundant component in the adsorbed protein layer when adsorbed from hard water.

Adsorbed protein layer composition of f-sand did not affect f-sand filter performance against any of the turbid soft and hard waters. F-sand filters had the highest capacity over 20

column volumes for kaolin, followed by the mixture of kaolin and humic acid, then humic acid. Water hardness did not have a significant effect on f-sand filter capacity, but did have a significant effect on number of column volumes at which 50% breakthrough is observed.

Chapter 8: Conclusions

8.1. Summary of dissertation

Micro-coagulation assays can be used in place of standard jar tests to evaluate performance of scarce coagulants. These well plate assays should be shaken for 15 minutes and allowed to settle for 3 h to produce critical coagulation concentrations and most effective coagulant dosages similar to those that would result from a jar test.

Many distinct cationic proteins comprise aqueous extracts of *M. oleifera* seeds. The majority of the individual or combined protein fractions reduce water turbidity with low protein dosages. Fatty acids do not significantly affect coagulation activity. To produce a water treatment process immune to coagulant concentration uncertainty, protein combinations should be used, as they are effective over broader concentration ranges. Therefore, additional protein purification is not warranted for field applications for drinking water treatment beyond aqueous extraction.

M. oleifera proteins are effective coagulants against kaolin, humic acid, and mixtures of kaolin and humic acid, demonstrating that these proteins can be used to reduce turbidity in a multi-component system. Coagulation occurs within a finite coagulant concentration range. This range broadens as water hardness increases. As humic acid concentration increases in mixtures, the range of effective coagulating protein concentrations broadens, and the critical coagulation concentration (CCC) increases. Increasing water hardness decreases the CCC for humic acid and mixtures, but has no effect on kaolin. The CCC is an order of magnitude higher for humic acid and the mixtures than it is for kaolin. Competitive adsorption between kaolin, humic acid, and the proteins creates a need for higher coagulant dosages in order to successfully clarify water, but it also broadens the protein concentration range for effective coagulation. It is likely that this

trend will persist as other predominantly negatively charged components, such as microbes, are added to the water to be treated.

The coagulation mechanism of *M. oleifera* proteins is adsorption and charge neutralization. The protein concentrations at which charge reversal and a spike in particle size occur closely resemble the median concentrations of the ranges of effective protein concentrations for kaolin, humic acid, and mixtures. The concentration at which charge reversal occurs was an order of magnitude lower for kaolin than for humic acid or the mixtures, though the mixtures required a higher protein concentration to cause charge reversal than humic acid alone. The particle size of the mixture is on the same order of magnitude as the particle size of kaolin, but is consistently smaller, suggesting that kaolin is somewhat less aggregated in the presence of humic acid.

Ellipsometry revealed that adsorption from a solution of all water-soluble *M. oleifera* proteins produces greater surface excess concentrations on silica surfaces than a solution of cationic proteins. Fatty acids do not interfere with the adsorption of *M. oleifera* seed proteins to silica. The effect of water hardness on *M. oleifera* seed protein adsorption is fairly modest. Proteins in soft or hard water adsorb to a greater extent to silica than proteins in deionized water at intermediate bulk concentrations, but to similar extents at low and high bulk concentrations. Adsorption most likely exceeds saturated monolayer coverage for each combination of protein fractionation and water hardness at higher bulk concentrations. *M. oleifera* proteins adsorbed to silica are resistant to desorption during freshwater rinsing but can be removed with concentrated sodium chloride solutions.

Streaming potential measurements showed that dilute solutions of *M. oleifera* proteins cause a net charge reversal of silica surfaces from negative to positive and that a solution of

cationic proteins will produce a more positive zeta potential than a solution of all-water-soluble proteins. This suggests that dilute solutions with lower levels of natural organic matter would be sufficient to produce effective functionalized sand (f-sand) with a net positive charge for use in potable water treatment in the developing world. Fatty acids and water harness hinder the extent of surface charge reversal caused by protein adsorption.

M. oleifera proteins selectively adsorb to silica sand granules. When sand adsorption sites are limited, the high cationic species dominate the adsorbed protein layer composition in both soft and hard water. As sand adsorption sites become abundant, the ratio of low cationic species to high cationic species within the adsorbed layer approaches unity. Non-cationic species are a negligible component of the adsorbed protein layer.

Adsorbed protein layer composition of f-sand does not affect f-sand filter performance against turbid soft and hard waters containing kaolin, humic acid, or a mixture of kaolin and humic acid. This finding is very significant, as using dilute solutions to create f-sand would conserve seed protein resource and reduce the amount of natural organic matter in contact with treated drinking water. The latter would reduce residual microbe growth and extend the shelf life of drinking water treated with *M. oleifera* proteins. F-sand filters had the highest capacity over 20 column volumes for kaolin, followed by the mixture, then humic acid. Water hardness did not have a significant effect on f-sand filter capacity, but did have a significant effect on number of column volumes at which 50% breakthrough is observed.

8.2. Original contributions

Micro-coagulation assays that implement volumes on the order of microliters to a few milliliters have been used in several studies to examine the turbidity reduction capabilities of *M.*

oleifera cationic proteins.[25,33,38,58,59] Yet, the correspondence between micro-coagulation assays that use micro- to low macro-volumes and the larger volume jar tests conventionally used in water treatment plants to evaluate coagulant performance was not established. In this dissertation, micro-coagulation assay was validated by determining the conditions under which the jar test and the micro-coagulation assay yield similar results. This was done using a kaolin suspension to model turbid water and aluminum potassium sulfate dodecahydrate (alum) as a coagulant. It was found that these well plate assays should be shaken for 15 minutes and allowed to settle for 3 h to produce critical coagulation concentrations and most effective coagulant dosages similar to those that would result from a jar test.

Aqueous extracts from *M. oleifera* seeds contain various cationic and non-cationic proteins, as well as other water-soluble compounds, and it was currently unknown if these component interactions have antagonistic or synergistic impacts on coagulant performance. Therefore, a systematic evaluation of the coagulation activities of extracts with varying levels of purification was needed to determine the protein fraction or combination of fractions that has high coagulation activity at low concentrations so that the inactive fractions might be eliminated to minimize the dissolved organic carbon added to water. In this dissertation, high performance liquid chromatography was used to isolate eight *M. oleifera* cationic protein fractions. The coagulation performances of these fractions were compared individually and in various combinations against kaolin clay suspensions in model freshwaters of varying hardness. It was found that combinations of the strongly cationic fractions, of all cationic fractions, and of all cationic and non-cationic fractions were effective across broad ranges of protein dosages. Therefore, additional protein purification beyond aqueous extraction is not warranted for field applications for drinking water treatment.

The coagulation activity of *M. oleifera* proteins has been tested on natural water sources as well as on model freshwaters. Natural waters vary widely in hardness and natural organic matter content. Therefore, a model study that systematically introduces competitive multi-component interactions that would exist in natural waters was required to reveal the mechanistic roles of different system components that are likely to be important in complex, highly variable natural water sources. In this dissertation, the influence of these interactions on the effective concentration range for kaolin coagulation by *M. oleifera* seed proteins was determined by varying humic acid concentration in model freshwaters with varying hardness. It was shown that *M. oleifera* proteins remain effective as coagulants when used to reduce turbidity in a multi-component system, but that competitive adsorption between model water components creates a need for higher coagulant dosages in order to successfully clarify water. However, this competitive adsorption, along with increasing water hardness, also broadens the protein concentration range for effective coagulation. It is likely that this trend will persist as other predominantly negatively charged components, such as microbes, are added to the water to be treated. These findings contribute to the development of methods to treat natural water using *M. oleifera* seed proteins.

Adsorption of *M. oleifera* seed proteins to silica surfaces had yet to be extensively studied. In this dissertation, the extent to which varying levels of *M. oleifera* extract purification affect adsorption to silica, the main constituent of sand, under various water conditions was determined. Ellipsometry was used to construct adsorption isotherms for the proteins adsorbed to the native oxide layer on silicon wafers, and a rotating disk streaming potential method[67,68] was used to determine the protein concentration at which these silica surfaces undergo charge reversal from net anionic to net cationic. It was found that water hardness has minimal effect on

protein adsorption, that protein fractionation reduces surface excess concentration but increases charge reversal at a given concentration, and that fatty acids do not affect adsorption but do hinder charge reversal. The latter is an important practical issue, as oil removed from the seeds is commonly sold as a commodity before using the seeds to treat drinking water[10]. Since the cationic character of the f-sand filter material is critical for solids removal and antimicrobial potency, these results will assist in determining the minimum protein concentration required to produce effective f-sand.

The effects of water hardness on *M. oleifera* protein adsorption to sand granules, the composition of the adsorbed protein layer on f-sand granules, and the influence of layer composition on f-sand filter efficiency had yet to be studied. In this dissertation, four different f-sands were created by exposing various quantities of sand to similar aliquots of protein solution. The supernatants of the protein solutions were collected, concentrated, and fractionated using a cation exchange column and high performance liquid chromatography. Three fractions were collected and quantified to determine the composition of the adsorbed protein layer on the f-sands as well as the percent of each fraction adsorbed to the sand granules. When packed into filters and tested against soft and hard turbid waters containing either kaolin, humic acid, or both, all four f-sand filters performed similarly, confirming that dilute protein solutions are sufficient to produce effective f-sand for use in potable water treatment. This finding is very significant, as creating f-sand with low protein coverage reduces the amount of natural organic matter in contact with treated drinking water, which would hinder residual microbe growth and extend the shelf life of drinking water treated with *M. oleifera* proteins.

8.3. Future work

8.3.1. Moringa oleifera proteins as coagulants

Although the coagulation activity of *Moringa oleifera* proteins has been tested against a variety of natural water sources and model freshwaters, the most complex model freshwater that has been studied contained only two components, kaolin and humic acid. The complexity of this model freshwater could be increased to include a species of bacteria to model microbes in natural water sources. The complexity could be further increased to include pollutants, such as dyes, fertilizers, or hormones.

8.3.2. Adsorption of Moringa oleifera proteins to silica

The adsorption of *Moringa oleifera* proteins to silica has only been studied using protein solutions in deionized water[66] or EPA model soft and hard freshwaters[65], neither of which contained any species representative of natural water components. Adsorption studies could be performed using proteins dissolved in natural water sources or in more realistic model waters, such as ones that contain kaolin to model particulates and humic acid to model natural organic matter.

8.3.3. F-sand filter development

To create a higher performance f-sand filter, the depth of the filter will likely need to be increased. Gravity filters used in municipal drinking water treatment plants are typically 0.6-1.8 m in depth, though some as deep at 4 m are in use[69]. Crittenden explains that particles must first be destabilized before passing through a filter bed in order to adhere to the filter media due to electrostatic repulsions between the particles and the filter media[69]. The adsorbed cationic proteins in our f-sand filters reverse the sand surface charge from negative to positive. This

changes the particles-media interactions from repulsive to attractive and eliminates the need to destabilize particles prior to filter use.

Pre-treatment of turbid water may still be a necessary step to increase filter performance. Incorporating coagulation, flocculation, and sedimentation steps with *M. oleifera* proteins before utilizing granular filtration with an f-sand filter would reduce the amount of particulate matter flowing through the filter, which would likely increase the longevity and efficiency of the f-sand filter. Such two-step processes have been shown to produce clean and safe drinking water[100–102]. The main concern with first using *M. oleifera* proteins as coagulants is the organic matter added to the treated drinking water. However, the f-sand filters, which are packed with adsorbent material, should be able to remove the organic matter from the coagulation step along with any residual particulate matter[103].

References

(1) Razis, A. F. A.; Ibrahim, M. D.; Kntayya, S. B. Health Benefits of Moringa Oleifera. *Asian Pacific J. Cancer Prev.* **2014**, *15* (20), 8571–8576.

(2) Moyo, B.; Masika, P. Nutritional Characterization of Moringa (Moringa Oleifera Lam.) Leaves. *African J. Biotechnol.* **2011**, *10* (60), 12925–12933.

(3) Hussain, S.; Malik, F.; Mahmood, S. An Exposition of Medicinal Preponderance of Moringa Oleifera (Lank.). *Pak. J. Pharm. Sci.* **2014**, *27* (2), 397–403.

(4) Ferreira, P. M. P.; Farias, D. F.; Oliveira, J. T. de A.; Carvalho, A. de F. U. Moringa Oleifera: Bioactive Compounds and Nutritional Potential. *Rev. Nutr.* **2008**, *21* (4), 431–437.

(5) Ebert, A. W. Potential of Underutilized Traditional Vegetables and Legume Crops to Contribute to Food and Nutritional Security, Income and More Sustainable Production Systems. *Sustain.* **2014**, *6* (1), 319–335.

(6) Dubey, D. K.; Dora, J.; Kumar, A.; Gulsan, R. K. A Multipurpose Tree- Moringa Oleifera. *Int. J. Pharm. Chem. Sci.* **2013**, *2* (1), 415–423.

(7) Anwar, F.; Latif, S.; Ashraf, M.; Gilani, A. H. Moringa Oleifera: A Food Plant with Multiple Medicinal Uses. *Phyther. Res.* **2007**, *21*, 17–25.

(8) Yin, C. Y. Emerging Usage of Plant-Based Coagulants for Water and Wastewater Treatment. *Process Biochem.* **2010**, *45* (9), 1437–1444.

(9) Kansal, S. K.; Kumari, A. Potential of M. Oleifera for the Treatment of Water and Wastewater. *Chem. Rev.* **2014**, *114* (9), 4993–5010.

(10) Lea, M. Bioremediation of Turbid Surface Water Using Seed Extract from Moringa Oleifera Lam. (Drumstick) Tree. *Curr. Protoc. Microbiol.* **2014**, *33* (G:1G.2), 1G.1-1G.8.

(11) Madsen, M.; Schlundt, J.; Omer, E. F. Effect of Water Coagulation by Seeds of Moringa Oleifera on Bacterial Concentrations. *J. Trop. Med. Hyg.* **1987**, *90* (3), 101.

(12) Bawa, L. M.; Djaneye-Boundjou, G.; Boukari, Y.; Sani, A. Coagulation of Some Humic Acid Solutions by Moringa Oleifera Lam Seeds: Effect on Chlorine Requirement. *Bull. Chem. Soc. Ethiop.* **2001**, *15* (2), 119–129.

(13) Katayon, S.; Noor Megat Mohd, M. J.; Asma, M.; Ghani Abdul, L. A.; Thamer, A. M.; Azni, I.; Ahmad, J.; Khor, B. C.; Suleyman, A. M. Effects of Storage Conditions of Moringa Oleifera Seeds on Its Performance in Coagulation. *Bioresour. Technol.* **2006**, *97* (13), 1455–1460.

(14) Katayon, S.; Ng, S. C.; Megat Johari, M. M. N.; Abdul Ghani, L. A. Preservation of Coagulation Efficiency of Moringa Oleifera, a Natural Coagulant. *Biotechnol. Bioprocess Eng.* **2006**, *11* (6), 489–495.

(15) Abdulsalam, S; Gital, A. A.; Misau, I. M.; Suleiman, M. S. Water Clarification Using Moringa Oleifera Seed Coagulant: Maiduguri Raw Water as a Case Study. *J. Food, Agric. Environ.* **2012**, *5* (4), 472–486.

(16) Katayon, S.; Megat Mohd Noor, M. J.; Kien Tat, W.; Abdul Halim, G.; Thamer, A. M.; Badronisa, Y. Effect of Natural Coagulant Application on Microfiltration Performance in Treatment of Secondary Oxidation Pond Effluent. *Desalination* **2007**, *204* (1–3), 204–212.

(17) Pritchard, M.; Mkandawire, T.; Edmondson, A.; O'Neill, J. G.; Kululanga, G. Potential of Using Plant Extracts for Purification of Shallow Well Water in Malawi. *Phys. Chem. Earth* **2009**, *34* (13–16), 799–805.

(18) Sarpong, G.; Richardson, C. P. Coagulation Efficiency of Moringa Oleifera for Removal of Turbidity and Reduction of Total Coliform as Compared to Aluminum Sulfate. *African J. Agric. Res.* **2010**, *5* (21), 2939–2944.

(19) Ndabigengesere, A.; Narasiah, K. S.; Talbot, B. G. Active Agents and Mechanism of Coagulation of Turbid Water Using Moringa Oleifera. *Water Res.* **1995**, *29* (2), 703–710.

(20) Nkurunziza, T.; Nduwayezu, J. B.; Banadda, E. N.; Nhapi, I. The Effect of Turbidity Levels and Moringa Oleifera Concentration on the Effectiveness of Coagulation in Water Treatment. *Water Sci. Technol.* **2009**, *59* (8), 1551–1558.

(21) Wilson, S. A.; Andrews, S. A. Impact of a Natural Coagulant Pretreatment for Colour Removal on Solar Water Disinfection (SODIS). *J. Water, Sanit. Hyg. Dev.* **2011**, *1* (1), 57.

(22) Freitas, J. H. E. S.; de Santana, K. V.; do Nascimento, A. C. C.; de Paiva, S. C.; de Moura, M. C.; Coelho, L. C. B. B.; de Oliveira, M. B. M.; Paiva, P. M. G.; do Nascimento, A. E.; Napoleão, T. H. Evaluation of Using Aluminum Sulfate and Water-Soluble Moringa Oleifera Seed Lectin to Reduce Turbidity and Toxicity of Polluted Stream Water. *Chemosphere* **2016**, *163* (1), 133–141.

(23) Ndabigengesere, A.; Narasiah, K. S. Use of Moringa Oleifera Seeds as a Primary Coagulant in Wastewater Treatment. *Environ. Technol.* **1998**, *19* (8), 789–800.

(24) Ndabigengesere, A.; Narasiah, K. S. Quality of Water Treated by Coagulation Using Moringa Oleifera Seeds. *Water Res.* **1998**, *32* (3), 781–791.

(25) Ghebremichael, K. A.; Gunaratna, K. R.; Henriksson, H.; Brumer, H.; Dalhammar, G. A Simple Purification and Activity Assay of the Coagulant Protein from Moringa Oleifera Seed. *Water Res.* **2005**, *39* (11), 2338–2344.

(26) National Research Council. *Lost Crops of Africa Volume II: Vegetables*; 2006.

(27) Jerri, H. A.; Adolfsen, K. J.; McCullough, L. R.; Velegol, D.; Velegol, S. B. Antimicrobial Sand via Adsorption of Cationic Moringa Oleifera Protein. *Langmuir* **2012**, *28* (4), 2262–2268.

(28) Xiong, B.; Piechowicz, B.; Wang, Z.; Marinaro, R.; Clement, E.; Carlin, T.; Uliana, A.; Kumar, M.; Velegol, S. B. Moringa Oleifera F-Sand Filters for Sustainable Water Purification. *Environ. Sci. Technol. Lett.* **2018**, *5* (1), 38–42.

(29) Li, L.; Pan, G. A Universal Method for Flocculating Harmful Algal Blooms in Marine and Fresh Waters Using Modified Sand. *Environ. Sci. Technol.* **2013**, *47* (9), 4555–4562.

(30) Nisha, R. R.; Jegathambal, P.; Parameswari, K.; Kirupa, K. Biocompatible Water Softening System Using Cationic Protein from Moringa Oleifera Extract. *Appl. Water Sci.*

2017, *7* (6), 2933–2941.

(31) Williams, F. E.; Lee, A. K.; Orandi, S.; Sims, S. K.; Lewis, D. M. *Moringa Oleifera* Functionalised Sand – Reuse with Non-Ionic Surfactant Dodecyl Glucoside. *J. Water Health* **2017**, *15* (6), 863–872.

(32) Gassenschmidt, U.; Jany, K. D.; Tauscher, B.; Niebergall, H. Isolation and Characterization of a Flocculating Protein from Moringa Oleifera Lam. *Biochim. Biophys. Acta* **1995**, *1243* (3), 477–481.

(33) Suarez, M.; Entenza, J. M.; Doerries, C.; Meyer, E.; Bourquin, L.; Sutherland, J.; Marison, I.; Moreillon, P.; Mermod, N. Expression of a Plant-Derived Peptide Harboring Water-Cleaning and Antimicrobial Activities. *Biotechnol. Bioeng.* **2003**, *81* (1), 13–20.

(34) Shebek, K.; Schantz, A. B.; Sines, I.; Lauser, K.; Velegol, S.; Kumar, M. The Flocculating Cationic Polypetide from Moringa Oleifera Seeds Damages Bacterial Cell Membranes by Causing Membrane Fusion. *Langmuir* **2015**, *31* (15), 4496–4502.

(35) Santos, A. F. S.; Argolo, A. C. C.; Coelho, L. C. B. B.; Paiva, P. M. G. Detection of Water Soluble Lectin and Antioxidant Component from Moringa Oleifera Seeds. *Water Res.* **2005**, *39* (6), 975–980.

(36) Madrona, G. S.; Branco, I. G.; Seolin, V. J.; Filho, B. de A. A.; Fagundes-Klen, M. R.; Bergamasco, R. Evaluation of Extracts of Moringa Oleifera Lam Seeds Obtained with NaCl and Their Effects on Water Treatment. *Acta Sci. - Technol.* **2012**, *34* (3), 289–293.

(37) Agrawal, H.; Shee, C.; Sharma, A. K. Isolation of a 66 kDa Protein with Coagulation Activity from Seeds of Moringa Oleifera. *Res. J. Agric. Biol. Sci.* **2007**, *3* (5), 418–421.

(38) Suarez, M.; Haenni, M.; Fisch, F.; Chodanowski, P.; Servis, C.; Michielin, O.; Freitag, R.; Moreillon, P.; Mermod, N. Structure-Function Characterization and Optimization of a Plant-Derived Antibacterial Peptide. *Antimicrob. Agents Chemother* **2005**, *49* (9), 3847–3857.

(39) Kwaambwa, H. M.; Maikokera, R. Infrared and Circular Dichroism Spectroscopic Characterisation of Secondary Structure Components of a Water Treatment Coagulant Protein Extracted from Moringa Oleifera Seeds. *Colloids Surfaces B Biointerfaces* **2008**, *64* (1), 118–125.

(40) Salazar Gámez, L. L.; Luna-delRisco, M.; Salazar Cano, R. Effect of Storage and Preparation Methods of Moringa Oleifera Seeds during the Coagulation Process. *Desalin. Water Treat.* **2015**, *57*, 1–8.

(41) Pritchard, M.; Craven, T.; Mkandawire, T.; Edmondson, A. S.; O'Neill, J. G. A Study of the Parameters Affecting the Effectiveness of Moringa Oleifera in Drinking Water Purification. *Phys. Chem. Earth* **2010**, *35* (13–14), 791–797.

(42) Golestanbagh, M.; Ahamad, I. S.; Idris, A.; Yunus, R. Effect of Storage of Shelled Moringa Oleifera Seeds from Reaping Time on Turbidity Removal. *J. Water Health* **2011**, *9* (3), 597–602.

(43) Nordmark, B. A.; Przybycien, T. M.; Tilton, R. D. Comparative Coagulation Performance Study of Moringa Oleifera Cationic Protein Fractions with Varying Water Hardness. *J.*

Environ. Chem. Eng. **2016**, *4* (4A), 4690–4698.

(44) Okuda, T.; Baes, a U.; Nishijima, W.; Okada, M. Coagulation Mechanism of Salt Solution-Extracted Active Component in Moringa Oleifera Seeds. *Water Res.* **2001**, *35* (3), 830–834.

(45) Okuda, T.; Baes, A. U.; Nishijima, W.; Okada, M. Improvement of Extraction Method of Coagulation Active Components From Moringa Oleifera Seed. **1999**, *33* (15), 3373–3378.

(46) Crittenden, J. C.; Trussell, R. R.; Hand, D. W.; Howe, K. J.; Tchobanoglous, G. Coagulation and Flocculation. In *MWH's Water Treatment: Principles and Design*; John Wiley & Sons, Inc: Hoboken, NJ, 2012; pp 541–639.

(47) Blaney, L. M. Lecture 8: Coagulation and Flocculation. ENCH 412: Environmental Physicochemical Processes. University of Maryland, Baltimore County. University of Maryland, Baltimore County 2013.

(48) Okuda, T.; Baes, A. U.; Nishijima, W.; Okada, M. Isolation and Characterization of Coagulant Extracted from Moringa Oleifera Seed by Salt Solution. *Water Res.* **2001**, *35* (2), 405–410.

(49) Beltrán-Heredia, J.; Sánchez-Martín, J.; Muñoz-Serrano, a.; Peres, J. a. Towards Overcoming TOC Increase in Wastewater Treated with Moringa Oleifera Seed Extract. *Chem. Eng. J.* **2012**, *188*, 40–46.

(50) Sánchez-Martín, J.; Ghebremichael, K.; Beltrán-Heredia, J. Comparison of Single-Step and Two-Step Purified Coagulants from Moringa Oleifera Seed for Turbidity and DOC Removal. *Bioresour. Technol.* **2010**, *101* (15), 6259–6261.

(51) Madrona, G. S.; Serpelloni, G. B.; Salcedo Vieira, A. M.; Nishi, L.; Cardoso, K. C.; Bergamasco, R. Study of the Effect of Saline Solution on the Extraction of the Moringa Oleifera Seed's Active Component for Water Treatment. *Water. Air. Soil Pollut.* **2010**, *211* (1–4), 409–415.

(52) Ghebremichael, K. A.; Gunaratna, K. R.; Dalhammar, G. Single-Step Ion Exchange Purification of the Coagulant Protein from Moringa Oleifera Seed. *Appl. Microbiol. Biotechnol.* **2006**, *70* (5), 526–532.

(53) Ghebremichael, Kebreab; Abaliwano, Juliet; Amy, G. Combined Natural Organic and Synthetic Inorganic Coagulants for Surface Water Treatment. *J. Water Supply Res. Technol.* **2009**, *58* (4), 267–276.

(54) Santos, A. F. S.; Carneiro-da-Cunha, M. G.; Teixeira, J. A.; Paiva, P. M. G.; Coelho, L. C. B. B.; Nogueira, R. Interaction of Moringa Oleifera Seed Lectin with Humic Acid. *Chem. Pap.* **2011**, *65* (4), 406–411.

(55) Santos, A. F. S.; Paiva, P. M. G.; Teixeira, J. A. C.; Brito, A. G.; Coelho, L. C. B. B.; Nogueira, R. Coagulant Properties of Moringa Oleifera Protein Preparations: Application to Humic Acid Removal. *Environ. Technol.* **2012**, *33* (1–3), 69–75.

(56) Sánchez-Martín, J.; Beltrán-Heredia, J.; Peres, J. A. Improvement of the Flocculation Process in Water Treatment by Using Moringa Oleifera Seeds Extract. *Brazilian J. Chem. Eng.* **2012**, *29* (3), 495–501.

(57) Ghebremichael, K. Overcoming the Drawbacks of Natural Coagulants for Drinking Water Treatment. *Water Sci. Technol. Water Supply* **2007**, 87–93.

(58) Okoli, C.; Boutonnet, M.; Järås, S.; Rajarao-Kuttuva, G. Protein-Functionalized Magnetic Iron Oxide Nanoparticles: Time Efficient Potential-Water Treatment. *J. Nanoparticle Res.* **2012**, *14* (10), 1194.

(59) Broin, M.; Santaella, C.; Cuine, S.; Kokou, K.; Peltier, G.; Joët, T. Flocculent Activity of a Recombinant Protein from Moringa Oleifera Lam. Seeds. *Appl. Microbiol. Biotechnol.* **2003**, *60* (1–2), 114–119.

(60) Amagloh, F. K.; Benang, A. Effectiveness of Moringa Oleifera Seed as Coagulant for Water Purification. *African J. Agric. Res.* **2009**, *4* (2), 119–123.

(61) Subramanium, S.; Nand, V.; Maata, M.; Koshy, K. Moringa Oleifera and Other Local Seeds in Water Purification in Developing Countries. *Res. J. Chem. Environ.* **2011**, *15* (2), 135–138.

(62) Ali, Syed Imran; MacDonaold, Morgan; Jincy, J.; Sampath, Arun; Vinothini, G.; Philip, Ligy; Hall, Kevin; Aronson, K. Efficacy of an Appropriate Point-of-Use Water Treatment Intervention for Low-Income Communities in India Utilizing Moringa Oleifera , Sari-Cloth Filtration and Solar UV Disinfection. *J. Water, Sanit. Hyg. Dev.* **2016**, *1* (2).

(63) Ferreira, R. S.; Napoleao, T. H.; Santos, A. F. S.; Sa, R. A.; Carneiro-da-Cunha, M. G.; Morais, M. M. C.; Silva-Lucca, R. A.; Oliva, M. L. V; Coelho, L. C. B. B.; Paiva, P. M. G. Coagulant and Antibacterial Activities of the Water-Soluble Seed Lectin from Moringa Oleifera. *Lett. Appl. Microbiol.* **2011**, *53* (2), 186–192.

(64) Gupta, V.; Hampton, M. a.; Stokes, J. R.; Nguyen, A. V.; Miller, J. D. Particle Interactions in Kaolinite Suspensions and Corresponding Aggregate Structures. *J. Colloid Interface Sci.* **2011**, *359* (1), 95–103.

(65) Nordmark, B. A.; Bechtel, T. M.; Riley, J. K.; Velegol, D.; Velegol, S. B.; Przybycien, T. M.; Tilton, R. D. Moringa Oleifera Seed Protein Adsorption to Silica: Effects of Water Hardness, Fractionation, and Fatty Acid Extraction. *Langmuir* **2018**, *34* (16), 4852–4860.

(66) Kwaambwa, H. M.; Hellsing, M.; Rennie, A. R. Adsorption of a Water Treatment Protein from Moringa Oleifera Seeds to a Silicon Oxide Surface Studied by Neutron Reflection. *Langmuir* **2010**, *26* (6), 3902–3910.

(67) Hoggard, J. D.; Sides, P. J.; Prieve, D. C. Measurement of the Streaming Potential and Streaming Current near a Rotating Disk to Determine Its Zeta Potential. *Langmuir* **2005**, *21* (16), 7433–7438.

(68) Sides, P. J.; Newman, J.; Hoggard, J. D.; Prieve, D. C. Calculation of the Streaming Potential near a Rotating Disk. *Langmuir* **2006**, *23* (22), 9765–9769.

(69) Crittenden, J. C.; Trussell, R. R.; Hand, D. W.; Howe, K. J.; Tchobanoglous, G. Granular Filtration. In *MWH's Water Treatment: Principles and Design*; John Wiley & Sons, Inc: Hoboken, NJ, 2012; pp 867–954.

(70) U.S Environmental Protection Agency Office of Water. *Methods for Measuring the Acute Toxicity of Effluents and Receiving Waters to Freshwater and Marine Organisms*;

Washington, DC, 2002.

(71) Thermo Scientific. Pierce ™ 660nm Protein Assay. **2013**.

(72) Hunter, R. J. *Foundations of Colloid Science*, 1st ed.; Clarendon Press: Oxford, 1986.

(73) Saigal, T.; Riley, J. K.; Golas, P. L.; Bodvik, R.; Claesson, P. M.; Matyjaszewski, K.; Tilton, R. D. Poly(Ethylene Oxide) Star Polymer Adsorption at the Silica/Aqueous Interface and Displacement by Linear Poly(Ethylene Oxide). *Langmuir* **2013**, *29* (12), 3999–4007.

(74) Benjamins, J.-W.; Jönsson, B.; Thuresson, K.; Nylander, T. New Experimental Setup To Use Ellipsometry To Study Liquid - Liquid and Liquid - Solid Interfaces. *Langmuir* **2002**, *18* (16), 6437–6444.

(75) Tilton, R. D. Scanning Angle Reflectometry and Its Application to Polymer Adsorption and Coadsorption with Surfactants. In *Colloid-Polymer Interactions: From Fundamentals to Practice*; Farinato, R. S., Dubin, P. L., Eds.; Wiley: New York, 1999; pp 331–363.

(76) de Feijter, J. A.; Benjamins, J.; Veer, F. A. Ellipsometry as a Tool to Study the Adsorption Behavior of Synthetic and Bioplymers at the Air-Water Interface. *Biopolymers* **1978**, *17* (7), 1759–1772.

(77) Ball, V.; Ramsden, J. J. Buffer Dependence of Refractive Index Increments. *Biopolymers* **1998**, *46* (7), 489–492.

(78) US Environmental Protection Agency. Drinking Water Contaminants http://water.epa.gov/drink/contaminants/index.cfm.

(79) Robeson, J. L.; Tilton, R. D. Spontaneous Reconfiguration of Adsorbed Lysozyme Layers Observed by Total Internal Reflection Fluorescence with a pH-Sensitive Fluorophore. **1996**, *7463* (14), 6104–6113.

(80) Daly, S. M.; Przybycien, T. M.; Tilton, R. D. Coverage-Dependent Orientation of Lysozyme Adsorbed on Silica. *Langmuir* **2003**, *19* (9), 3848–3857.

(81) Lin, S.; Kohn, J. E.; Siino, J.; Yee, D. C.; Urban, M. Precision Plus Protein ™ Dual Xtra Standards — New Protein Standards with an Extended Range from 2 to 250 kD. *Electrophor. Bio-Rad Laboritories, Inc.* **2010**, 14–17.

(82) Kelly, S. M.; Jess, T. J.; Price, N. C. How to Study Proteins by Circular Dichroism. *Biochim. Biophys. Acta* **2005**, *1751*, 119–139.

(83) Berg, J. C. *An Introduction to Interfaces and Colloids: The Bridge to Nanoscience*, 1st ed.; World Scientificc Publishing Co. Pte. Ltd, 2010.

(84) Norde, W. The Adsorption of Human Plasma Albumin and Bovine Pancreas Ribonuclease at Negatively Charged Polystyrene Surfaces. **1978**, *66* (2).

(85) Arai, T.; Norde, W. The Behavior of Some Model Proteins at Solid-Liquid Interfaces 1. Adsorption from Single Protein Solutions. *Colloids and Surfaces* **1990**, *51*, 1–15.

(86) Malvern. *Dynamic Light Scattering Common Terms Defined*; 2011.

(87) Angelico, R.; Ceglie, A.; He, J. Z.; Liu, Y. R.; Palumbo, G.; Colombo, C. Particle Size,

Charge and Colloidal Stability of Humic Acids Coprecipitated with Ferrihydrite. *Chemosphere* **2014**, *99* (1), 239–247.

(88) Palafox, J. O.; Navarrete, A.; Sacramento-Rivero, J. C.; Rubio-Atoche, C.; Escoffie, P. A.; Rocha-Uribe, J. A. Extraction and Characterization of Oil from Moringa Oleifera Using Supercritical CO2 and Traditional Solvents. **2012**, *3* (12A), 946–949.

(89) Daly, S. M.; Przybycien, T. M.; Tilton, R. D. Adsorption of Poly(ethylene Glycol)-Modified Lysozyme to Silica. *Langmuir* **2005**, *21* (4), 1328–1337.

(90) Sing, K. S. W. Reporting Physisorption Data for Gas/solid Systems with Special Reference to the Determination of Surface Area and Porosity. *Pure Appl. Chem.* **1982**, *54* (11), 2201–2218.

(91) Tilton, R. D.; Robertson, C. R.; Gast, A. P. Lateral Diffusion of Bovine Serum Albumin Adsorbed at the Solid-Liquid Interface. *J. Colloid Interface Sci.* **1990**, *137* (1), 192–203.

(92) Tilton, R. D.; Gast, A. P.; Robertson, C. R. Surface Diffusion of Interacting Proteins: Effect of Concentration on the Lateral Mobility of Adsorbed Bovine Serum Albumin. *Biophys. J.* **1990**, *58* (5), 1321–1326.

(93) Rabe, T. E.; Tilton, R. D. Surface Diffusion of Adsorbed Proteins in the Vicinity of the Substrate Glass Transition Temperature. *J. Colloid Interface Sci.* **1993**, *159* (1), 243–245.

(94) Robeson, J. L.; Tilton, R. D. Effect of Concentration Quenching on Fluorescence Recovery after Photobleaching Measurements. *Biophys. J.* **1995**, *68* (5), 2145–2155.

(95) Talbot, J.; Schaaf, P. Random Sequential Adsorption of Mixtures. *Phys. Rev. A* **1989**, *40* (1), 422–427.

(96) Ullah, A.; Mariutti, R. B.; Masood, R.; Caruso, I. P.; Gravatim Costa, G. H.; Millena De Freita, C.; Santos, C. R.; Zanphorlin, L. M.; Rossini Mutton, M. J.; Murakami, M. T.; et al. Crystal Structure of Mature 2S Albumin from Moringa Oleifera Seeds. *Biochem. Biophys. Res. Commun.* **2015**, *468* (1–2), 365–371.

(97) Erickson, H. P. Size and Shape of Protein Molecules at the Nanometer Level Determined by Sedimentation, Gel Filtration, and Electron Microscopy. *Biol. Proced. Online* **2009**, *11* (1), 32–51.

(98) Norde, W.; Rouwendal, E. Streaming Potential Measurements as a Tool to Study Protein Adsorption Kinetics. *J. Colloid Interface Sci.* **1990**, *139* (1), 169–176.

(99) Adamczyk, Z.; Sadlej, K.; Wajnryb, E.; Nattich, M.; Ekiel-Jezewska, M. L.; Bławzdziewicz, J. Streaming Potential Studies of Colloid, Polyelectrolyte and Protein Deposition. *Adv. Colloid Interface Sci.* **2010**, *153* (1–2), 1–29.

(100) Zaman, S.; Begum, A.; Rabbani, K. S.; Bari, L. Low Cost and Sustainable Surface Water Purification Methods Using Moringa Seeds and Scallop Powder Followed by Bio-Sand Filtration. *Water Sci. Technol. Water Supply* **2017**, *17* (1), 125–137.

(101) Beltrán-Heredia, J.; Sánchez-Martín, J. Improvement of Water Treatment Pilot Plant with Moringa Oleifera Extract as Flocculant Agent. *Environ. Technol.* **2009**, *30* (6), 525–534.

(102) Franco, M. Water Treatment by Multistage Filtration System with Natural Coagulant from

Moringa Oleifera Seeds. *Eng. Agric.* **2012**, *32* (5), 988–996.

(103) Crittenden, J. C.; Trussell, R. R.; Hand, D. W.; Howe, K. J.; Tchobanoglous, G. Adsorption. In *MWH's Water Treatment: Principles and Design*; John Wiley & Sons, Inc: Hoboken, NJ, 2012; pp 1245–1357.